Engineered Design of Fiber Reinforced Precast Refractory Material for Taconite Processing Furnaces

A THESIS
SUBMITTED TO THE FACULTY OF THE GRADUATE SCHOOL
OF THE UNIVERSITY OF MINNESOTA
BY

Robb Alex Peterson

IN PARTIAL FULFILLMENT OF THE REQUIREMENTS
FOR THE DEGREE OF
MASTER OF SCIENCE

Eshan V. Dave

February 2014

ACKNOWLEDGEMENTS

I would like to thank Cliffs Natural Resources for their support, in particular the management at Northshore Mining, who fully supported and recognized the importance of this research for both personal growth and in continued innovation of refractory maintenance.
I would also like to thank the Allied Mineral Products team led by Dr. Dana Goski who fully supported and encourage this study. Without their support this study would have not taken place on such a through and professional level.
In addition, I would like to thank the faculty and staff at the University of Minnesota Duluth: Dr. Eshan V. Dave who was a helpful advisor that was enthusiastic about the subject matter throughout this whole process, Moe Benda for encouraging me along the way, along with Mark Roberts, Jill Bergman, and Jay Dailey.

DEDICATION

I would like to dedicate this effort to my late brother Erik who had been an inspiration throughout my graduate education. I would like to also dedicate this to my invaluable support system: Tina, Audrey, Dennis, Tommy, and Francine.

ABSTRACT

Northern Minnesota's iron mines are the starting point for the majority of the steel that gets produced in the United States. Their taconite processing plants use heat in furnaces to oxidize and indurate iron in the final stage of making a taconite pellet. Facilities can increase efficiencies when refractory service life is maintained. Efficiencies gained include: less fuel used, better quality control, better furnace control, and less mechanical component maintenance. Furnace refractory linings fail when the cracks that develop in them are uncontrolled or too large. These failures allow heat and gases retained by the lining to reach structural or mechanical components. Furnace control and efficiencies are also compromised when heat and gases are allowed to short circuit or escape the system.

These failures are primarily the result of thermal of shock and expansion. It is common place to add stainless steel needle reinforcement to a monolithic refractory in an effort to counteract these effects. This study used several standard ASTM testing procedures to test 65% alumina mullite based refractory samples with 304 and 406 grade stainless steel needles. Mechanical property data gathered was used to analyze performance. The study found that adding reinforcement does not increase initial Compression and Cold Modulus of Ruptures strengths, however, after prolonged heat and thermal shock exposure, needles help maintain integrity and mechanical properties of samples. The study also found that corrosion due to oxidation was a major contributing factor to the way needles performed; and concluded that a concentration of 3% 406 "Alfa 1" stainless steel reinforcing needles added to the working lining of a taconite furnace is recommended.

Table of Contents

LIST OF TABLES

LIST OF FIGURES

CHAPTER 1: INTRODUCTION, MOTIVATION, AND BACKGROUND

1.1 History of the Iron Range

Early natives and pioneers came to Northern Minnesota to harvest natural resources. In the beginning, it was in search of animals and animal furs. Later on, it would be timber. And in the 1850s, explorers would come for what was underneath the top soil. At first, they walked right over the raw iron ore in search of gold, but, with industrialization and modern steel-making processes, the iron underneath the ground would spark 160 years of economic development and change to the landscape [1].

After the easy-to-mine raw ore was gone the much harder taconite rock was left. The reserves of taconite on the Mesabi Iron Range were staggering and estimated to be able to last over 100 years. But taconite is not pure iron; it is a hard rock with iron particles in it. There was a need to develop a process to extract the iron units and have a way of feeding the existing steel making blast furnaces, if the Mesabi Iron Range were to survive.

Figure 1: Sherman Open Pit Mine 1960

1.2 History of Taconite Processing

Taconite processing reached economic viability in the 1950s and it involved crushing, grinding, separating, filtering, balling (agglomerating), oxidizing, and indurating. The end product is a concentrated iron ore pellet of 3/8 inch diameter that can be easily conveyed and shipped to a blast furnace to make steel, thus replacing the demand for the natural ore that was running out.

Refractory is used to line the furnaces where taconite pellets are oxidized and indurated. It is the construction material that contains heat inside the furnace. Heat and oxygen need to be added to convert the magnetite to hematite while the pellet is hardened for transportation.

Refractories are a category of technical ceramics that are blended mixes of crystalline oxides [2] and are products that have the ability to contain high heat. They must be durable to resist wear and corrosion, and also must be able to insulate. Refractory's role in a taconite furnace is to hold the heat in and protect the structure of the furnace. Since taconite furnaces are a continuous firing process and not a batch process, the furnaces must conveyor the ore at a certain rate through the furnace based on production rates and temperature.

Figure 2: Furnace No. 1 Northshore Mining - Silver Bay, MN - 1955

1.3 Induration of Taconite: Process and Purpose

There are two main styles of taconite-processing furnaces in the world today, and both styles are still operating on Minnesota's Iron Range today. Both types of these furnaces were developed in the 1950s and 1960s, and the basic design has not changed much today. As a matter of note, the two new furnaces that are being constructed in the United States today are both versions of the original 1950's style, and the world's oldest two furnaces are still active at Northshore Mining in Silver Bay, MN (Furnaces 5 and 6).

The two styles of furnaces are the “straight-grate” design (Figure 3) and a “grate-kiln-cooler” design (Figure 4). Straight grate style refractory components are what will be focused on in this study.

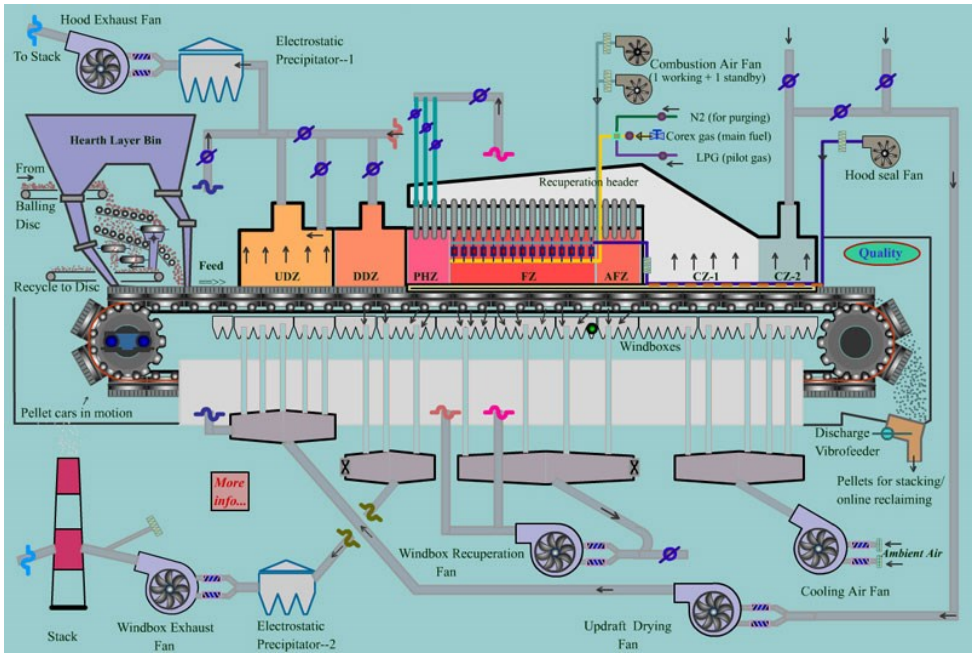

Figure 3: Straight-Grate Furnace [30]

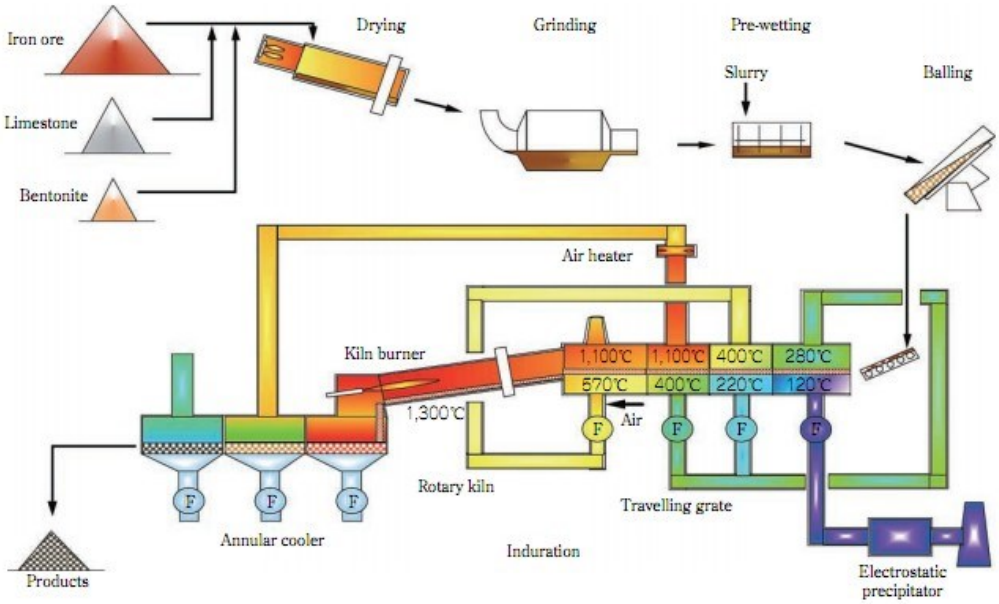

Figure 4: Grate-Kiln-Cooler Furnace [31]

Refractory design in this application has to withstand temperatures in excess of 2300 degrees F while handling abrasion, fuel chemical degradation, thermal shock, along with mechanical loads and expansion issues.

This study will focus on heat retention, thermal shock, mechanical loading, and expansion design issues.

The furnace lining itself consists of several different components put together as one complete liner package. A straight-grate furnace will have monolithic walls and an interlocking brick roof. A monolithic design is a joint free lining that is made up of smaller granular sized particles that are bonded together to form shapes required. It can be gunned, rammed, poured in place, shotcreted, or cast ahead of time in a precast piece.

Figure 5: Furnace No. 6 Northshore Mining - Silver Bay, MN - 1958

Figure 6: Furnace No. 12 Northshore Mining - Silver Bay, MN - 2013

1.4 Refractory Management

In mining and processing taconite, refractory is a relatively small cost to the overall price of the final product. In the past, a single manager was responsible for the management of refractory maintenance along with other fulltime duties. Refractories are difficult to manage from the perspective of their work environment, the operating temperatures are high and maintenance access is limited. Usually, access is available only once per year during a scheduled maintenance shut-down. Most managers will not take chances with new products because the risk to production if a failure occurs is too high. Plant engineering does not normally get involved; therefore, all the expertise lies with the manufacturers and contractors. The typical environment is not conducive to implementing improvements and innovation. This study is an attempt to create a case to break away from that model.

1.5 Recent Innovations of Refractory (Precast and Shotcrete)

Starting in the late 1990s, precast refractories in Minnesota's Iron Range taconite furnaces were just coming into use. Shotcreting refractories would soon follow. Areas that had to be formed and poured prior to this were now either being assembled with precast, shotcreted, or both. These procedures offered two main advantages: tighter quality control and ease of installation. Precast pieces can be formed, poured, and cured in a shop environment maximizing your quality. They are also relatively easy and expeditious to install. Both precast and shotcrete far outpace formed-

in-place for speed of installation. Because downtime on a taconite furnace is extremely expensive in lost production, saving time is critical.

Precast refractory pieces typically perform well in areas where geometric constraints and quality are critical to the application. Shotcrete performs well in large coverage areas. Major maintenance downs where refractory tasks controlled critical path where in many cases were cut down by a third. Problems that took a furnace down for unscheduled maintenance due to refractory have decreased in frequency.

Figure 7: Furnace No. 12 Northshore Mining - Silver Bay, MN - 2013

This study will focus on a precast component design. The data and results that are gathered and analyzed in this study are easily transferable to a shotcrete design because the product makeup is so similar, with the major difference being how they are applied.

CHAPTER 2: LITERATURE REVIEW

2.1 Literature Review Overview

A literature review was performed at the beginning of the study and continued throughout the project. It was in an effort to find information and material written about reinforced refractory from books, journal articles, and technical papers. This study was in search of a way to improve and maximize reinforcement performance in a taconite processing furnace. It wanted to see what areas had not been investigated and identify voids in current research. See Table 2 at the end of this chapter for a summary matrix of the literature reviewed. Several different searches were performed online, through the University of Minnesota computer system, and with industrial manufacturers. Because of design complexity and the extreme temperatures that refractories see, it was important to understand standards on how refractories were tested and that our data would be comparable to other products. The review would also give insights to practices and procedures of sampling and testing.

The overall subject of refractory is large; however, the focus of this study was narrowed to reinforced refractory and how it was related to primary failure modes in a straight grate taconite furnace.

2.2 Handbooks and Basic Information

Several of the books found were of a general nature and took a broad look at refractory types, components, and designs. They had a wide broad sweep of all the areas in which refractories are used. They performed well as a valuable benchmark for topics and concepts. They were available to reference into specific subjects when needed. They also made excellent references and were able to bring concepts together for the study. Harbison-Walker (1992) "Modern Refractory Practices" [3] explained basic concepts and properties. These topics included expansion, cold crushing strength, modulus of rupture, work of fracture, modulus of elasticity to name a few. It also explained failure modes such as thermal and mechanical spalling, along with the stresses and strains related to them. The book elaborated on stress- stain relationships and confining refractory during thermal cycles. Permanent and reversible expansion was explained as well. These were valuable in calculating stresses [3].

Charles A. Schacht authored two books of reference on refractories. One was a design guide entitled "Refractory Linings" in Chapter 16, "Tensile Fracture" [4]; he goes over rapid heat up and cool down cycles that deteriorate lining and states: He states: "Thermal stress fracture is recognized as a principal wear mechanism…" He also goes on to explain that nonlinear temperature gradients create cracks during rapid heat up and cool down cycles, thus explaining

thermal stress and shock degradation [4]. Schacht's information was valuable in foreshadowing one of our main issues in our study.

Schacht also describes Modulus of Rupture three point bending test, crack initiation, and Stress Controlled vs. Strain Controlled loads along with Work of Fracture Test and crack propagation. In his handbook "Refractories Handbook" Schacht talks about (Chapter 16) Testing of Refractory Materials and (Chapter 17) Refractory Lining Design and Installation along with other concepts reiterated by other texts [5].

All of this was important to understand refractory behaviors under their anticipated loads and give a better overall understanding of the project.

The "Handbook of Industrial Refractories Technology" by Carniglia and Barna [2] gives a good history of refractory, covers many of the basic concepts of refractory design, and goes into depth on what refractories are best suited for particular applications. The basic philosophy was: the selection process is largely dependent on what material is being processed and how. The book covered the reduction process of making iron and steel, but did not cover refractory applications in the iron ore oxidation process.

2.3 ASTM Standards

The second group of literature that was of value was the American Society for Testing and Materials or ASTM standards. ASTM standards for testing and definitions are of the utmost importance during this study. They allow benchmarking of different types of materials and products and a consistency of comparison. Several documents defined elements of refractory components and properties while other standards defined testing procedures.

Many ASTM standards were reviewed for this project including: refractory definitions, mixing procedures, testing procedures, and calculations. Many of these will be reviewed in the upcoming chapter on testing and data processing.

2.4 Manufacturers' Information and Data on Reinforcing and Oxidation

Base information on needle corrosion would be fruitful because of the reinforcement selection. The third and last group of literature that was reviewed was specific journal articles and papers on the subject of reinforcement in refractory.

Two needle manufacturers' (Ribbon Technologies and Fibercon) papers, along with some datasheets they supplied, were valuable and interesting in studying and reviewing behaviors of stainless steel reinforcement alloys in refractories.

The subject of corrosion proved to be a major failure mode suspect when talking about using steel reinforcing needle as reinforcement. RibTec's paper on "Hot Corrosion of Steel Fiber in

Refractories" states that the higher the chrome content of the steel alloy, the more resistance to corrosion [6]. This reasoning holds true when the transitioning from 304 to 310 where both the Chrome and Nickel contents are increased (Table 1). In the end, 310 performs better in a hot corrosive environment; however, the chart and our evidence in testing indicate that an alloy with aluminum will perform well in a hot corrosion environment. Fibercon's 406 "Alpha" needles performed better with a little less chrome and some aluminum. This was explained in Fibercon's product bulletin sheet by the formation of Aluminum Oxide (Al_2O_3) vs. Chromium Oxide (Cr_2O_3). This study was interested enough in the material to prescribe it in our study.

Table 1: FIBERCON Standard Alloys (Recreated from [7])

	Alloy			
	304	310	330	406
Chromium, %	18-20	24-26	17-19	12-14
Nickel, %	8-10	19-22	33-37	-
Aluminum, %	-	-	-	3

When a metal alloys corrode, they get brittle and form a scale on their surface; at the same time, thermal cycles force the metal to expand and contract. This growth causes stresses in the refractory because the metal and ceramic have differing thermal expansion rates. These differential expansions crack and break down the refractory and result in a lack of strength and ductility. The reinforcing needles are relied upon to supply strength, ductility, and flexibility. When corrosion occurs, they lose their effectiveness.

In the RibTec articles, however, they state that the corrosion tests were done to exposed needles and not needles embedded in refractory. This study will gather data from refractory samples embedded with needles. This embedment or protection, may be advantageous, but was never explored. The speculation is that the refractory encasing the needles slows the oxidation because it is less exposed to the air, direct heat, and flame.

Figure 8: Furnace No. 5 Northshore Mining - Silver Bay, MN – 2013; In-service sample extraction

Sulfur and other corrosion were talked about, but, because of the use of natural gas in the furnaces, it is not really an issue in this furnace design at hand.

2.5 Design of Fiber Reinforced Composite

Monolithic composite refractory materials are inherently strong in compression and can handle high stress controlled loads. However, as heat is added to a furnace, thermal expansion occurs, inducing additional strain controlled loading on refractory shapes. Strains cause movements and flexure in the material. It is important for that material to be as ductile as possible while retaining its strength. Ductility and resistance to bending stresses are key indications on how well these materials can handle strain-controlled loads in a furnace application. Fiber reinforcement, in particular, stainless steel needles are commonly added to refractories to add ductility and flexibility in an effort to counter act crack formation.

In addition, fibers help control cracking due to thermal and bond phase change (from hydraulic to ceramic) shrinkage.

2.6 Other Published Literature

A number of other articles addressed reinforced refractory. They helped in the thought process of this study; however, they were less relevant than the others. This study was to be more about the reinforcement in the refractory and less about how they interact with each other in the refractory, in other words: we were not looking at bonding, development, or geometric design. The study assumed that this was not going to be a variable and bonding would be complete.

The journal article "Pullout of Steel Fibres from a Refractory Castable Experiment and Modeling" talked about how temperature, geometry, and the angle of inclination had an influence on effective pullout strength [8]. The length and angle of embedment and how they affected bonding strength were looked at. Angle-of-pull, along with friction were influences on what

introduced spalling. Inclination of the fiber is interesting and relevant, but not as controllable in our project. It was assumed that the mix would be homogenous because of the mixing procedure followed. Our study assumed that the crimped needles would be fully bonded in the refractory material.

In another article titled "Evaluation of Dispersiblity of Stainless Fiber in Reinforced Cartable Refractories" a use of consistent mixing and vibrating was used to ensure proper dispersement. [9] ASTM C 862 "Standard Practice for Preparing Refractory Concrete Specimens by Casting" prescribes ways of mixing refractory in an effort to get a consistency in a mix as well [10]. This ASTM test was followed in our study and through reinforcement dispersement was assumed.

"A Study of Reinforced Refractory Concrete" [11] tested reinforced refractory with metal reinforcements; the variable was different steel alloy fibers sized around 25-30mm at 0.6-0.8mm diameter at 2% by weight which is a similar situation in our study. They cured the samples to 932 °F and ultrasound while raised to 1400 °C (2552 °F) was used to determine Modulus of Elasticity [E=f(t)]. Cold Compressive Strength (CCS), Cold Ultimate Bending, and Density were the only physical tests done; it was not explained how these tests were performed. The study concluded that Fe-Cr-Ni had the greatest reduction effect on Modulus of Elasticity (E)

"Strength of Reinforced Refractory Materials" [12] an older study from 1976 examines reinforcement in an effort to use refractory in a structural application. "Refractory oxide single crystals" are used as reinforcement. They are a "laminar crystals of corundum" (a-Al_2O_3) and titanium oxide.

The size of crystals was 0.2-0.5 mm at 20-25 μ diameter which is much smaller and of different shape than the reinforcement in this study. Testing measured a bar under a bending load and measured tensile and compressive stress and strain in the bar under load which was essentially a modulus of rupture test.

Their study concluded that it was nonlinear under load and single breaking force information is insufficient and not as valuable as deformation under load with refractory as with most heterogeneous material. And strength and deformability decreases when reinforced with crystals are used. This was not a desirable outcome.

The last article reviewed was the "Use of Carbon Fibers in Refractory Materials" [13] In their study they used carbon fibers that were 15mm at 0.3mm diameter (which is equivalent size to this study), but different material to this study. They mentioned that the larger the fibers, the better the results, but did not explain why. Reinforcing to maintain integrity after hairline cracks was the goal and a recurring theme in these studies. The study claimed an increase in fracture toughness and not necessarily strength. Ultimate compressive breaking strength test was

performed tests were the only test performed. Graphite fibers maintain better after heat vs. polypropylene. The study recommended in-service testing, but did not explain or recommend temperatures. The integrity statement and conclusion was believable, but no data to back up results. The study was not necessarily relevant because of the temperature limitations of the carbon fiber.

2.7 Summary of Published Literature

A matrix was generated (Table 2) to summarize the information gathered by the literature review and to help support a direction for this study. This study justified looking into reinforcing refractory with stainless steel needles embedded in a hard face refractory material at taconite furnace processing conditions.

Table 2: Research Decision Matrix

Material	Was information found on this material during the literature review?	Was it tested in refractory (in taconite furnace conditions)?	Was it tested in similar temperature condition to a taconite furnace?	Is it reasonable to assume that this material could meet the following performance parameters for a taconite furnace?				
				Furnace Temp	Corrosion	Expansion	Sizing	Shape
Reinforcement Bar	n	-	-	y	y	n	n	y
Carbon Fibers	y	y/n	n	n	y	y	y	y
Crystals	y	y	y	y	y	y	n	n
Metal Needles of different physical types and sizes	y	y	y	y	y	y	y	y
Metal Needles of different chemistries(304, 310, 406)	y	n	y	y	y	y	y	y

The following are main themes found in the literature and how they were used in this study:

• Handbooks and basic reference information revealed that thermal shocking was a major failure mode in refractories; this study confirmed that this was a major problem in the design case at hand and the study was an effort to resist this.

• ASTM documents were an important resource to not only understand standard procedures performed, but to also understand reasoning behind these procedures.

• Manufacturers' papers, bulletins, and data sheets were valuable sources of information because they gave specific information to needles used in reinforcing refractory applications. These studies not only discussed needle reinforcement's role in preventing breakdown of refractory, but discussed how the needle would fail and breakdown when exposed to thermal loading and what properties and chemistries would be the best to counteract this. This information helped link gathered data to the study's major findings in section 7.2.1.
• Papers were a good source of foundational reading, but many of the variables, materials, and issues were in large un-relatable to the specifics in this study.

CHAPTER 3: DESIGN CONDITIONS AND CONSIDERATIONS OF A TACONITE FURNACE

3.1 General Design Conditions

This study coincided with upcoming relines of the two larger furnaces at Northshore Mining. These furnaces have not had a total refractory overhaul since they were built in the 1960s. They have, however, had maintenance and various wall sections replaced over the years but never a complete reline.

The emphasis of this study and design will be on precast monolithic refractory block referred to as a curb. The curb is positioned at the bottom of the wall, in the firebox of a "Straight Grate" type furnace above the traveling grate. Figure 9 shows cross sectional drawing, while Figure 10 shows a closer view of the original gap tolerances. Figure 11 shows a picture of the main furnace chamber during construction.

The curbs and walls of this furnace are of a monolithic refractory construction. Monolithic simply refers to smaller components cast into a one piece construction. A typical refractory wall in this type of furnace consists of three main components: insulation, hard-face (or working lining) and the anchoring system.

Monolithic walls can be cast-in-place, pneumatically gunned in place, shotcreted, or precast. Again, the focus of this study will be a hard-face working lining in a precast refractory piece.

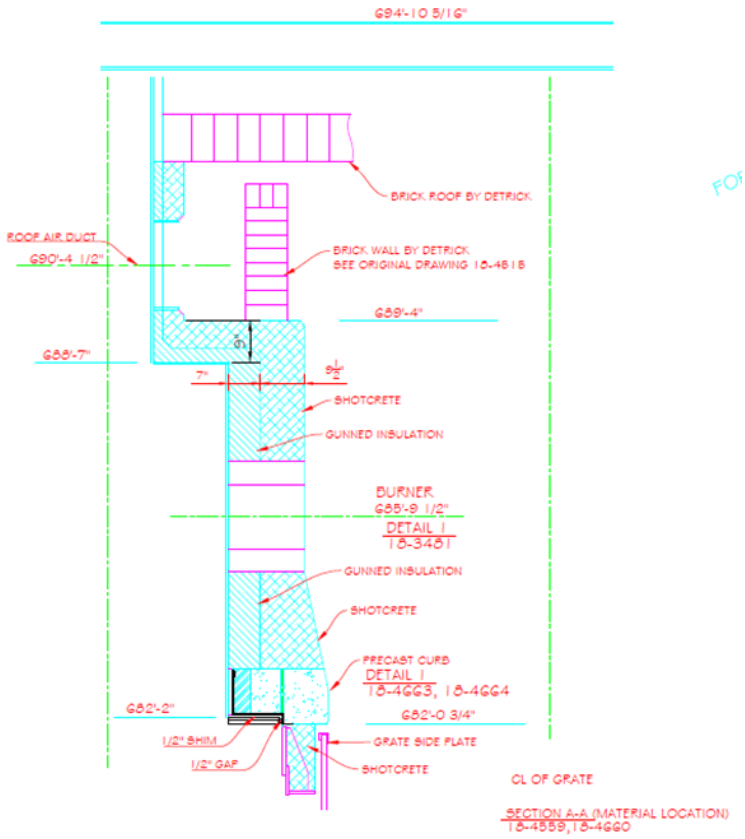

Figure 9: Drawing Cross Section of Original Design of Refractory Lining – Furnace No. 12

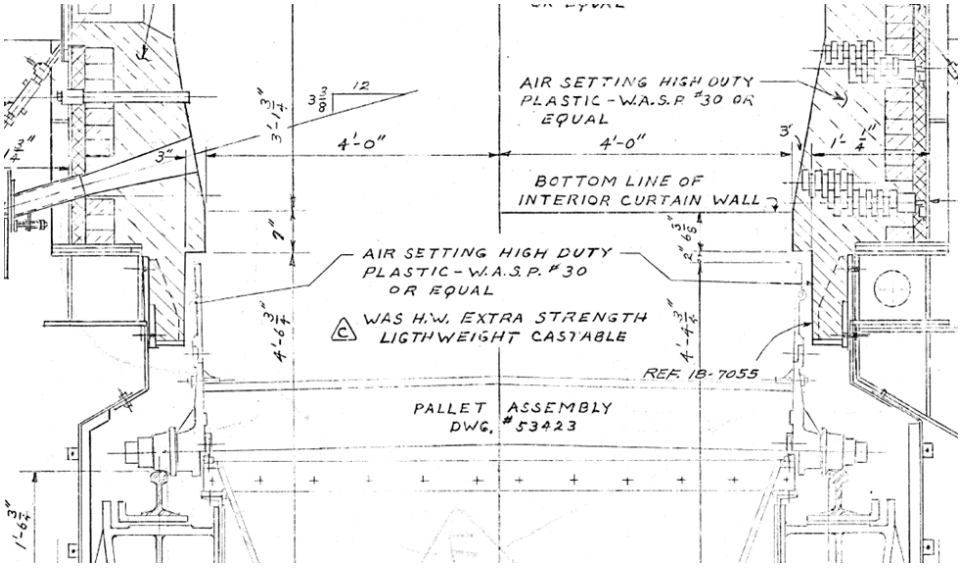

Figure 10: Close up of Drawing Cross Section of Original Design of Refractory Lining – Furnace No. 12

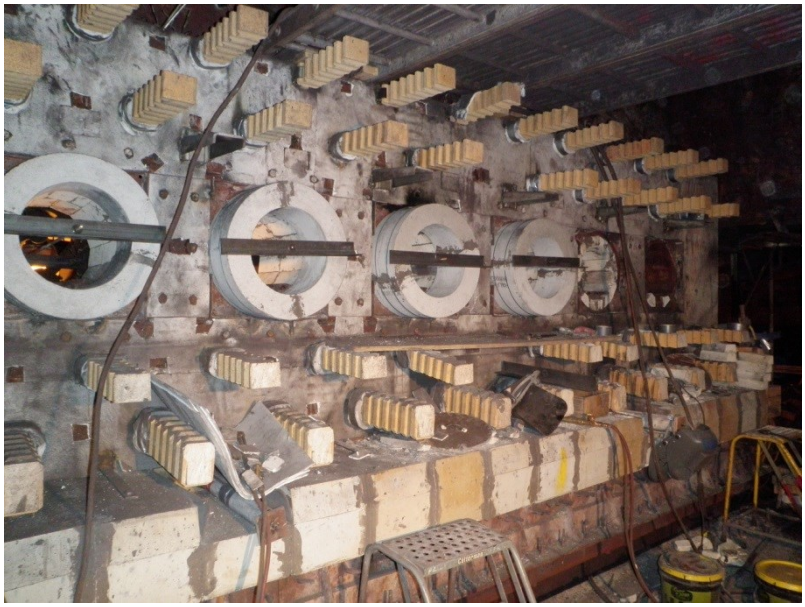

Figure 11: Furnace No. 12 Northshore Mining - Silver Bay, MN - 2013

As mentioned, the precast curbs (shown at the bottom of the wall in Figure 11) need careful consideration when it comes to their geometric profile. It is the area at the bottom of the wall where the stationary refractory wall meets the moving pallet cars filled with taconite pellets. The profile has to match the shape of the furnace's stationary wall on top and has to meet the clearance specifications of the traveling grate beneath it. This bottom clearance of two inches is a critical "seal" for the furnace. The curb of the wall is crucial for several reasons: operational efficiency, process control, and maintenance. In the past, sections have been "gunned" in or cast-in-place creating a curb that would hold up with limited integrity.

When that seal area is compromised, heat can penetrate through and damage the mechanical grate car components and structural steel. Heat loss increases inefficiencies on the furnace and makes it harder to control the furnace for quality reasons. This is where the design was focused. The design needed to be of a high quality material that could hold up to thermal shock and mechanical loads from the wall above. Expansion needed to be considered and the piece needed to be small enough so manpower could set them into place.

Meeting and maintaining those clearances is the most critical part of the design. With simple geometry clearance specifications could be met (shown in Figure 12), but maintaining the integrity of the shape during service was the difficulty in the design challenge. A precast piece design was selected instead of a cast-in-place or shotcrete because quality control measures could easily be monitored. In a quality controlled shop environment properties such as the geometry, the way the material is mixed, and the way it is fired could be monitored and documented. Figure 13 shows a 3D rendering of this curb piece.

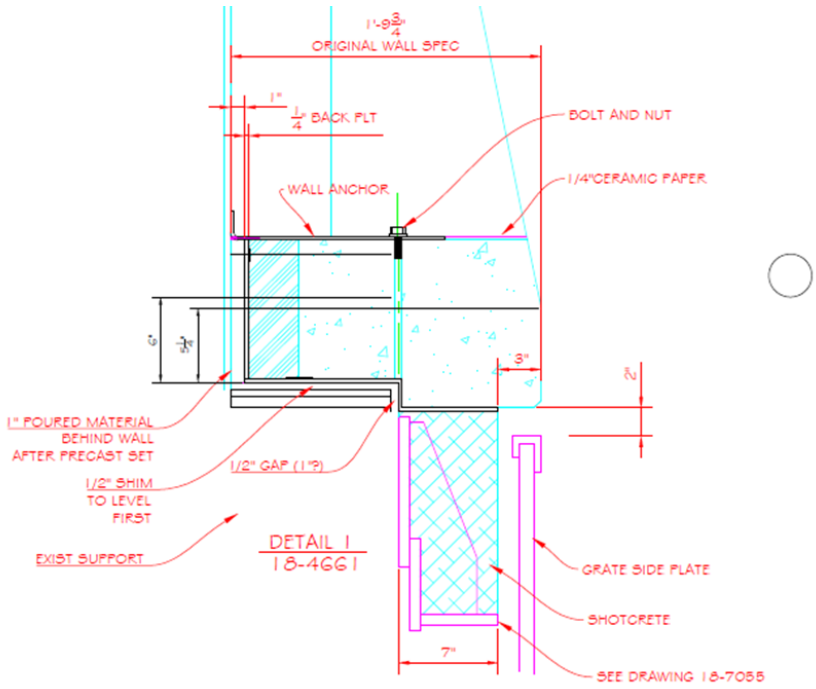

Figure 12: CAD Drawing Cross Section of Newly Designed Refractory Lining – Furnace No. 12

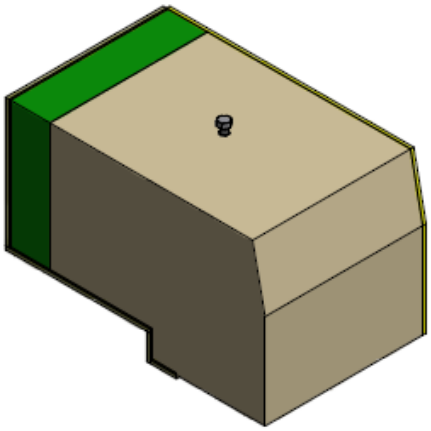

Figure 13: 3D Rendering of Newly Designed Precast Curb – Furnace No. 12

Taconite furnaces run upwards of 2000 degrees Fahrenheit in their hot zone. Typically, the fireboxes hottest spot is 2300 °F. This study will be focusing on the hot face material and as seen in by this snapshot in Figure 14 from thermo couples of a running furnace the temperature ranges from 1536 °F to 2349 °F. A temperature profile was created in Vesuvius's heat flow calculation software to run the thermal calculations and obtain a temperature profile within the precast shape (Figure 15). The Thermal Conductivity (K) values given in the products material data sheets were used to calculate the profile.

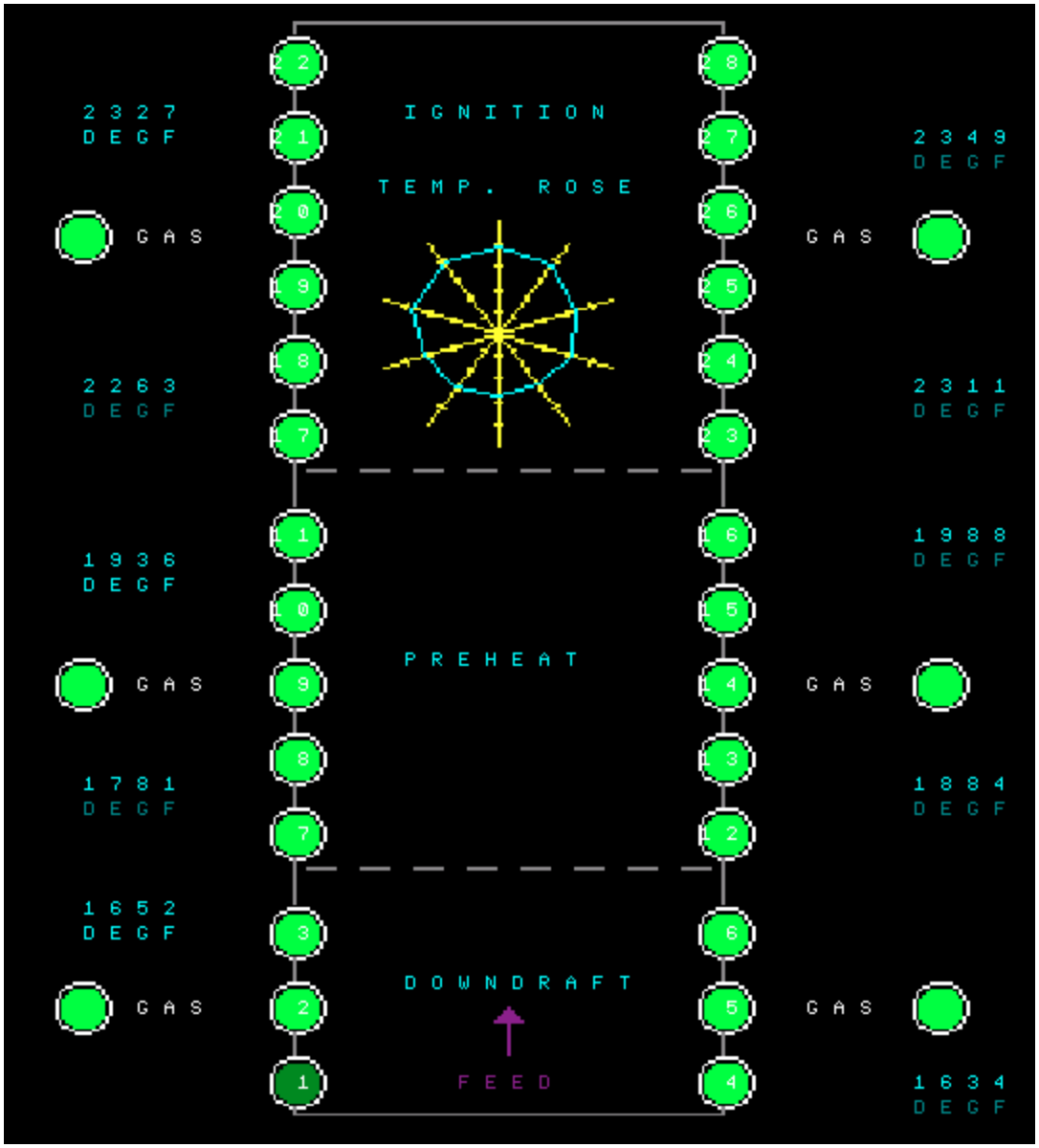

Figure 14: Snapshot of Process Control Screen on Taconite Furnace Showing Operating Temperatures

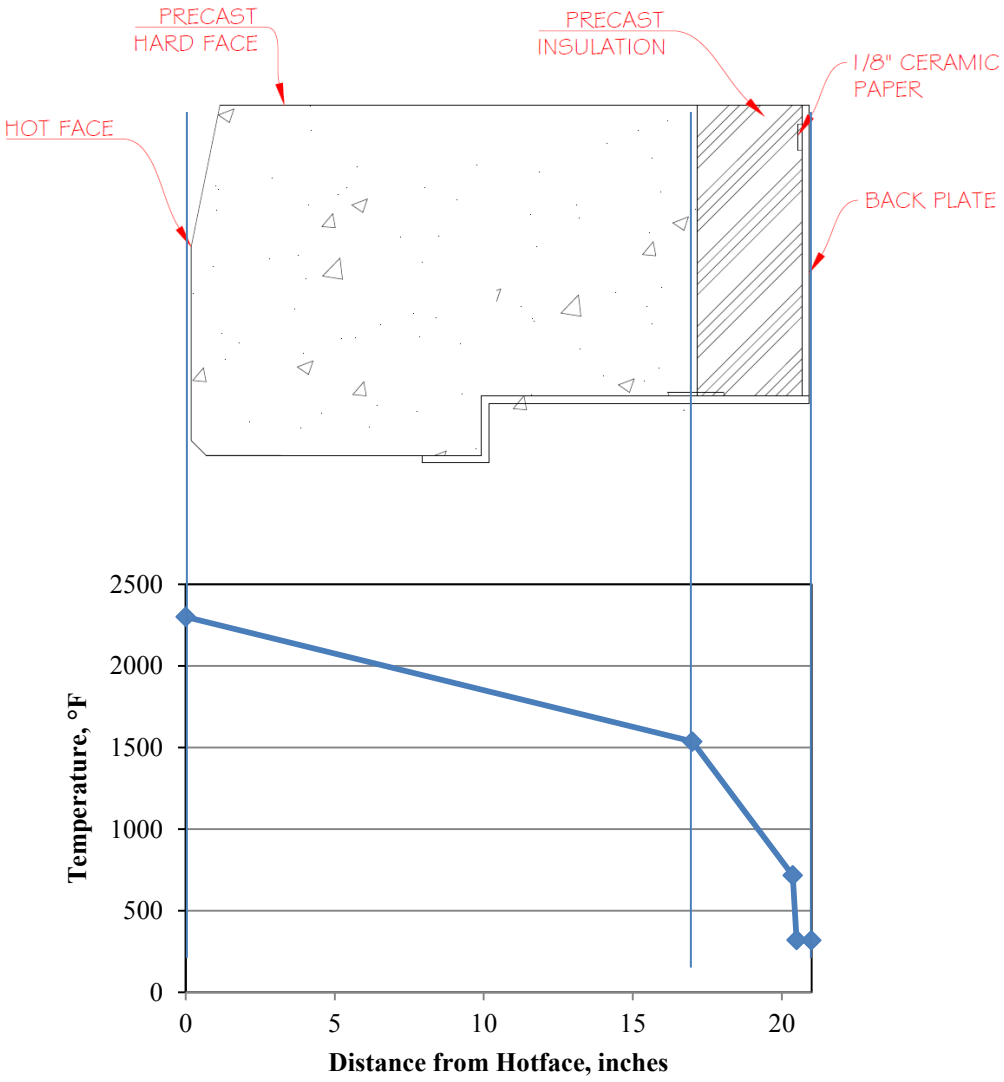

Figure 15: Calculated Temperature Profile of Curb Cross Section

3.2 Loading Conditions

Like most industrial processing facility components that come close, or touch processed material, it is subject to multiple mechanical, structural, thermal, abrasion, and chemical loads.

3.2.1 Stress Controlled Loads

Because this curb block is in the bottom of the wall, it experiences mechanical loading due to the weight of the refractory wall on top of it. It will experience compression and a small amount of

bending. Based on 163 lbs. per cubic foot and a 10 feet high wall, compressive forces only reach about 11 psi. This magnitude of loading is minimal compared to capabilities of up to 20,000 psi for this type of material. Similarly, bending forces could be 50 psi for that same 10 foot high wall, while material capacity for that same material can handle upwards of 4000 psi.

3.2.2 Thermal Shock and Thermal Cycling Loads

Although taconite furnaces are a 24 hour, 7 day a week operation, they periodically go down for operating upset conditions and planned maintenance outages. The furnace is also an environment of inconsistent temperature profiles and intermittent direct flame impingement. These conditions create thermal shock loads on the refractory. Thermal shock loads causes differential expansion gradients along with cyclical expansion and contraction.

3.2.3 Strain Controlled Loads

In addition to the thermal shock and cycling, material like refractory expands as it heats up and contracts when it cools down. The refractory is confined by the exterior structure of the furnace. Because of this, restrained and confined refractory will experience stresses if not allowed to expand. This loading can be extremely high and is typically engineered out with expansion joints; however, because of imperfections, non-uniformity, and imperfect installations this type of loading can still exist. To properly design for expansion, two fundamental characteristics must be understood. The first is a permanent linear expansion and the second is a reversible expansion. After refractory is poured and set, it changes phase when heat is added in the curing process. The material changes from a hydraulic phase to a ceramic phase. This phase change it is permanent. When that piece cools down for the first time it generally shrinks compared to its original size. This is called “permanent linear expansion” (Figure 16). Every heat cycle after that is a consistent reversible linear-elastic expansion (Figure 17).

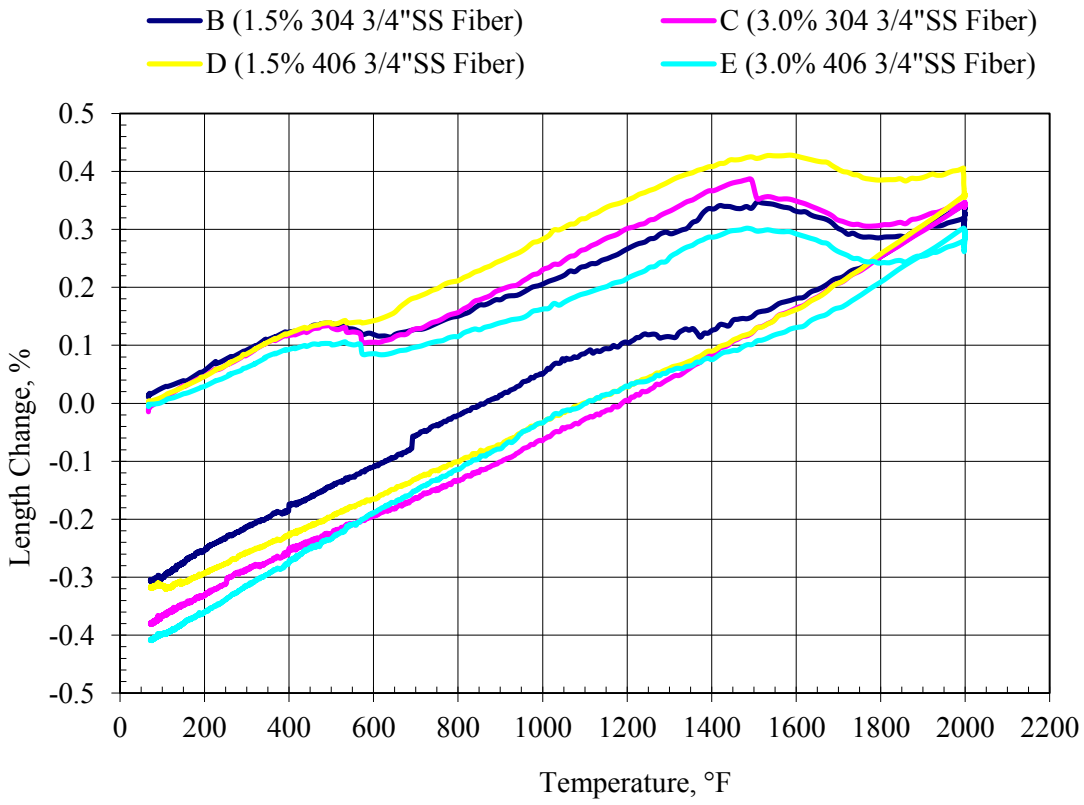

Figure 16: Thermal Dilation; First Run, Permanent Linear Expansion

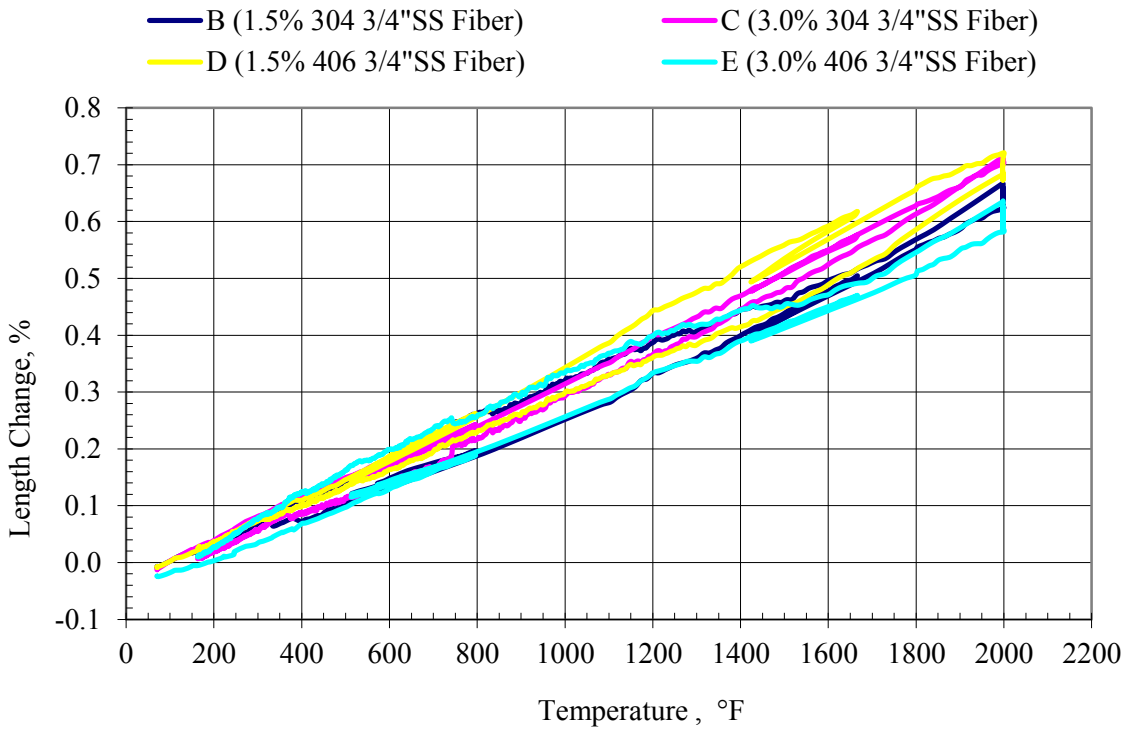

Figure 17: Thermal Dilation; Second Run, Reversible Expansion

3.3 Other Design Considerations

A design consideration in any refractory system should be corrosion of the refractory due to the impurities of the fuels. In this case, because natural gas is the primary fuel and the corrosion failure mode is not seen in this type of furnace, it was not explored in this study.

There is no evidence that airborne dust particles contribute to any significant abrasion of the refractory. In addition, processed materials (iron ore) rarely touch the refractory in this type of furnace. Also, there is no evidence of this type of failure mode in this type of furnace. Therefore, abrasion was not considered.

3.4 Recent History of Relines on Furnaces No. 5 and No. 6

Northshore Mining's smaller furnaces were relined in 2011 and 2012. Components were carefully considered and decisions were made based on past performance of tried products (Figure 18).

Although the refractory materials that used were of high quality, products had come from different suppliers and they were not engineered together. Overall, they performed well with the exception of a few expansion issues. There was not enough allowance in the roof air brick causing it to start to buckle when it heated up (Figure 19). In the precast curb, expansion allowance for all the curbs was taken up at the ends of the walls and not placed in between each individual piece. The curbs could not float together and caused a strain controlled load which allowed the front face of the curb to spall off and deteriorated the seal (Figure 19).

Lessons learned on these two furnaces proved valuable for design and decision making of the two large furnaces (Furnaces 11 and 12).

However, going forward, the impact risk to production would be higher because the throughput rates on those large furnaces are twice that of their smaller counter parts (Furnaces 5 and 6).

Figure 18: Furnace No. 6 Northshore Mining - Silver Bay, MN - 2011

Figure 19: Furnace No. 6 Northshore Mining - Silver Bay, MN - 2012

3.5 Furnace 12 Reline Design and Construction

This study, engineering, and a bid process to reline Furnace 12 commenced at the same time. So decisions had to be made before the complete results were in. However, there was enough anecdotal evidence to support the decision to specify 3% of 406 needles in the precast and 1.5% of 406 needles in shotcrete. Engineering calculations would support conservative expansion joints of ¼ inch between every curb and expansion; ¾ of an inch every 10ft of shotcreted wall.

The actual construction process of the Furnace 12 reline was done in June of 2013 and lasted 14 days. It involved demolition, preparation, installation, and a dry-out/heat up schedule (Figures 16 and 17). The project was invaluable in relating research with design and application. Figure 20 shows demolition by remote control robots and installation of lining components inside Furnace 12 while Figure 21 shows the finished product just before heat up.

Furnace 11, which is scheduled to be done at a later date, will have the full benefit of this study along with seeing how well Furnace 12 has performed.

Figure 20: Furnace 12 Remote Demolition and Relining

Figure 21: Furnace No. 12 Northshore Mining - Silver Bay, MN – 2012 - Furnace Reline

CHAPTER 4: TESTING PLAN, TESTING IMPLEMENTATION, DATA GATHERING, AND DATA PROCESSING

4.1 Testing Prescription Development

After all the design loading conditions on the refractory were considered, the next step was to focus on what materials, variables, and conditions would be most advantageous to test against each other in an effort to maximize value in this study.

The purpose of the study was to find what type of reinforcement addition would be most beneficial to add to the refractory design of a precast hardface curb in a straight grate furnace. Northshore Mining's furnaces and other taconite furnaces around the Range use a variety of 60 to 70% alumina hardface products. One product manufactured by Allied Mineral Products is a product called Tuffcrete 65M. It is a low cement mullite based monolithic that can be cast or shotcreted [15]. Mullite is a form of alumina [16] that is either found naturally or blended out of other alumina sources. This material has been used in many Minnesota Iron Range taconite processing plants in both precast and shotcrete applications. As stated before, the monolithic refractory material itself is not the variable in this study. It is, however, the backbone of lining system and a high quality, time tested product was desired for the base and control.

4.2 Needle Reinforcement Considerations

Next, consideration was given to what type of reinforcement would be added to the mixture. The reinforcement material should help resist cracks and crack propagation due to thermal cycling and resist other loading conditions already established in Chapter 3.

Stainless steel needles are a common and readily available reinforcement for high temperature, high alumina refractories. By nature of the product, they have the following variables associated with them: type or grade of stainless steel to be used, size, length, profile, and the concentration or percent in the mix. This study was not focusing on bonding strength, so it was decided to focus on two variables: grade of stainless and concentration in the mix.

It made sense for the study to test two popular needles already in use, the first being a traditional 304 stainless steel and the second being a 406 "Alpha 1" stainless steel. The 304 needle is a chrome-nickel stainless alloy. The second, the 406, Alfa needle is a chrome-aluminum alloy. They both resist corrosion by absorbing oxygen and creating and protective layer of oxidation. The 304 forms Cr_2O_3 and the 406 forms Al_2O_3. The 406 is considered to produce a better protective layer by the manufacturer [17].

304 has been historically been the choice in taconite furnaces for economic reasons. Table 3 shows the chemistry and physical properties of these needles.

Table 3: Material Data Sheets for Reinforcing Needles, 304 and 406 (Reproduced from [18], [19])

MATERIAL DATA SHEET—304 SLIT-SHEET FIBERS

REVISION DATE: 15/03/07
PRODUCT TYPE: Stainless Steel Fibers
MANUFACTURING PROCESS: Slit-Sheet Method
SHAPE: Straight & Deformed

TYPICAL CHEMISTRY & PHYSICAL PROPERTIES:
(Metallurgy is typical, conforming to AISI standards)

% kg	C	Mn	Si	P	S	Cr	Ni	Fe + trace elements
max	0.08	2.0	0.75	0.045	0.03	18—20	8—10,5	balance

Melting Range °F: 2550—2650

Critical Oxidation °F
Cyclic: 1500
Continuous: 1650

Specific Gravity g/cm3: 7.87
Tensile strength MPa (min) @ 20 °C: 515—640 (min) @ 20 °C

TYPICAL DIMENSIONS:

Length	1/2"	3/4"	1"	1 3/8"
Typical Equiv. Ø	0.5	0.50	0.5	0.84
Typical Aspect Ratio (ℓ/Ø)	24	38	50	42
Typical Fiber Count/kg	48,500	32,000	24,000	6,600

These Fibers are manufactured to the requirements of ASTM A820/A820M-06 Type III which specifies the following dimensional tolerances:
Length and **Equivalent diameter** +/- 10%
Aspect Ratio +/- 15%

MATERIAL DATA SHEET—406 ALFA-1 SLIT-SHEET FIBERS

REVISION DATE: 15/03/07
PRODUCT TYPE: Stainless Steel Fibers
MANUFACTURING PROCESS: Slit-Sheet Method
SHAPE: Straight & Deformed

TYPICAL CHEMISTRY & PHYSICAL PROPERTIES:
(Metallurgy is typical, conforming to AISI standards)

% kg	C	Mn	Si	Ti	Cr	Al	Fe
max	0.025	0.035	0.30	0.40	13	3.0	balance

Melting Range °F: 2650—2760

Critical Oxidation °F
Cyclic: 1800—1900
Continuous: 2050—2275

Specific Gravity g/cm3: 7.87
Tensile strength MPa (min) @ 20 °C: 524 (min) @ 20 °C

TYPICAL DIMENSIONS:

Length	1/2"	3/4"	1"	1 3/8"
Typical Equiv. Ø	0.5	0.50	0.5	0.84
Typical Aspect Ratio (ℓ/Ø)	24	38	50	42
Typical Fiber Count/kg	48,500	32,000	24,000	6,600

These Fibers are manufactured to the requirements of ASTM A820/A820M-06 Type III which specifies the following dimensional tolerances:
Length and **Equivalent diameter** +/- 10%
Aspect Ratio +/- 15%

4.2.1 Needle Geometry

All needles that were used in this study had the same geometry. Needles were ¾ inch long, 0.02 inches in effective diameter. They were manufactured by a company called Fibercon International. Needles are of a crimped or ribbed style shown in Figure 22. They are made using a "Slit-Sheet" method. This involves shearing off the needles from a crimped coil or a crimped strip. The deformations help obtain full development with the refractory concrete in the shortest length possible. These types of needles are also a common geometry in additions to refractory because of their ability to bond and develop into a cured refractory and their optimal aspect ratio.

Figure 22: Typical Stainless Steel Needle ¾ inch Long

4.2.2 Needle Concentration

The other design variable pertaining to the needles was the concentration in the mix. One of the goals was to find an effective concentration of needles without changing the basic properties of the monolithic refractory. Previous concentrations that Northshore and other taconite producers have been in the 0 to 3% range. In this study, 0, 1.5%, and 3% of both types of needles would be tried in an effort to understand how mechanical properties are affected.

After the chosen formulation was decided upon, the type and number of tests would have to be looked into. The standard tests for strength were chosen to get a comparison to the tech data sheets and standard five replicate samples prescribed by most ASTM standard tests was also chosen. Amongst the physical strength tests that were done, the study wanted to explore thermal shock and thermal expansion behaviors. Cracking as a result of thermal shock is a common failure mode with refractory. Thermal expansion has caused stresses and failures in furnace walls inside straight-grate furnaces in the past. It was important to fully understand what kind of loading and stress was induced into the system due to the effects of thermal expansion.

During the construction phase of a furnace reline and as the material is placed, dried, and cured in the furnace, it goes through expansion and contraction along with water loss and ceramic curing. It is important to understand the initial green strength (dried) of a material as well as the strength and characteristics at fully cured (fired) in an operating situation.

Green strength is important for consideration during the heat up process. With this study a lower temperature benchmark was important along with a higher benchmark at furnace operating temperatures. Half would be dried to 230 °F and the others were cured to 2000 °F. Five replicate samples of each type would be tested. See Table 4 for final testing prescription.

Table 4: Test Prescription

	Alloy				
		304		**406**	
	% needles				
Sample Notation	**A**	**B**	**C**	**D**	**E**
Types of Tests	0.0%	1.5%	3.0%	1.5%	3.0%
Cold Crushing Strength (ASTM C-133)					
Dried to 230°F	5	5	5	5	5
Fired to 2000°F	5	5	5	5	5
Modulus of Rupture (ASTM C-133)					
Dried to 230°F	5	5	5	5	5
Fired to 2000°F	5	5	5	5	5
Hot Modulus of Rupture @ 2000°F					
Fired to 2000°F **(ASTM C-583)**	5	5	5	5	5
Other Tests (ASTM C-1419,20,914)					
Thermal Dilation Test (ASTM C-832)	1	1	1	1	1
Thermal Shock Test w/ CMOR after (ASTM C-1171)	5	5	5	5	5
Destructive tests done to existing curbs: CCS and CMOR					
Furnace 5 (406 needles) at 3%	two curbs pulled one out of service (service 6 months)				
Furnace 5 (406 needles) at 3%	spare curb that has not seen service				
Furnace 6 (304 needles) at 3%	will not test				

4.3 Testing Facility

Allied Mineral Products was requested to host the testing of the refractory. The materials lab at the University of Minnesota Duluth did not have the facility equipped for this type of testing. As well as being a manufacturer of refractory products, Allied Mineral Products has a full service lab to facilitate all the testing required to ASTM standards.

After the prescription plan was agreed upon, a trip was arranged to Allied Mineral Products in Columbus, OH for the week of March 4th, 2013.

4.4 Testing and Data Processing

4.4.1 Sample preparation

The prescribed mixes were prepared with 6% municipal tap water as to be consistent with manufactures material specifications and then poured into 3 different sizes of molds: one type for Cold Modulus of Rupture (CMOR) test, one type for Hot Modulus of Rupture (HMOR) test, and one type for the Thermal Dilation test.

The "Soap" sized used for the CMOR tests were poured in gang molds shown in Figure 23. Compression and Thermal Shock tests were also performed with pieces originating with these same size samples. Making of these samples closely follows ASTM procedure C862 [21]. Soap-sized brick samples have been the standard for refractory sampling for many years. A standard straight brick has nominal dimensions of 9 inch x 4 ½ inch x 2 ½ inches. A soap size is a half a standard straight brick, which has nominal dimensions of 9 inch x 2 ¼ inch x 2 ½ inches [20].

HMOR tests required a smaller 1 inch x 1 inch x 6 inch sample [22]. These were also made in a similar gang style molds and of the prescribed formulations.

Cylindrical specimens were cast for the thermal dilation test. ASTM procedure C832 calls for 1 ½ inch x 1 ½ inch x 4 ½ inch long rectangular specimen [23]. The cylinder in this study was 2 inch diameter x 5 ¾ inch long. However, this change would not be significant to the test results.

All test samples were either dried to 230 °F or fired to 2000 °F depending on the test prescription matrix. See Figures 24 and 25.

Figure 23: Gang Soap Sample Mold

Figure 24: Soap Samples after Drying and Curing

Figure 25: Thermal Shock and Thermal Dilation Test Samples

4.4.2 Compression Test

Samples for this test were cut from the spent samples from the CMOR tests. Each sample was cut by a diamond blade saw to a nominal 2 inch height; the width and length were measured with calipers and recorded. The samples were loaded one at a time into the hydraulic compression testing machine with bedding material on the top and bottom as shown in Figure 26. A computer recorded the load and compression position over time. This procedure also closely followed ASTM 133 [24].

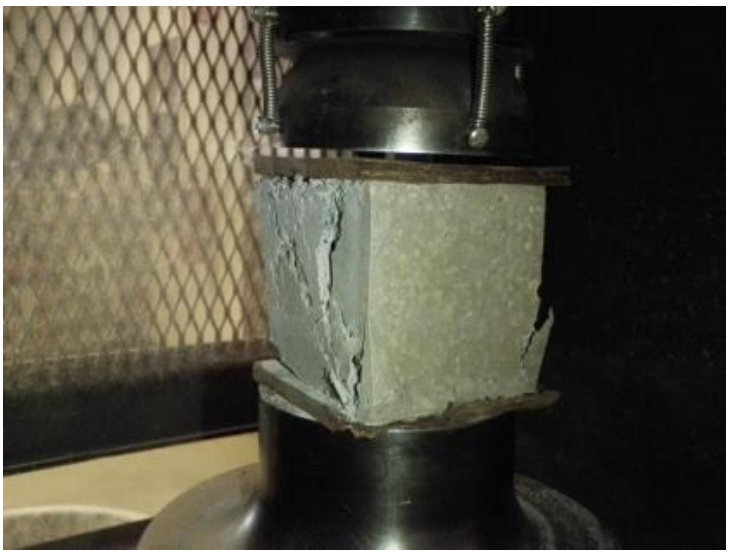

Figure 26: Compression Test

At the start of the test, the operator entered width and thickness of the sample. The compression testing machine fed load, time, and position data into a computer. The computer generated a spreadsheet file containing data points for each position in inches and load in pound force every $1/10^{th}$ of a second (Table 5). Points were generated up to the peak force and beyond up to 20% of the peak load loss, at which point the test stopped automatically. The program also used the width and thickness inputs to calculate a stress in pounds per square inch for each data point. Peak load and cross sectional area were used to calculate the maximum cold crushing strength for all samples.

This data was brought into a master spreadsheet where a stress vs. position curve (stress/strain) was generated (Figure 27). The graph is linear in the middle, which one would expect. There is flatness in the beginning which represents a compression of the bedding. This is prescribed by ASTM 133 and prevents point loading and also protects the equipment. This portion of the curve can be normalized for analysis purposes.

Table 5: Sample of Typical Data Generated from Cold Compressive Test

Counter #	30211		Width	Thickness
	CCS		2.228	2.380
Sample #	A2	Dried to 230F		
	Partner Data Point File			
	Start of Test Wed 06 Mar 2013 10:33:55	y	x	
	Time (min)	Stress (psi)	Position (in)	Load (lbf)
	7.84333	13691.4	0.1658	72600
	7.845	13693.28	0.1659	72610
	7.84667	13697.05	0.1661	72630
	7.84833	13698.94	0.1661	72640
	7.85	13700.83	0.1663	72650
	7.85167	13702.71	0.1665	72660
	7.85333	13702.71	0.1665	72660
	7.855	13704.6	0.1667	72670
	7.85667	13706.48	0.1669	72680
	7.85833	13706.48	0.1672	72680
	7.86	13698.94	0.1674	72640
	7.86167	13566.93	0.1694	71940
	7.86333	12827.67	0.1768	68020
	7.865	11854.56	0.1844	62860
	7.86667	11271.83	0.1924	59770
	7.86833	10551.43	0.2002	55950

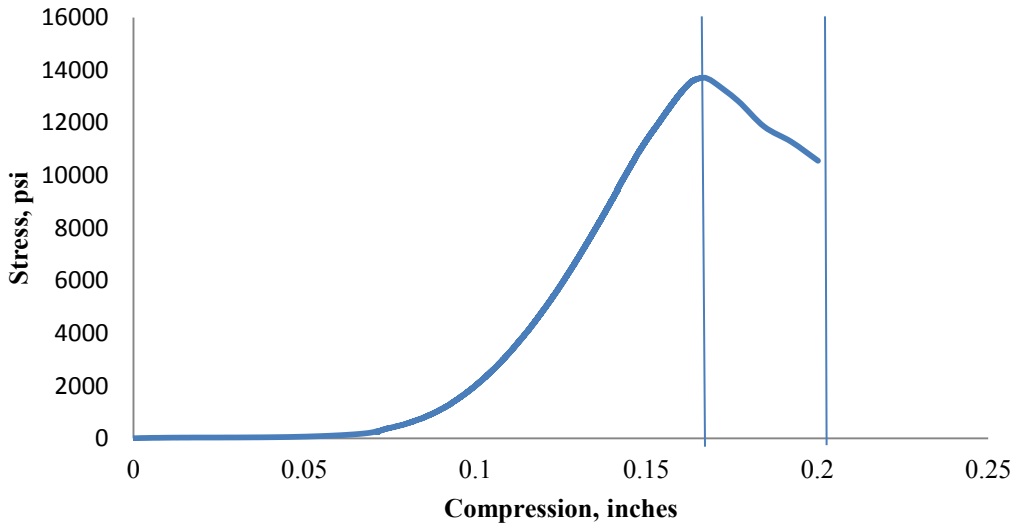

Figure 27: Stress - Deflection from Compression Test

4.4.3 Cold Modulus of Rupture (CMOR) Test

As with the compression testing, each soap-sized sample bar was measured with calipers, weighed, and documented (Figure 28). The sample was then placed into a CMOR machine and a bending test with a 7" span was performed that closely followed ASTM C-133 [24] (Figure 29 and 30).

Figure 28: Samples Being Weighed and Measured

Figure 29: CMOR Machine

Figure 30: CMOR Machine

Figure 31: Extensometer on CMOR machine

At the start of the test, the operator entered the height and thickness of the sample along with the bending span. The CMOR testing machine fed load, time, and position (Figure 31) data into a computer. The change in position would be the deflection of the bar at mid-span and position of the load. The computer then generated a spreadsheet file containing data points for each position in inches and load in pound force every $1/10^{th}$ of a second (Table 6). Points were generated up to the peak force and beyond up to 60% of the peak load loss, at which point the test had stopped automatically.

Table 6: Sample of Typical Data Generated from Cold Modulus of Rupture Test

Counter #	34613		Span	Width	Thickness	S
	CMOR		7	2.2095	2.5030	2.3
Sample #	A1	Dried to 230F				
	Partner Data Point File					y
	Start of Test Mon 04 Mar 2013 09:51:38		y	x		flexural
	Time (min)	Position (in)	Load (lbf)	Position (in)	Work (lbf-in)	Stress (psi)
	0	0.0405	110	0	0.0228	83.4
	0.00167	0.0407	118	0.0002	0	89.5
	0.00333	0.0407	123	0.0002	0	93.3
	0.005	0.0407	125	0.0002	0	94.8
	0.00667	0.0407	126	0.0002	0	95.6
	0.00833	0.0407	125	0.0002	0	94.8
	0.01	0.0407	124	0.0002	0	94.1

4.4.4 Strength

The CMOR data on the spreadsheet was processed in the effort to find out a number of properties of each sample and to find out what the add mixtures did to each sample. With the data off the CMOR machine, the study could find strength, work of fracture, and energy of fracture properties.

Strength or Modulus of Rupture was a basic Strength and Material's equation using the peak load, the span, and the cross sectional geometry. It was simply the peak load that the sample attained. It is equivalent to the peak bending stress experienced in the sample testing.

$$MOR = \frac{3PL}{2bd^2}$$

Where:

MOR = Modulus of rupture, lbf/in^2

P = maximum applied at rupture, lbf

L = span between supports, inches

b = width of specimen, inches

d = depth of specimen, inches [24]

4.4.5 Work of Fracture Initiation

With the data that was generated for these tests a modified Work of Fracture (WOF) could be generated. Work of fracture is the work required to fracture or crack the sample to failure. Throughout the rest of this study, WOF will be calculated up to the point of crack initiation. This initiation would happen at peak load. To calculate this, a load vs. deflection curve would have to

be generated and then the area below that curve could be calculated using integration. This was done by using the trapezoidal rule.

The deflection would have to be calculated by normalizing the position reading from the data. The load and deflection curve was then plotted as seen in Figure 32. Work of Fracture or Fracture toughness is the ability of a material to resist a crack or fracture. A line was fit to the curve; however, it was more accurate to calculate the area under the data points using the trapezoidal rule.

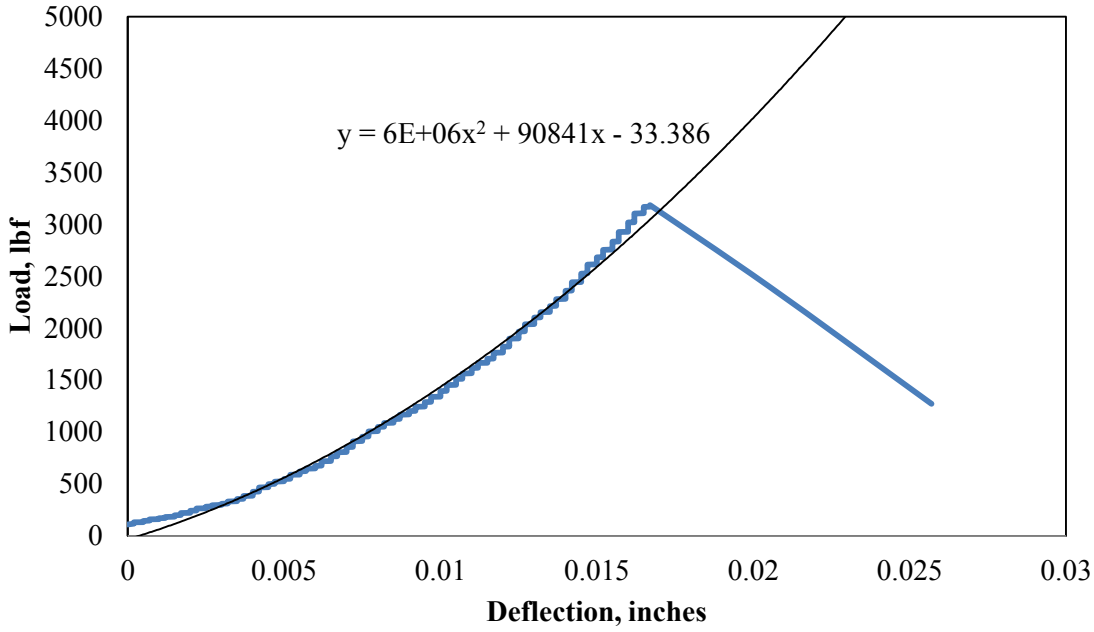

Figure 32: Load – Deflection from Modulus of Rupture (Work of Fracture)

4.4.6 Energy of Fracture Initiation

Energy of Fracture (EOF) was calculated in a very similar way. In this case, Energy of Fracture up to the peak load was calculated. It involved taking the area under the stress strain curve (Figure 33). Neither WOF nor EOF was given in the manufacturer's data sheets, so this data was not comparable to any other. However, it was valuable information to have because it would allow us to see what energy it took to break a sample and start propagating a crack.

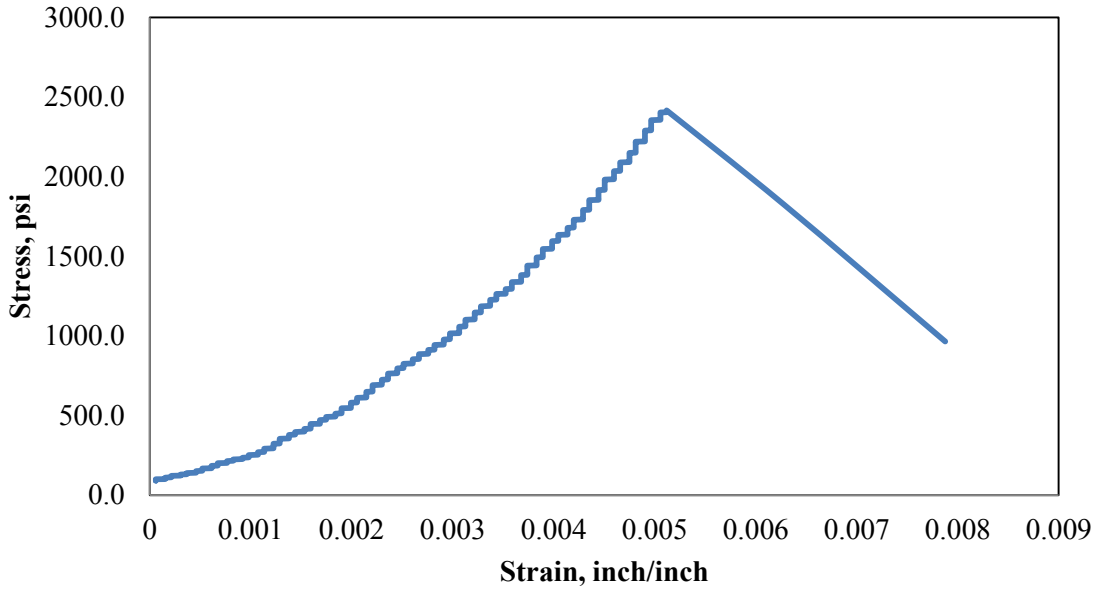

Figure 33: Stress - Strain from Modulus of Rupture (Energy of Fracture)

4.4.7 Hot Modulus of Rupture

Modulus of Rupture at an Elevated Temperature or Hot Modulus of Rupture (HMOR) was performed for pre-fired samples of all five formulations. HMOR data was gathered from more of a manual convention. These tests closely follow ASTM C583. The test was a 1 inch x 1 inch x 6 inch beam bending test. The calculation is the same for HMOR as it is for CMOR. The sample was broken at a 5 inch span while being heated at 2000 °F. The force at mid span was generated by a water column on a lever. Water height at rupture was recorded and then the weight of the water and the distance away could be used to calculate the force (Figure 34 and 35).

Figure 34: Hot Modulus of Rupture Testing Machine

Figure 35: Hot Modulus of Rupture Testing Machine

4.4.8 Thermal Shock

The data that was generated and analyzed for the thermal shock test was the done with the same procedure as the CMOR data that was generated with the full-sized soap bars fired to 2000 °F, however, the samples were cut in half. One side was thermally shocked prior to the CMOR tests while the other side was not.

The thermal shocking test closely follows ASTM C1171 and describes five cycles through the furnace to a temperature of 2200 °F [25]. All cycles involved cooling at room temperature and the heat up in the furnace (Figure 36 and 37). The idea of this test is to see how much cracking and thermal shock breakdown the samples experience. After the cycles, the CMOR test will gauge how well they perform against the control side of the CMOR test. It is no different than the CMOR test previously explained, but with the exception of a bending test on a 4 inch span versus a 7 inch span.

Figure 36: Thermal Shock Testing

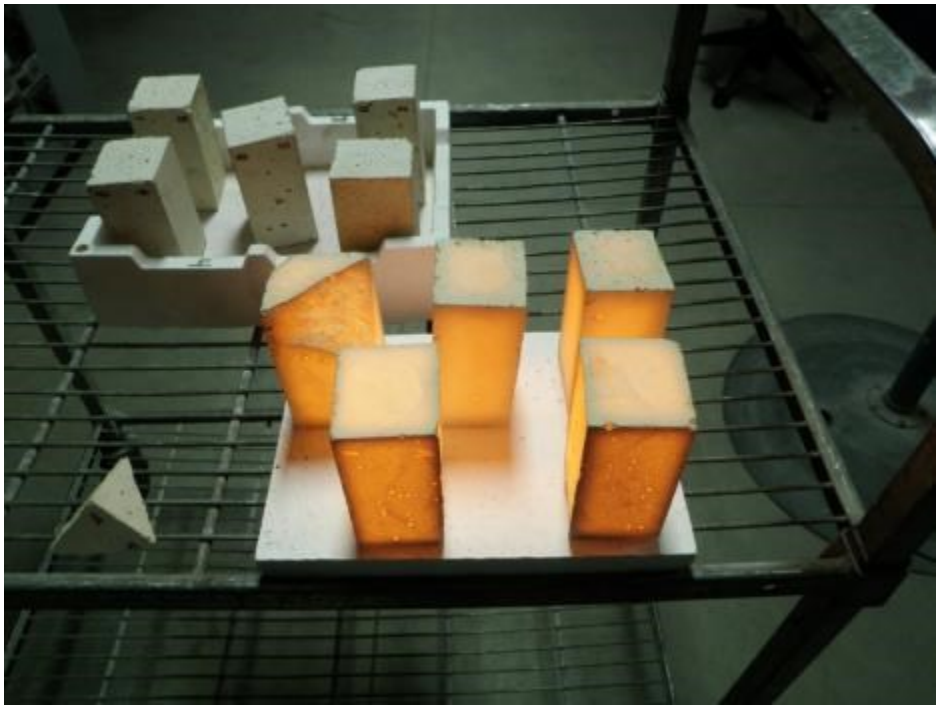

Figure 37: Thermal Shock Testing

4.4.9 Ultrasonic Testing

Sonic velocities were measured from samples that underwent thermal shock and compared to sonic velocity measurements taken from their un-shocked counterparts. Readings were taken in microseconds and then divided by the length of the sample in inches.

$$\nu = \frac{L}{t}$$

Where:

ν = signal velocity, in/s

t = time, μs

L = Length, inches

Young's Modulus (E) could be calculated with the data gathered by using these velocities along with the samples density. The slower the signal the more inclusions, discontinuities, and cracking present in the samples [26]. A slower velocity will produce a lower E value and less elastic sample.

$$E = \rho v^2$$

Where:

E = Young's Modulus of Elasticity, psi

ρ = density, lbs/in^3

v = signal velocity, in/s

4.4.10 Thermal Dilation

Thermal dilation testing would give valuable information on the thermal expansion that one would expect to see in the furnace. The expansion information would allow for a calculation of expansion joints to minimize stain controlled stress in the material. ASTM C832 is the standard test to measure linear expansion during heat loading [23] (Figures 38 and 39).

The sample pieces were cylindrical in shape placed in a furnace with probe attached that measured the linear expansion of the piece over a prescribed heat ramp and time.

Since the refractory goes through a ceramic bonding and phase change process at higher temperature while curing, the coefficient of expansion will change from the initial heat up while green vs. subsequent heat ups. After the initial heat up, a second run was taken to look at this change.

Figure 38: Thermal Dilation Test

Figure 39: Thermal Dilation Test

4.4.11 Other Tests

Tests for porosity and bulk density were also performed on these samples (ASTM C-20 [27] and ASTM C-914 [28]).

4.4.12 In-service samples

The testing plan also strived to gather "in-service" samples of refractory that had been placed in a furnace and have seen duty. Furnace 5 and 6 would give an opportunity to do just that. In gathering information for the Furnace 12 design, it would be beneficial to extract some these in-service samples. They could tell us about actual performances for known samples. During the process of this study Furnace 5 and Furnace 6 were idled for production demand reasons. The study extracted curb samples out of Furnace 5 (Figure 40). The curbs consisted of a 3% 406 needle content (Furnace 6 was 3% 304).

Samples were brought to the UMD Civil Engineering lab and rough cut (Figure 41). The samples were then shipped to Allied Mineral Products in Columbus where they were categorized, labeled, and tested (Figure 42). Compression and CMOR tests were performed with as many sample sizes that could be extracted.

Figure 40: In-service Furnace 6 Curbs, before Extraction

Figure 41: In-service samples after cutting at UMD

Figure 42: In-service Samples before Testing

CHAPTER 5: RESULTS AND ANALYSIS

5.1 Cold Compressive Strength (CCS) Test Data Analysis

Much like concrete, Cold Compressive Strength (CCS) data is important to refractory design because refractories are inherently strong in compression and have been designed for systems that take advantage of this property. Thermal expansion, along with mechanical live and dead loads, put the material into compression.

The results of this study found that compression strength data for dried and fired samples shown in Figures 43 and 44 indicate a similar trend. Both dried and fired samples have stronger unreinforced compression strength properties compared to those with reinforcing. Cross sectional and effective areas of the actual refractory are reduced when needles are added. This will cause actual stresses to be higher in the refractory relative to the same point load because of reduced cross-section. Reduced volume and cross sectional area is only about 1% at a 3% by addition of needles. This effect of this is probably small. However, uniaxial unconfined compression strength relies on circumferential tension to hold it in place. Reinforcing causes discontinuities and disruptions in the uniformity of the refractory and most likely reduces its compressive strength.

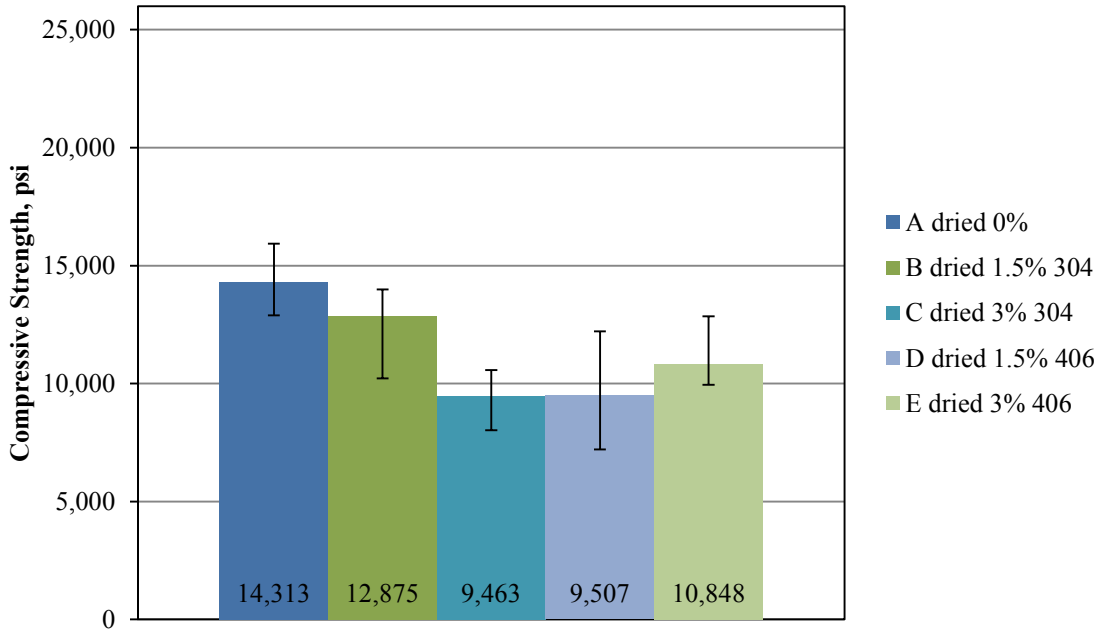

Figure 43: Cold Compressive Strength – Dried Samples

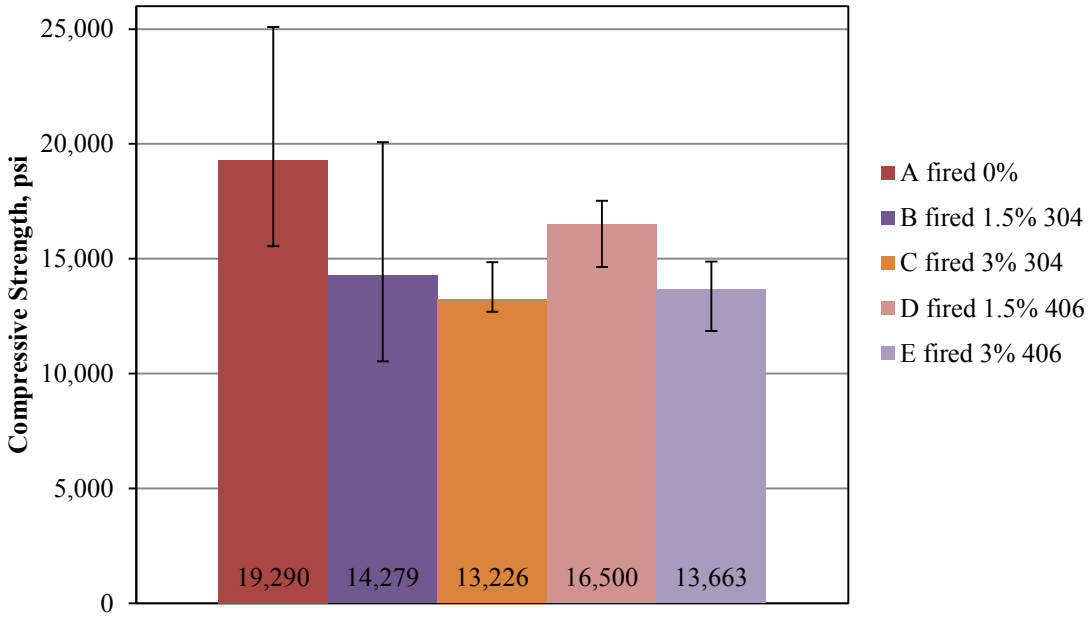

Figure 44: Cold Compressive Strength – Fired Samples

If dried compression data numbers are compared from this study with the data supplied on the manufacturer's data sheets for vibration cast data, the unreinforced data gathered was 24% lower (Table 7). When fired samples were compared, they matched well.

Table 7: Cold Compressive Strength of Unreinforced TuffCrete 65M

	Temperature, °F	Cold Compressive Strength, psi
This Study	230	14,313
Manufacturer's Data Sheet		18,910
This Study	2000	19,290
Manufacturer's Data Sheet		21,035

In all cases fired samples in the ceramic phase perform better in compression than those in the dried or hydraulic phase (Figure 45).

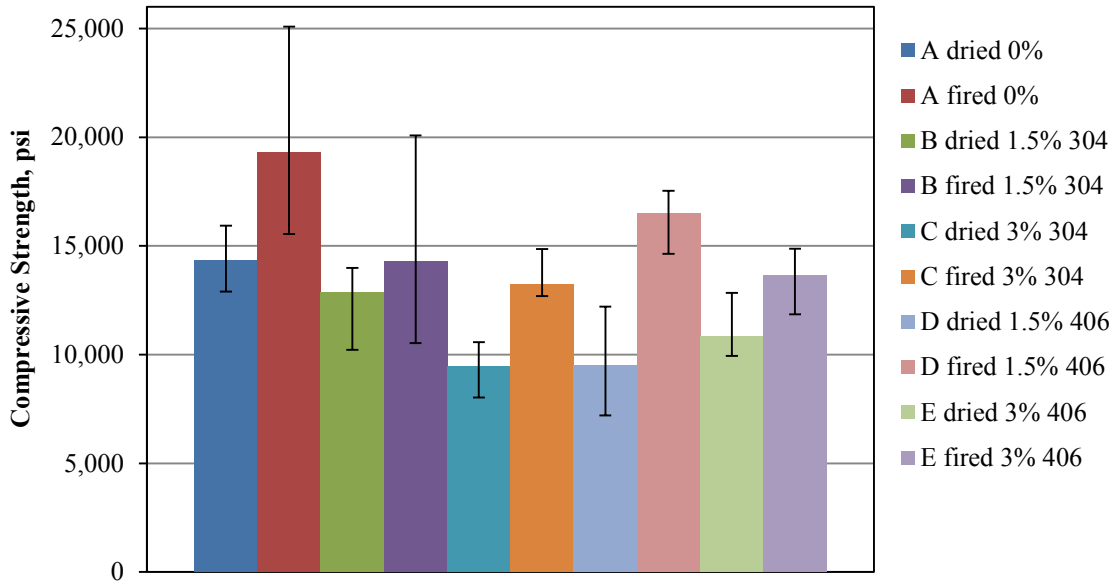

Figure 45: Cold Compressive Strength – Dried and Fired Samples

Although it would not be adequate to look at compression results alone, compression strength and data is useful in several ways. These results tell us that this material is strong in compression, how it compares to other similar refractory materials, and the material can handle a considerable amount of compression when needed.

In this type of furnace, real stress controlled compressive loads in a static installation at a room temperature environment are low (11 psi). However, if the material achieves operating temperature without being allowed to properly expand compressive stresses can be as high 3,100 psi (assuming 0.65% growth and a Modulus of Elasticity of 475,000 psi and as calculated by compression data gathered in this study – see Chapter 6).

5.2 Cold Modulus of Rupture (CMOR) Data Analysis: Strength

Refractory designs do not typically put refractory into tension. However, there are certain situations where refractory will experience bending or tensile loads. The CMOR data gives us insight to what the reaction to this type of load may be.

CMOR or peak strength data is relatively flat across the board (Figure 46) similar to compression properties, however, both dried and fired samples decreased slightly with added reinforcement (Figures 47 and 48). This may be caused by a similar degradation as seen with the compression properties; where needles displace or introduce discontinuities in the refractory that decrease the strength.

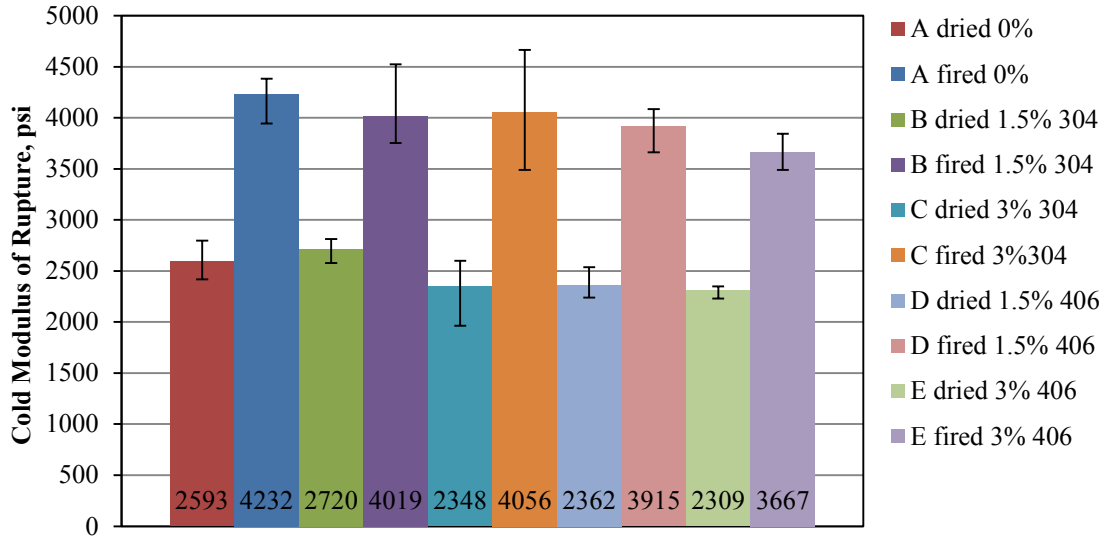

Figure 46: Cold Modulus of Rupture Strength – Dried and Fired Samples

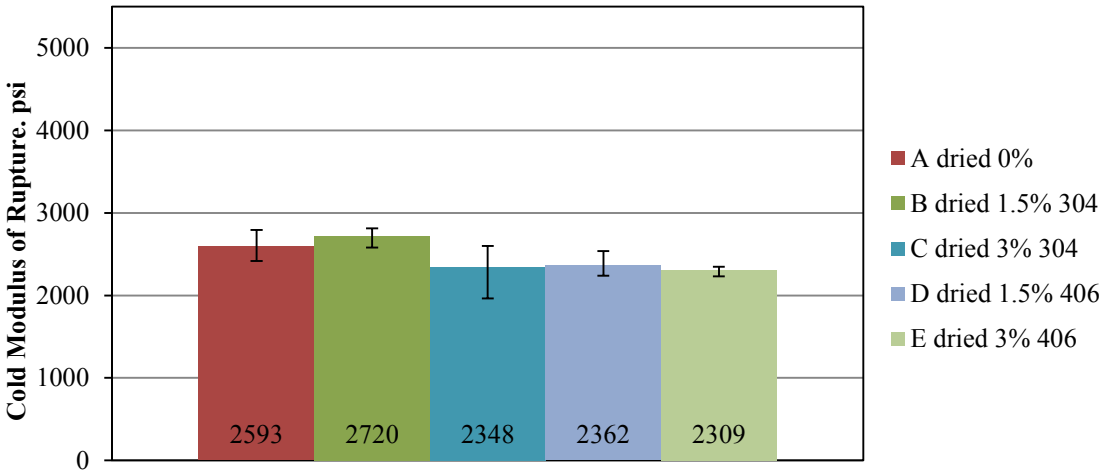

Figure 47: Cold Modulus of Rupture Strength – Dried Samples

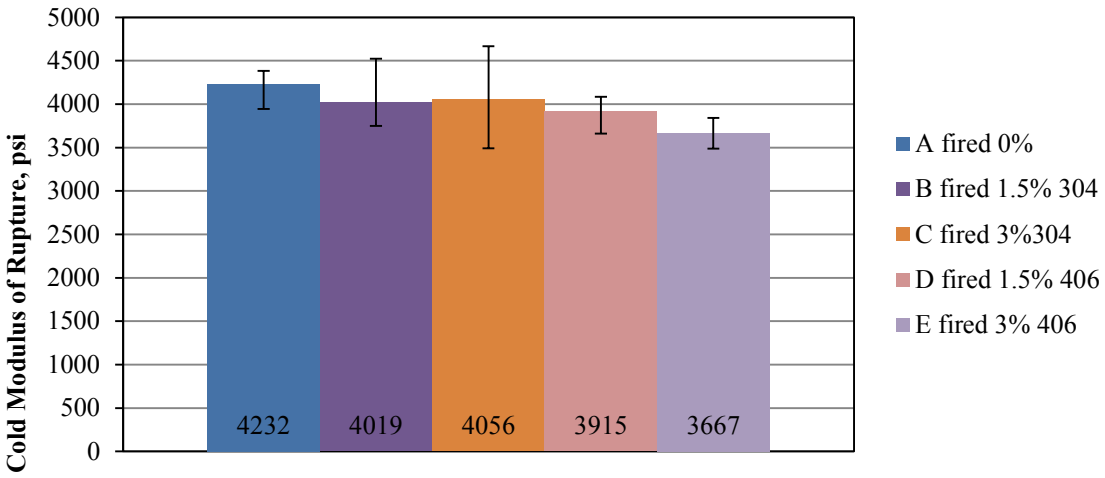

Figure 48: Cold Modulus of Rupture Strength – Fired Samples

The study prescribed reinforcing at 1.5% and 3% by weight which calculates to approximately 0.5 and 1% by volume (and cross sectional area) (Figure 49). The study concluded that a reinforced sample in an un-shocked and un-cracked form is less strong than its unreinforced counterpart.

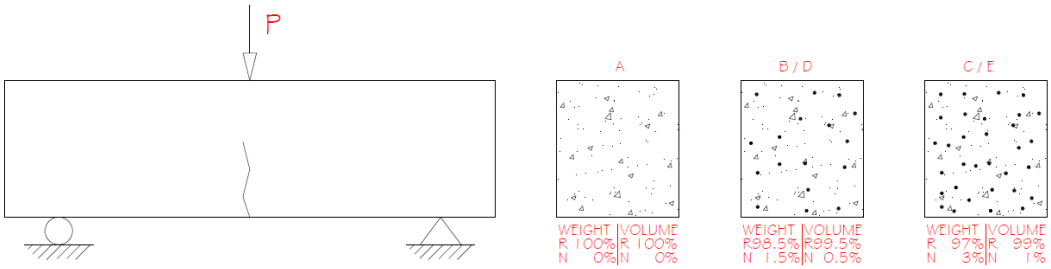

Figure 49: CMOR Beam and Cross Sections (R = Refractory; N = Needles)

When a sample broken in the CMOR machine was inspected visual evidence (Figure 50) showed that most of the needles broke as opposed to pulling out from the material (a bonding failure or lack of development). In both dried and fired sample situations it appeared that was true and confirmed an assumption made by the study in Chapter 2 where fully bonded needles were assumed.

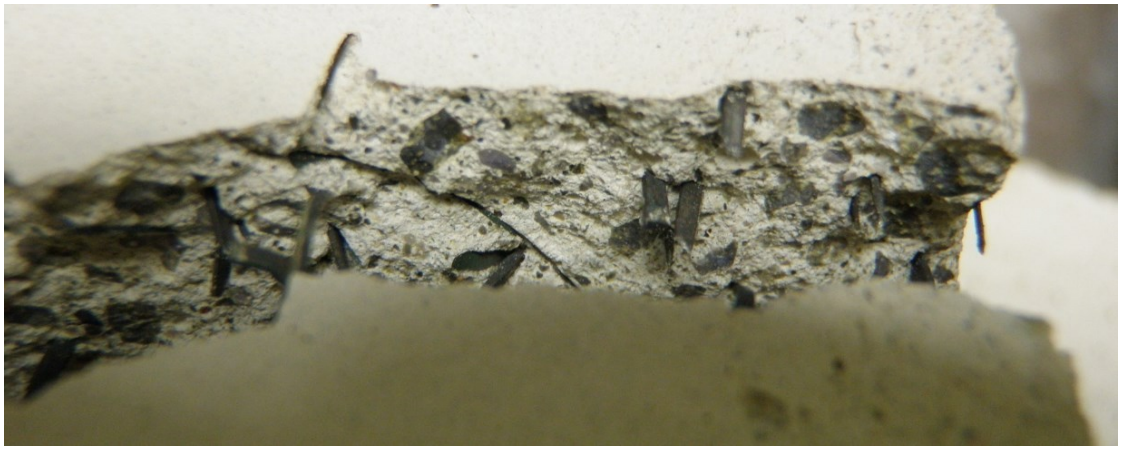

Figure 50: CMOR Beam Failure Showing Broken Needles

Reinforcing needles are, however, placed randomly in the mix and their orientation is typically not controlled. So unlike bars in concrete, where reinforcing can be strategically placed in areas where cracks would be assumed to arise and development length can be assured, needles cannot be placed with accuracy. This leads some needles not be split equally across the crack (Figure 51). And depending on the length of development and the phase of the refractory (hydraulic being softer and requiring slightly more length to bond vs. a harder ceramic phase) all needles may not be 100% developed in the refractory.

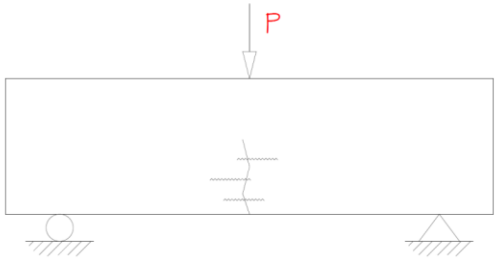

Figure 51: CMOR Beam Showing Needles and Crack

The data shows that dried (hydraulic phase) refractory samples with 304 needles at 3% concentration have approximately the same strength as 406 needles at the same concentration (Figure 43). This would indicate that during this softer hydraulic phase, not as many needles are fully engaged as in the ceramic phase. Results in the ceramic phase show that samples with 304 needles are 10% stronger than samples with 406 needles of the same concentration (Figure 46). This may be explained by seeing the material data sheet information in Table 8 where 304 needles are explained to have a raw data specification range that is 24% higher than the 406 specification.

Table 8: Material Data Sheets for 304 and 406 Stainless Needles (Reproduced from [18],[19])

MATERIAL DATA SHEET—304 SLIT-SHEET FIBERS

REVISION DATE: 15/03/07
PRODUCT TYPE: Stainless Steel Fibers
MANUFACTURING PROCESS: Slit-Sheet Method
SHAPE: Straight & Deformed

TYPICAL CHEMISTRY & PHYSICAL PROPERTIES:
(Metallurgy is typical, conforming to AISI standards)

% kg	C	Mn	Si	P	S	Cr	Ni	Fe + trace elements
max	0.08	2.0	0.75	0.045	0.03	18—20	8—10,5	balance

Melting Range °F: 2550—2650

Critical Oxidation °F
Cyclic: 1500
Continuous: 1650

Specific Gravity g/cm3: 7.87
Tensile strength MPa (min) @ 20 °C: 515—640 (min) @ 20 °C

MATERIAL DATA SHEET—406 ALFA-1 SLIT-SHEET FIBERS

REVISION DATE: 15/03/07
PRODUCT TYPE: Stainless Steel Fibers
MANUFACTURING PROCESS: Slit-Sheet Method
SHAPE: Straight & Deformed

TYPICAL CHEMISTRY & PHYSICAL PROPERTIES:
(Metallurgy is typical, conforming to AISI standards)

% kg	C	Mn	Si	Ti	Cr	Al	Fe
max	0.025	0.035	0.30	0.40	13	3.0	balance

Melting Range °F: 2650—2760

Critical Oxidation °F
Cyclic: 1800—1900
Continuous: 2050—2275

Specific Gravity g/cm3: 7.87
Tensile strength MPa (min) @ 20 °C: 524 (min) @ 20 °C

The study found that unreinforced CMOR test data matched closely the manufacturer's data sheets (Table 9) and indicate tests performed in this study were consistent with manufacturer's practices, material, and data.

Table 9: Comparison of CMOR Data with This Study and Manufacturers Data

	Temperature, °F	Cold Modulus of Rupture, psi
This Study	230	2,593
Manufacturer's Data Sheet		2,700
This Study	2000	4,232
Manufacturer's Data Sheet		4,725

In this type of furnace, bending loads in a static installation at room temperature situation are at 7 times lower than what this material can handle. However, if the material achieves operating temperature without being allowed to properly expand, loads could be higher.

5.3.1 Cold Modulus of Rupture (CMOR) Data Analysis: Work of Fracture (WOF)

Although calculated, EOF data shadowed all WOF data and was intentionally left out as it did not add value to this section. When analyzing WOF and EOF similar trends emerged as they did with the strength information. Although there was not a gradual trend downward as with strength, the data showed lower property values for samples with 406 needles (see Figures 54 and 55). There was a significant step change when 406 needles were introduced (Figure 54 and 55). While 304 and 406 samples have a similar strength (CMOR,) 406 samples have a much lower WOF, which would reveal a less ductile 406 sample. This would also translate to less deflection at the same breaking strength.

However, according to a Fibercon (email dated 9/27/13) adding Aluminum slightly drops the Modulus of Elasticity (E). And as seen by the following equations a lower E value means a higher strain and higher ductility. (Also see Chapter 6 for further evaluation of E.)

$$\sigma = E\varepsilon$$

Or

$$\varepsilon = \sigma/E$$

Where

ε = Strain

σ = Stress

E = Modulus of Elasticity

In this study WOF to the peak load was calculated. Figures 52 and 53 shows data from a representative sample of similar strength but different formulation(both dried and fired CMOR data).This data shows that needles in both cases hold the sample together better after crack initiation, exhibiting a higher ductility (Figures 52 and 53). And 304 sampled hold together best in both cases, which also supports earlier evidence that 304 steel may be of higher strength than 406.

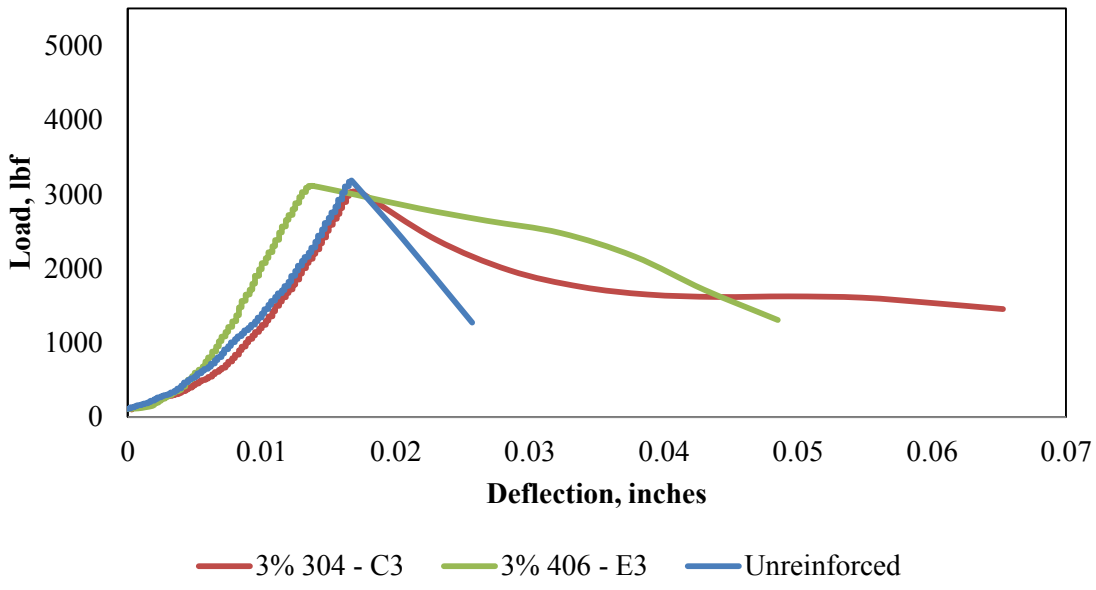

Figure 52: Load – Deflection Curves from Dried CMOR Samples

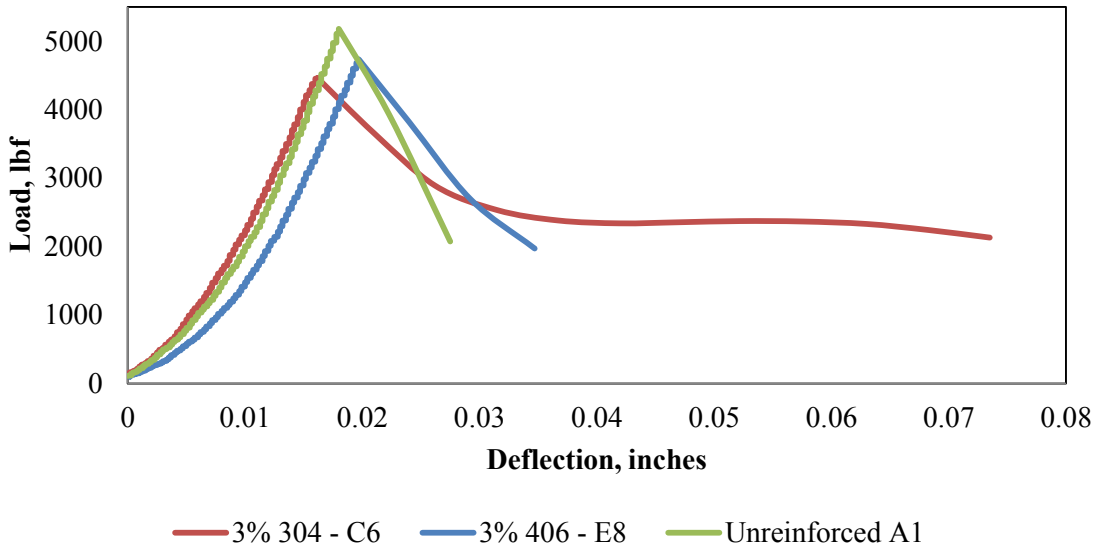

Figure 53: Load – Deflection Curves from Fired CMOR Samples

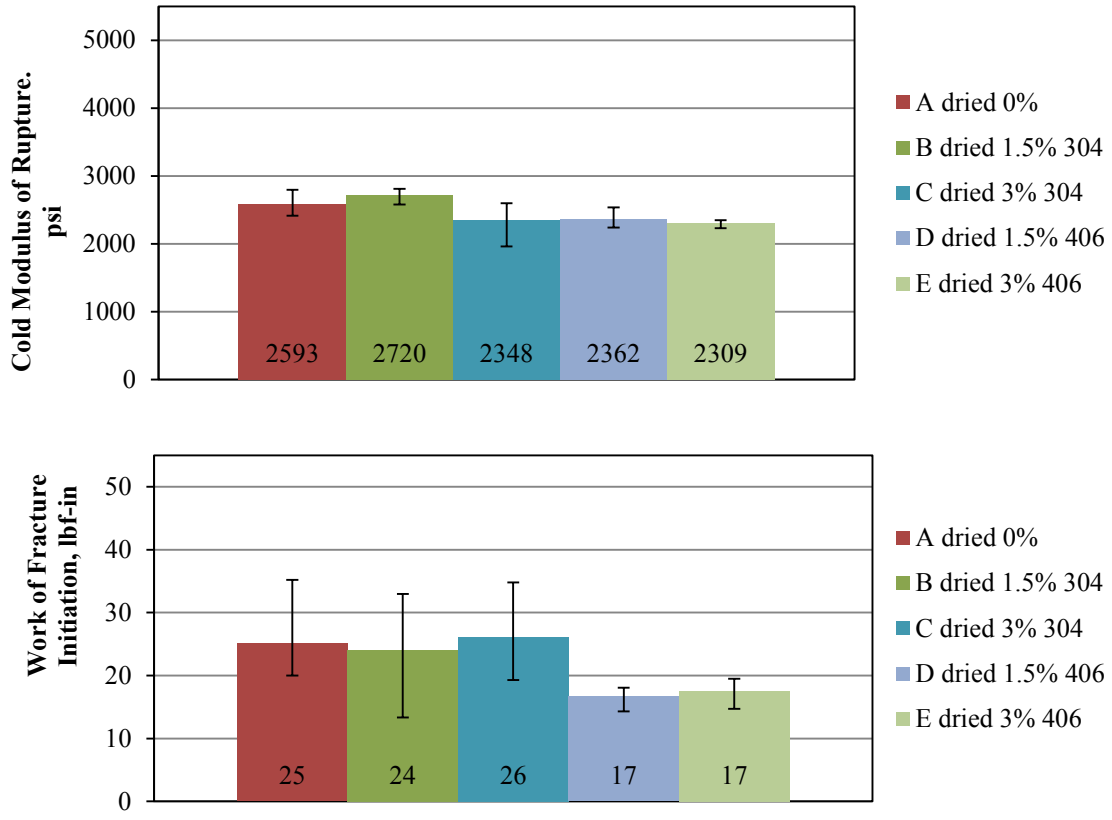

Figure 54: CMOR Strength vs. WOF for Dried Samples

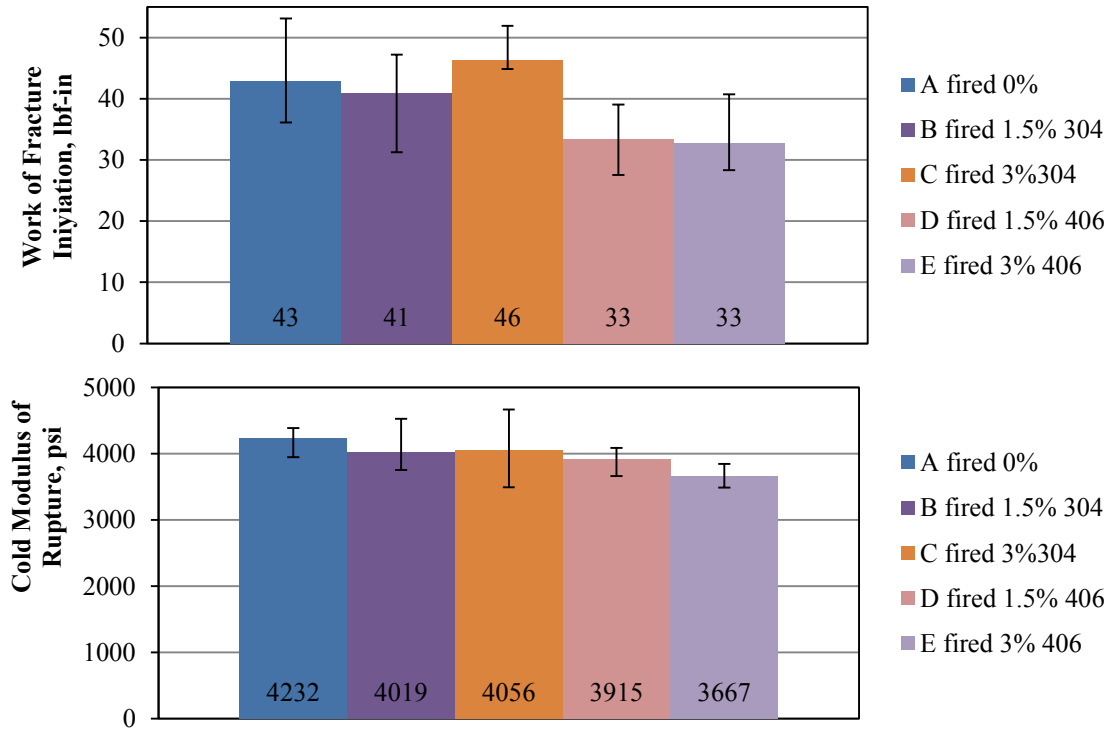

Figure 55: CMOR Strength vs. WOF for Fired Samples

Work and energy calculation are important because they reflect ductility and flexibility properties in a material. And that flexibility is important because in this type of wall system as a less brittle structure will bend instead of break reducing failures.

5.3.2 Comparison of Short and Long CMOR Tests

Fired samples from CMOR test were compared against the controlled (un-shocked) sample from the thermal shock test. CMOR test off the first run were done at a 7 inch span. Controlled samples of the thermal shock test were done at a 4 inch span. WOF data was significantly higher as expected because more work is required to break a shorter sample (comparing Figure 50 with Figure 52). However, the failure mode of a shorter sample with that type of aspect ratio may not always be a true bending failure as intended in the testing. ASTM C-1171 recommends individual 1 inch x 1 inch x 6 inch samples and if other sizes are used they should be cut parallel to the longest dimension. This study used a soap sized (2 ¼ inch x 2 ½ inch x 9 inch sample) bar and cut the samples perpendicular to the longest dimension. Some of the samples appeared to have a shear type failure (Figure 56). ASTM C-78 "Flexural Strength of Concrete" goes even further to ensure a bending failure by using a three point bending test. This data needed to be scrutinized closely as different failure modes may skew data.

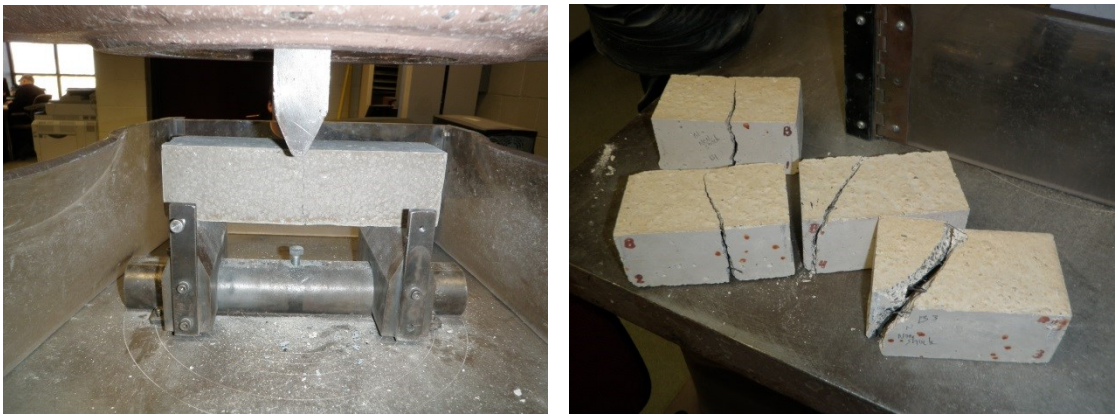

Figure 56: CMOR Comparison of Long and Short Sample Failure Modes

5.4 Hot Modulus of Rupture (HMOR) Analysis

The HMOR test gives a peak bending strength. Because of the nature of the test is so heat intensive, it is difficult to gather any incremental load-deflection data as received with the CMOR. Therefore, Work of Fracture and Energy of Fracture could not be calculated. Needles more than likely have a less representative effect in this test because a smaller cross section to needle size ratio (with ¾ long needles and 1 inch square cross section) of the sample has less chance of being a well-blended heterogeneous mix.

HMOR data continues the trend seen in the CMOR data of 406 samples being weaker than 304 samples (Figure 54) which supports the theory of 304 alloy needles supplied being stronger than 406. Evidence also shows in this case as well as CMOR case that the needles did break and did not pull out confirming full bonding to the refractory.

The data also reveals two other trends. The first trend is unreinforced samples are stronger than reinforced (Figure 57) (similar to CMOR data). The other trend shows that samples tested at higher temperatures are approximately 10% higher than the fired samples tested at room temperature (CMOR data). Refractory not only retains its strength at high temperatures but show slightly higher data (Figure 58).

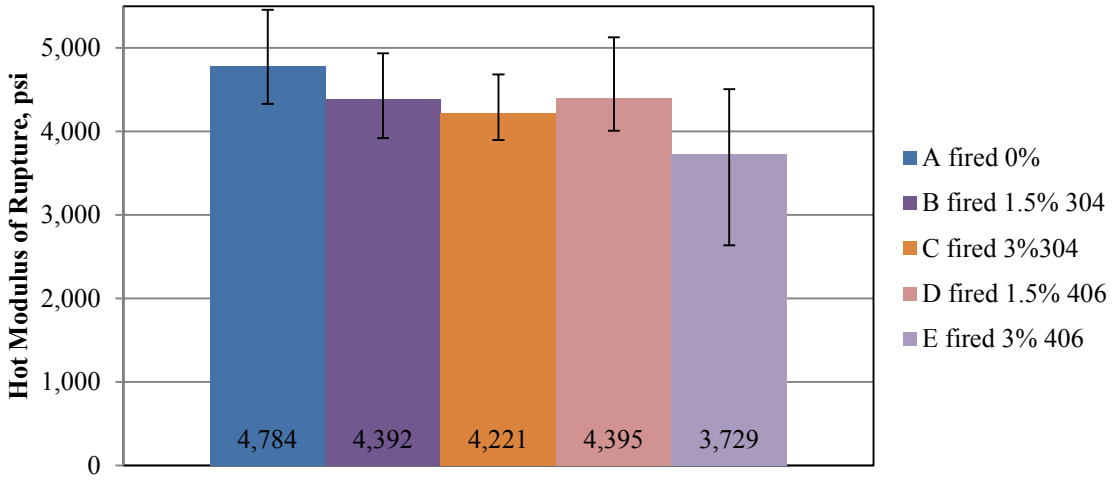

Figure 57: HMOR Strength

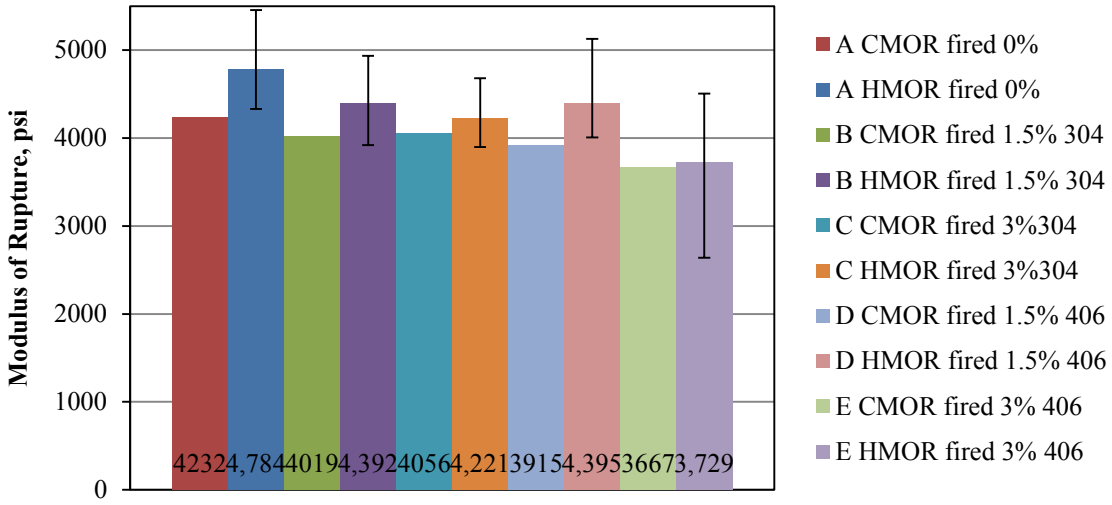

Figure 58: CMOR vs. HMOR Strength

The HMOR test indicates the strength of a material while in service. This makes it the most meaningful and relative strength test. The data generated from this test does not match the manufacturer's data for an unreinforced sample very well (Table 10), however, it was consistent across the test and shows HMOR outperforms CMOR at equivalent temperatures, which was consistent with this study.

Table 10: Comparison of HMOR and CMOR Data of This Study to Manufacturer's Data

Test		Temperature, °F	psi
Hot Modulus of Rupture	This Study	2000	4,784
	Manufacturer's Data Sheet		6,375
Cold Modulus of Rupture	This Study	room	4,232
	Manufacturer's Data Sheet		4,725

5.5 Thermal Shock Data Test Analysis

The Thermal Shock data proved to be the most outstanding and revealing data of this study. This two part analysis of each block; the CMOR and Ultrasonic speed data (destructive and nondestructive) show a significant strength reduction caused by thermal shock on unreinforced samples and the effect of adding reinforcement.

After the prescribed shock test, properties of strength and Work of Fracture would break in the other direction when shock and un-shock data was compared. Thermal cracking starts to induce small cracks in the samples as they are cycled. Needle reinforcement holds these samples together retaining strength and WOF properties. Higher values appeared with increased needle content and when 406 needles were used vs. 304 alloy (Figure 59).

This data proved challenging to interpret because many of the shocked sample data points did not create a smooth, traditional bending failure curve creating doubt of a true MOR test (refer to Section 5.3.2 in this chapter). Figure 60 also shows the 3% 304 (C) Work of Fracture higher than others; however, a clear MOR failure point was not obvious. Figure 61 shows all the 3% concentration fired sample plotted curves (304-top; 406-bottom). 406 samples exhibited a smooth more traditional bending failure curve, while 304 samples failed unconventionally and needed more data interpretation. A cracked sample increases the chances of a failure mode other than bending. As a matter of note, many of the un-shocked samples failed in a traditional bending mode. A different size sample or a larger sample set would have helped this portion of the analysis. (See Appendix B for raw data.)

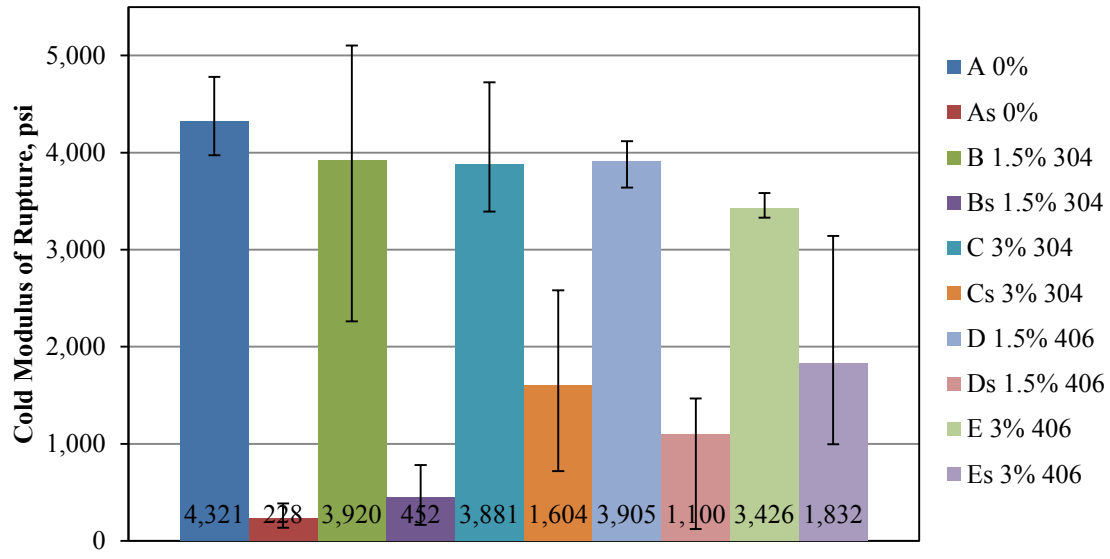

Figure 59: CMOR Strength Data of Shocked vs. Un-shocked

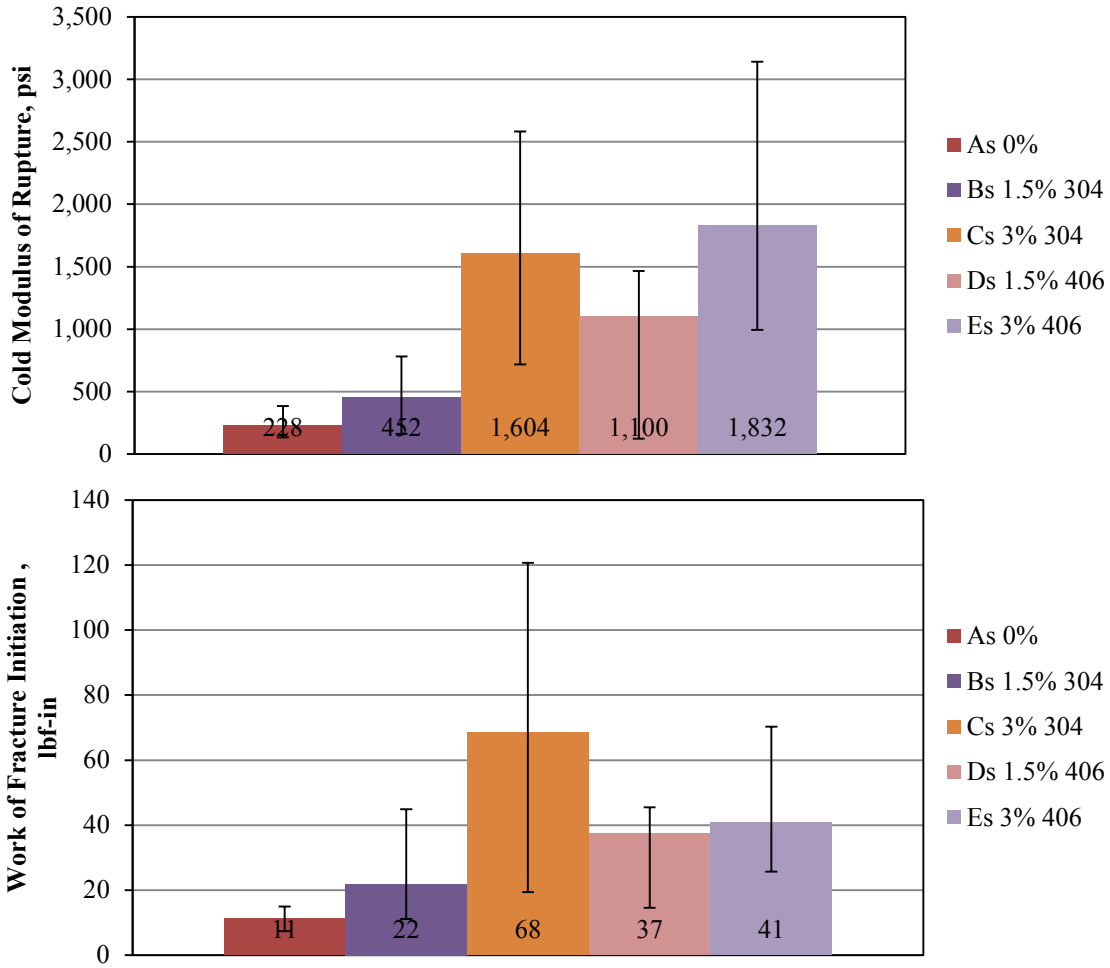

Figure 60: CMOR Strength and WOF Data of Shocked Samples

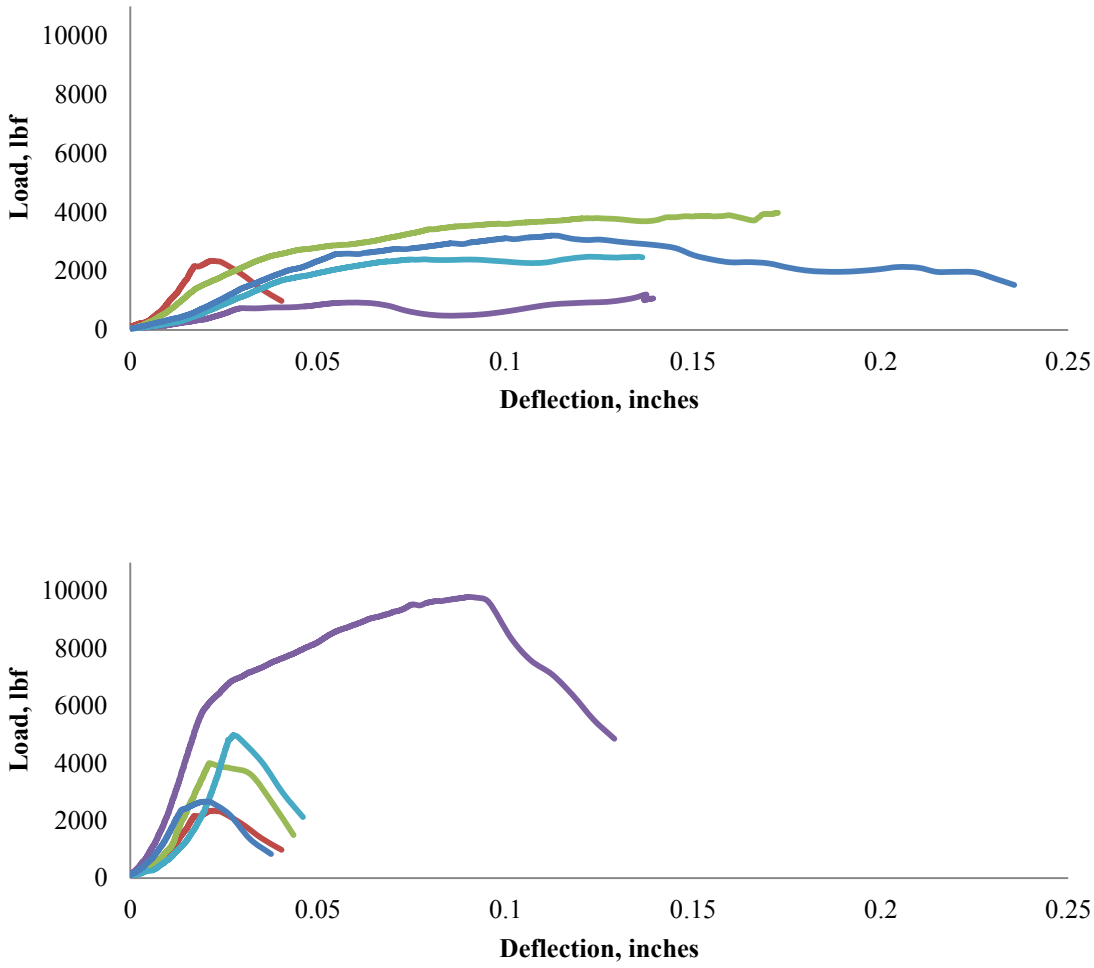

Figure 61: CMOR data of Shocked samples of 3% 304 (top); Shocked samples of 3% 406 (bottom)

Nondistructive sonic velocity measurements were taken of all sample formulas during this test and show that they have a good corralation with the losses in strength and Work of Fracture as seen in the distructive CMOR test (Table 11).

Table 11: Properties Percentage Loss of Properties after Shocking

Sample	Needle Type	Needles Content, %	Strength Loss, %	Work of Fracture Loss, %	Sonic Velocity Loss, %
A	na	0.0	95	89	63
B	304	1.5	88	77	63
C	304	3.0	59	23	48
D	406	1.5	72	57	46
E	406	3	47	48	44

Aggregates, binders, and in this case, stainless steel needles, do not expand at the same rate in this heterogeneous refractory mix. These unequal expansion rates and differential thermal gradients cause internal stresses in the monolithic. Resilience after thermal shock cycles depends on how well those materials react to those stresses.

However, when thermal shock stresses start to break down the material and micro cracking develops, needles hold that material together so it retains its strength and integrity. Needles also control the cracking from a few large ones to many small ones. This is advantageous because it prevents large sections of lining to fail.

5.5.1 Differential Particle Expansion Issues

As mentioned earlier, the results start to show a larger data separation of 406 needles in their outperformance of 304. These break away starts to make sense when properties of these needles are explored.

The first property looked into is needle thermal expansion. As mentioned before, the differential expansion rates of materials in the refractory create stresses, cracking, and breakdown. So the closer the materials expansion rates are matched, the less the damage that will occur. As seen by Table 12, properties of 406 stainless have a much closer expansion rate to the Tuff Crete 65M refractory used in this study. Therefore, the 406 alloy does a better job in limiting failure in a thermal shock situation.

Table 12: Coefficient of Thermal Expansion for Alloys and Refractory Materials

Alloy	Coefficient of Thermal Expansion ($\times 10^{-6}$ inch/inch/°F)
304	10.4
310	8.6
406	7.1
TC65M	3.4

5.5.2 Needle Corrosion

The other damaging property to a needle reinforced design is corrosion. Corrosion breaks down the needles when heat and oxygen are absorbed turning a metal into a metal-oxide. Corrosion occurs when certain environmental and material situations are present. Visual evidence of needle coloration in the samples of this test can be seen in Figure 62. On the left (in Figure 62) is a sample with 304 needles and on the right is a sample with 406 needles. The needles already

exhibit a corrosion darkening after only five cycles to 2200 °F, while the 406 alloy needles are still of the original gray color.

Figure 62: Needles Shown after Firing 304 (Left) 406 (Right)

When corroding, an iron based product like steel, is turned into iron oxide. Chrome is added to steel to make stainless steel which is resistant to corrosion. The stainless steel is resistant to corrosion because chrome combines with the oxygen to make a protective chromium-oxide layer on the surface of the metal. Typically the more chrome, the more protection against corrosion (Table 13). Studies show that in the case of going from 304 to 310 this is true [6][29]; however, the 406 stainless alloy containing lower chrome and a small amount of aluminum outperforms both chrome only alloys. The 406 alloy creates an aluminum oxide surface layer as opposed to a chromium oxide layer as a protective barrier. This protective layer does not break down until a higher temperature.

Table 13: Elemental Make Up of Needle (Recreated from [7])

	Alloy			
	304	310	330	406
Chromium, %	18-20	24-26	17-19	12-14
Nickel, %	8-10	19-22	33-37	-
Aluminum, %	-	-	-	3
Melting Temperature, °F	2552-2651	2552-2651	2451-2606	2651-2759
Maximum Service Temperature, °F	1814	2102	2120	2300

Table 14 shows that all stainless steels have temperature limits of design where even the protective coating is no longer adequate to protect against corrosion. This is called their critical oxidation temperature. Critical oxidation has both a cyclical and continuous value assigned to each alloy. Continuous values are higher because a steady state has fewer tendencies to disrupt the protective oxide layer (i.e. less expansion and contraction).

Table 14: Critical Oxidation Temperatures (Recreated from [18],[19])

	Alloy	
	304	406
	Critical Oxidation, °F	
Cyclic	1500	1800-1900
Continuous	1650	2050-2275

Other ways to understand oxidation and corrosion of the needle reinforcement is to look at weight gain and cycles to failure. Weight gain suggests that when alloy oxidizes it takes on additional weight because of the chemical absorption of the oxygen. Figure 63 shows how much weight is gained at certain temperatures. Figure 64 shows the number of thermal cycles an alloy can handle before failure. Data on both of these tables continue to support 304 alloy needle being inferior to the 406 (ALFA I) needle.

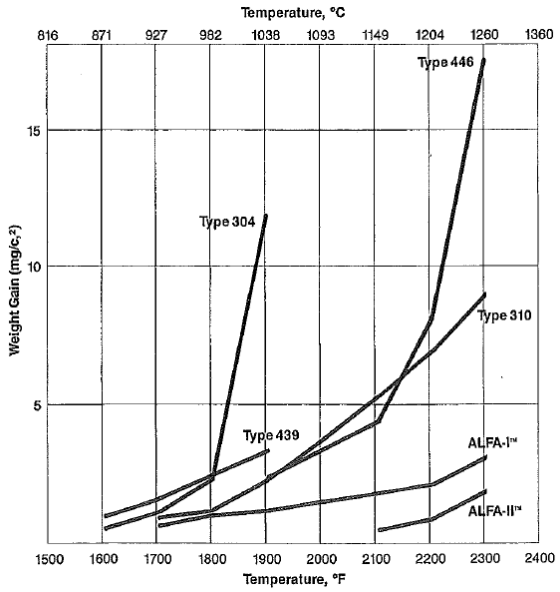

Figure 63: Weight Gain Due to Corrosion of Alloys (Reproduced from [29])

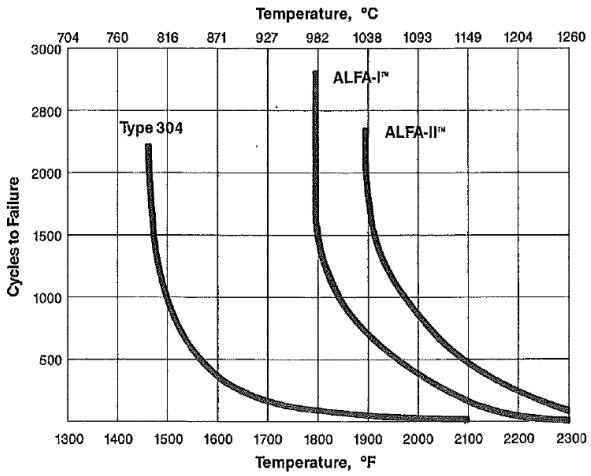

Figure 64: Cycles to Failure of Alloys at Temperatures (Copied from [29])

If the original design conditions that were laid out in Chapter 3 are looked at again, they expose the fact that the needles lie in the hard face refractory where temperatures range from 2300 °F to 1500 °F (Figure 65). This information helps explains why 304 needle samples first produced a stronger material until thermal shock is factored in. Then 304 samples lose much of their mechanical properties because the optimal temperature limits for 304 are exceeded while 406 is still functional.

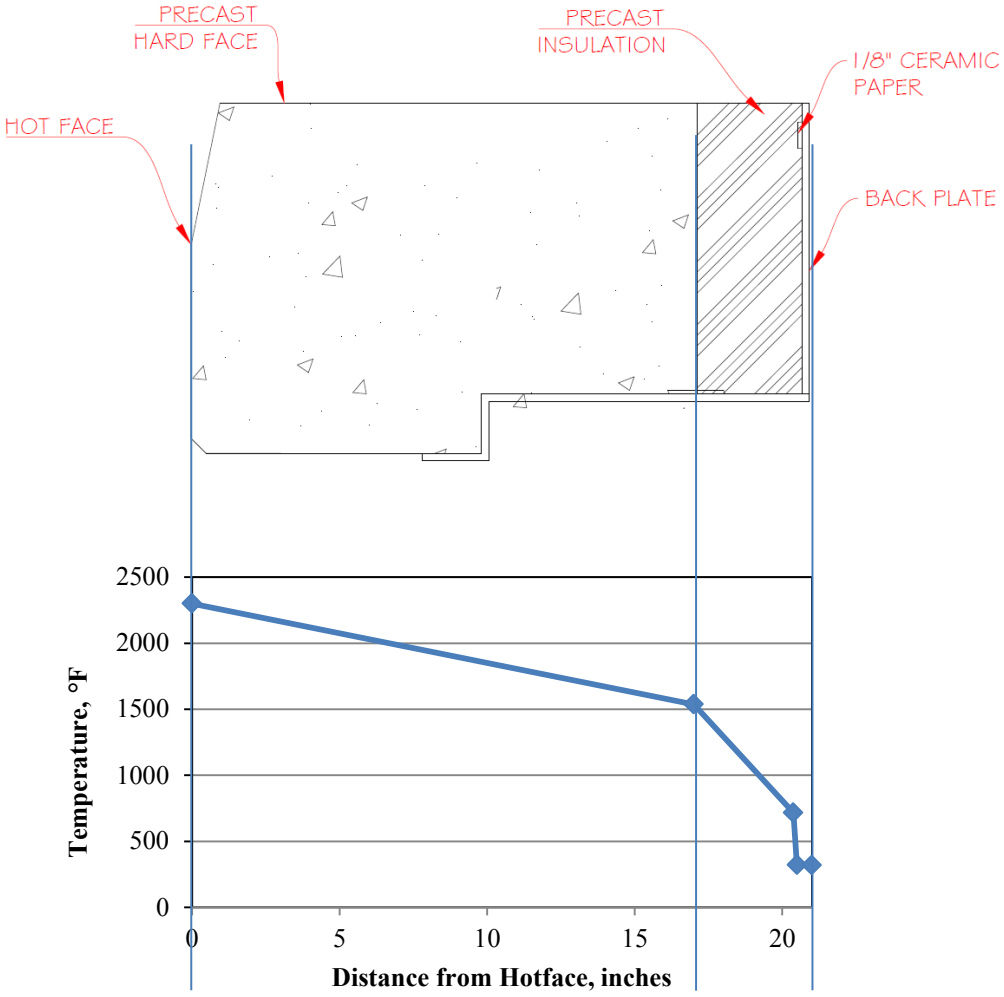

Figure 65: Calculated Temperature Profile of Curb Cross Section

5.5.3 Other Needle Considerations

Even though needle properties are dissimilar to the refractory properties and may contribute to cracking as explained in 5.5.2, in a thermal shock situation they hold the refractory material together and help control the cracks from one or two large ones to many small ones. Because the cracks are small the needles will now help hold the material together and increase strength and ductility.

If design conditions of the furnace are recalled; compression and MOR data is important and the properties should be adequate to the furnace design. Factors-of-safety in those design numbers should also be adequate. However, after thermal shock is analyzed, it is far more important that

the liner maintains its basic integrity and "stays on the wall" in an in-service application. This is to protect the insulation layers and the structure.

When investigating information on needles the manufacturers use the terms "continuous" or "cyclical" to describe the service loads the needles will see. A taconite processing furnace is not a cyclical batch process; however, it is not truly a steady state condition either. The study had to factor this into consideration and future furnace designs should consider this as well.

When researching needle reinforcement it was discovered that all of the testing done on these alloys were done with the metal directly exposed to heat and air. In the furnace, the needles are buried inside the refractory and somewhat protected from the direct heat and oxygen. This would have an effect on the expected results; however, the trends in the data show a consistency with the researched thermal cycle data.

5.6 Thermal Dilation

As referenced in the earlier testing chapter, this test was done in done in two runs. An initial run up to 2000 °F through a phase change and then back down to room temperature was completed. The second was another run up to 2000 °F (in a stable ceramic phase) and then back down to room temperature.

The first run displayed geometrical changes that were non-linear and non-elastic. When the sample had cooled it had shrunk by 0.4% (Figure 66). This is typical of this type of refractory material heating up through a phase change from hydraulic phase to a ceramic phase. The second run (and presumably every run after that) displayed a linear elastic behavior, expanding when heated and cooling back down to original size (Figure 67). Slight differences between reinforced and unreinforced samples are seen, but all displayed similar respective data point patterns (Figure 66 and 67).

An actual precast piece delivered from the manufacturer is dried to 700 degrees F after it is cast at room temperature. It is then shipped and installed in the furnace and it then goes up to 2000 °F with the initial heat up of the furnace.

The dry out at the manufacturer is done in an effort to eliminate any water in the form of steam being released during furnace heat up and causing liner failures. This is one major advantage to a precast piece. However, as seen in Figure 61 it has not completed its phase change. For a designer of a furnace lining, the true behavior of a precast piece in furnace conditions is not known because this phase change is not complete. Information for thermal expansion given on manufacturer's data sheets only references the initial run.

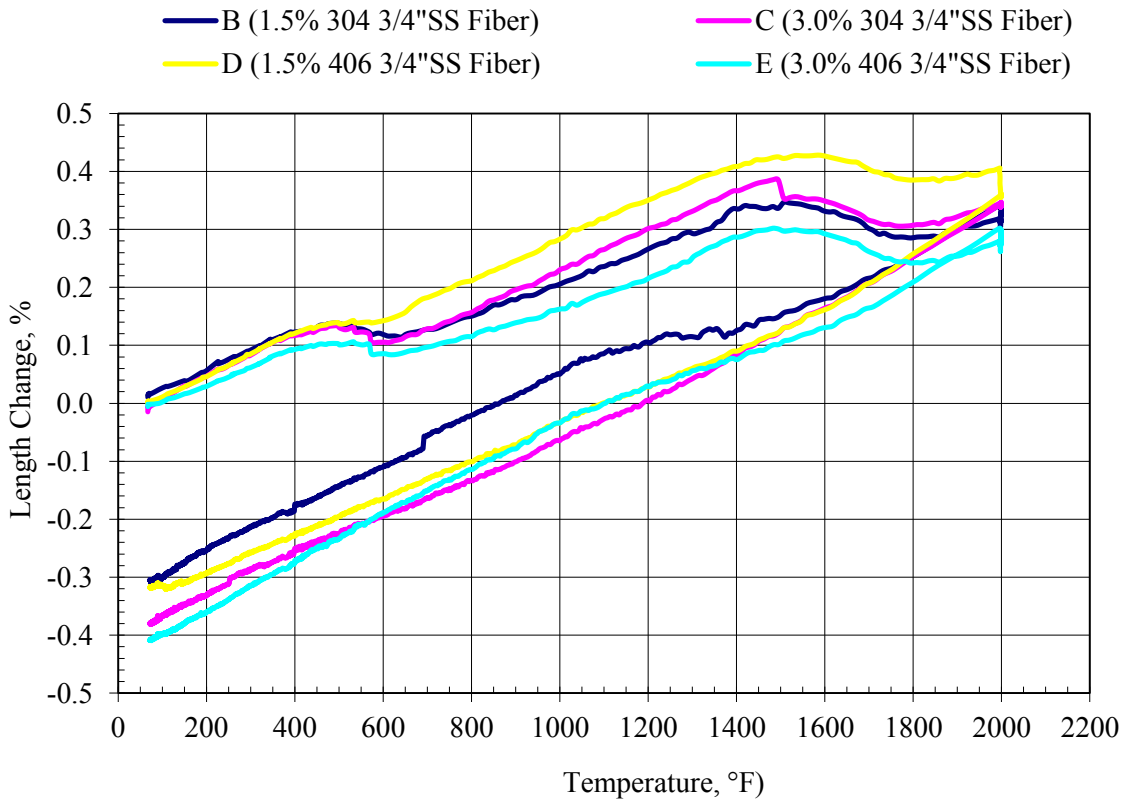

Figure 66: Thermal Dilation Test; Temperature vs. Change in Length of First Run to 2000 F

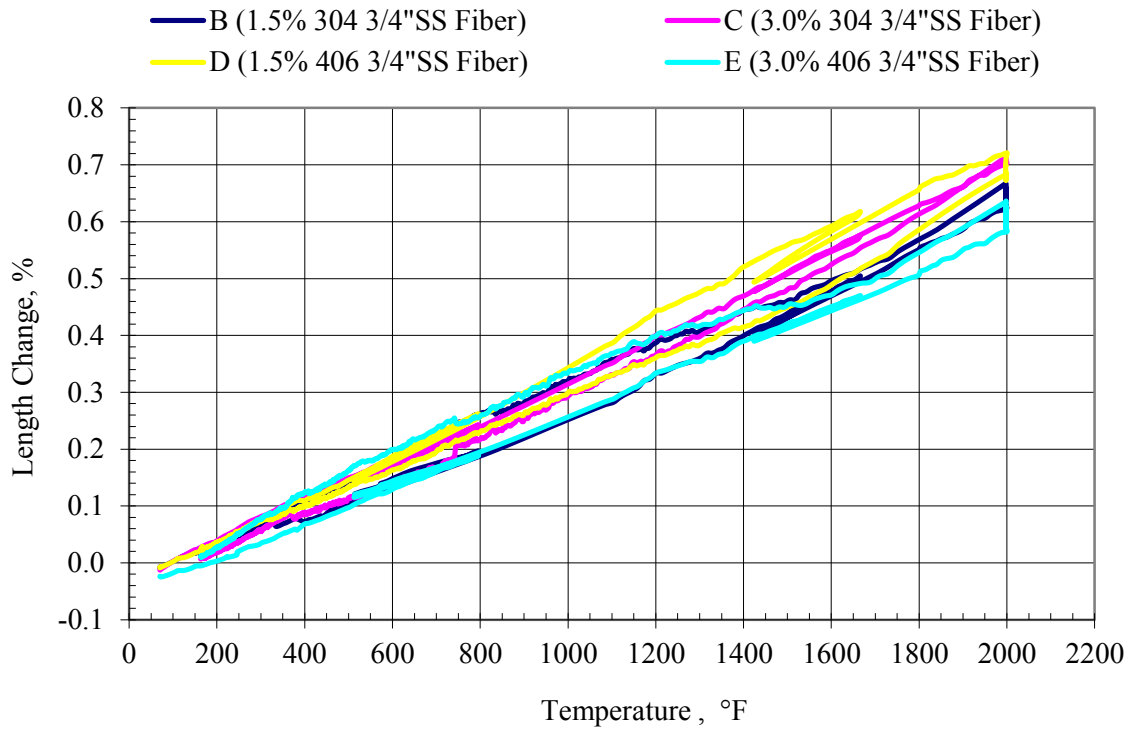

Figure 67: Thermal Dilation Test; Temperature vs. Change in Length of Second Run to 2000 F

Information gathered during this thermal dilation test is valuable for calculating expansion joints and stresses caused by thermal expansions being constrained. Thermal expansion failure can cause complete lining failure and thermal expansion is often ignored or misunderstood, however with the proper expansion joints engineered into the liner it is one of the most preventable failures.

Information gathered in this study was well matched to the manufacturer's data sheets.

5.7 In-service samples

Samples were taken from precast curbs that have been in-service in Northshore Mining Furnace Number 5 for approximately 6 months. Samples from hot face "D," the cold face "B," and in-between "C," were taken (Figure 68). One control sample of the same material that had not been in the furnace "A" was taken as well. These samples were all TuffCrete 65M with 3% 406 needles. Needles exhibited oxidation where cracks exposed the needles to air. Saws cut through the un-cracked portion of the samples revealed far less corrosion (Figures8 and 68 sample "D"). When the compression tests were completed of in-service samples, most of the data showed a slight decrease in compressive strength versus the controlled samples in this study (Figure 69; Table 15). However, the sample from the cold face and the sample that had not seen service both showed approximately 50% loss in CMOR data (Figure 69; Table 15). And curb samples still retained ½ of its original compression strength as compared to the data sheet and what our study shows. It was interesting to note, the sample that had not seen service "A," was only at about ½ strength after testing. "C" and "D" samples were most likely exposed to thermal shock. This explains reduction in strength. Reduction in "B" samples strengths vs. "A" samples were most likely due to the incomplete phase change from a hydraulic bond to a ceramic bond. This is evident when looking at a thermal profile of the curb (Figure 65).

All these could be explained by a few things: the numbers are comparable to thermal shock numbers, and non-in-service samples may have absorbed moisture in storage environment.

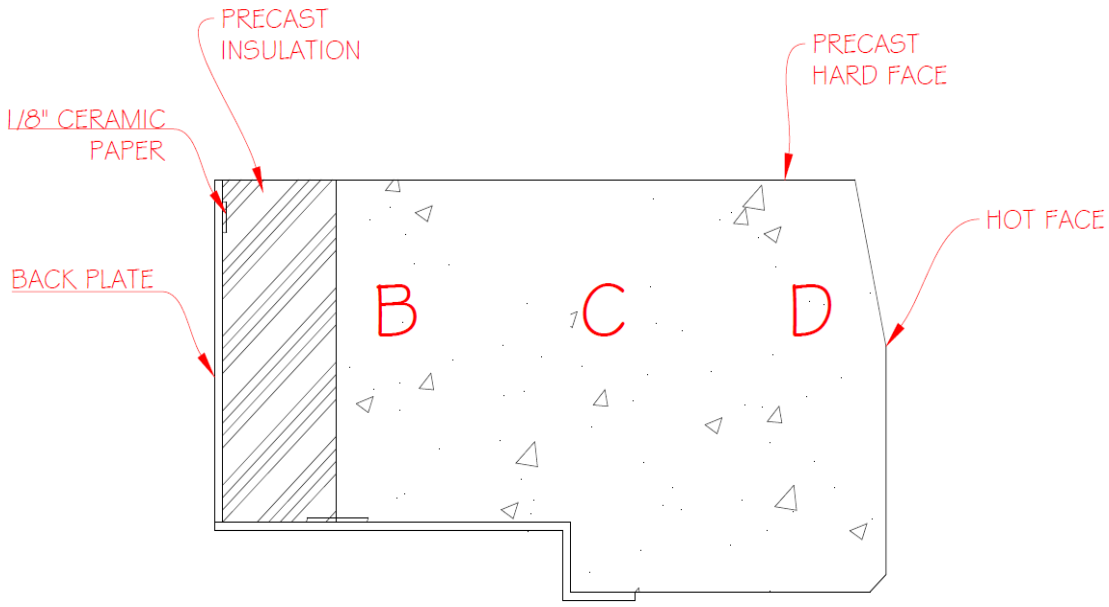

Figure 68: In-Service Samples Labled and Shown in Lab (A: No service, B: Cold Face C: Middle D: Hot face)

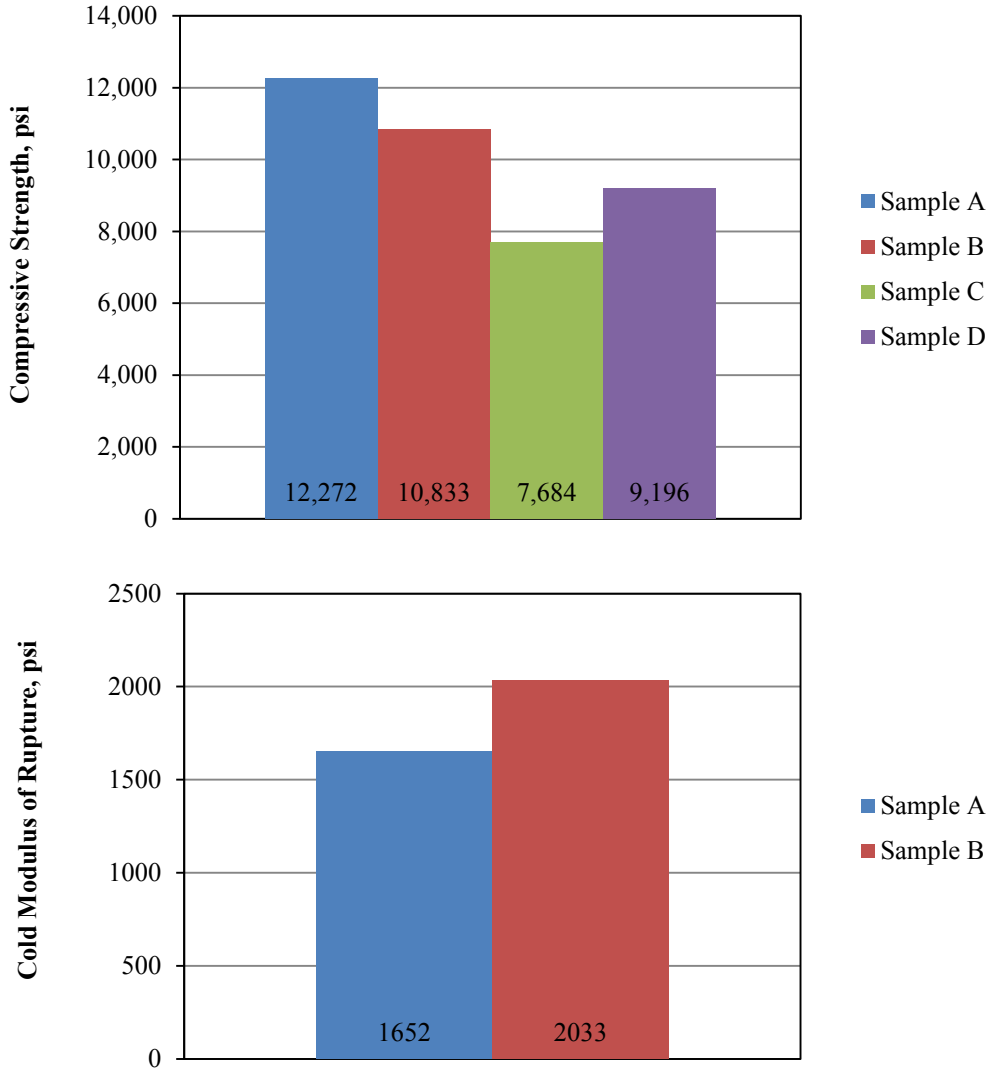

Figure 69: Compression and CMOR Data of In-service Samples

Table 15: Compression and CMOR Data of In-service Samples

Test	Sample	Position	psi
Compression	In-service (3%-406)	A	12,272
		B	10,833
		C	7,684
		D	9,196
	This Study (3%-406)		10,848
	Manufacturer's Data (unreinforced)		21,035
Cold Modulus of Rupture	In-service (3%-406)	A	1,652
	-	B	2,033
	This Study (3%-406)		3,667
	Manufacturer's Data (unreinforced)		4,725

CHAPTER 6: STRESS ANALYSIS

6.1 Stress Analysis Overview

This study strived to understand the stresses that a precast curb may potentially see during furnace operation so that an effective design could be established. In Chapter 3, an overview of general loading conditions was explained. In this chapter, specific calculated pressures were looked into based on thermal loading conditions in a strain controlled environment. Those pressures were fed into a finite element model to look at stress ranges and the nature of stresses that the refractory piece may experience.

6.2 Stress and Strain Calculations

In order to calculate the compressive pressures parallel with the wall, (pressures acting on the side of the curb) created by a confined curb in a high temperature environment, Hooke's Law can be applied. If the curb is restrained to move, it will experience a pressure relative to the expansion rate the material.

$$\sigma = E\varepsilon$$

Where

σ = Stress (Pressure)

ε = Strain

E = Modulus of Elasticity

6.2.1 Thermal Profile

The first step in calculating strain is to calculate a thermal profile based on the loading conditions and material properties of the precast block. This was done by knowing the maximum hot face temperature of a curb (2300 °F as seen in Chapter 3) and the Thermal Conductivity Coefficient (K) of the material (Figure 70). These calculations were done assuming a steady state condition.

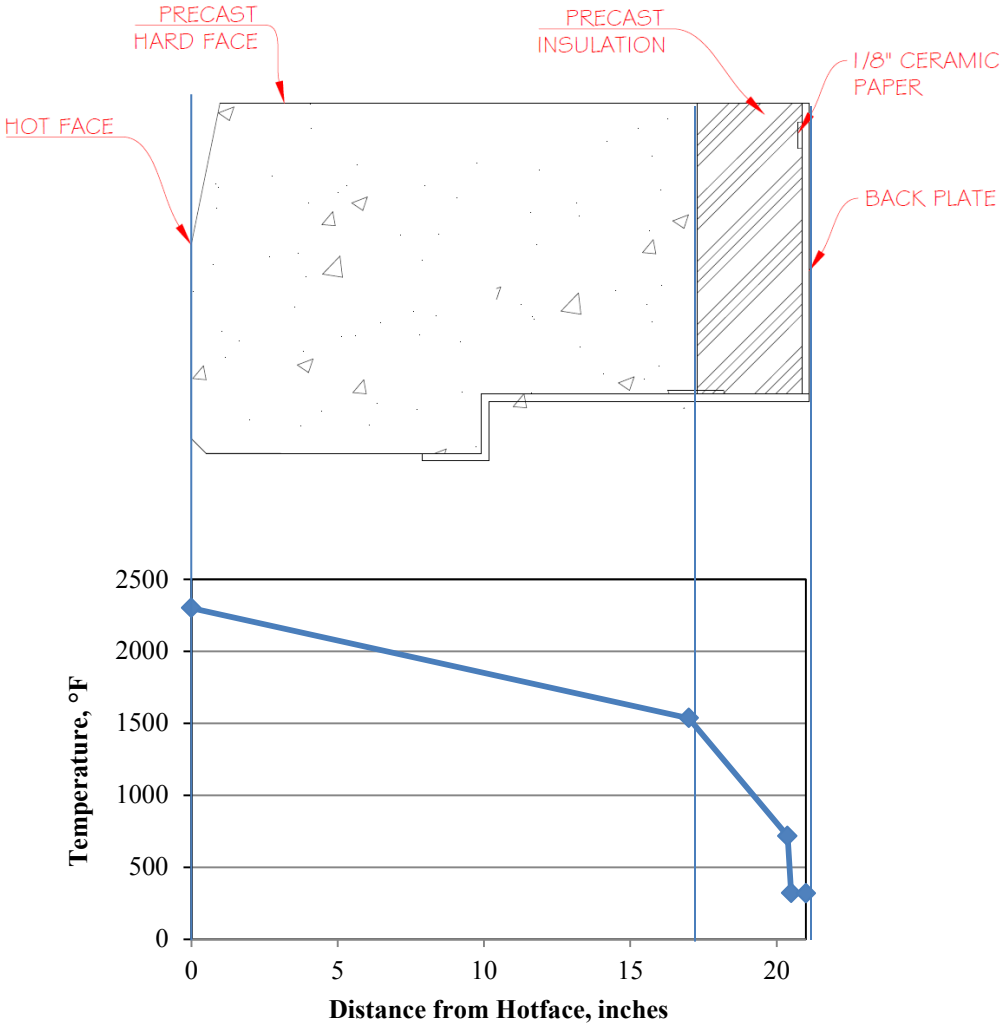

Figure 70: Calculated Temperature Profile of Curb Cross Section

6.2.2 Strain Profile

After the thermal profile was established, stain (ε) due to these temperatures would have to be understood.

Strains based on temperature changes were established in Chapters 4 and 5 when the thermal dilation tests were done to calculate expansions (Figure 67). This information was then used to create a strain profile (Figure 71).

Figure 71: Curb Strain Profile

6.2.3 Modulus of Elasticity Calculation

Modulus of Elasticity (E) values could be derived from this material's compression test results data (Chapter 4). Stress vs. strain slopes of all fired sample compression curves were measured (Figures 72 and 73) and an average of (475,000 psi) was established.

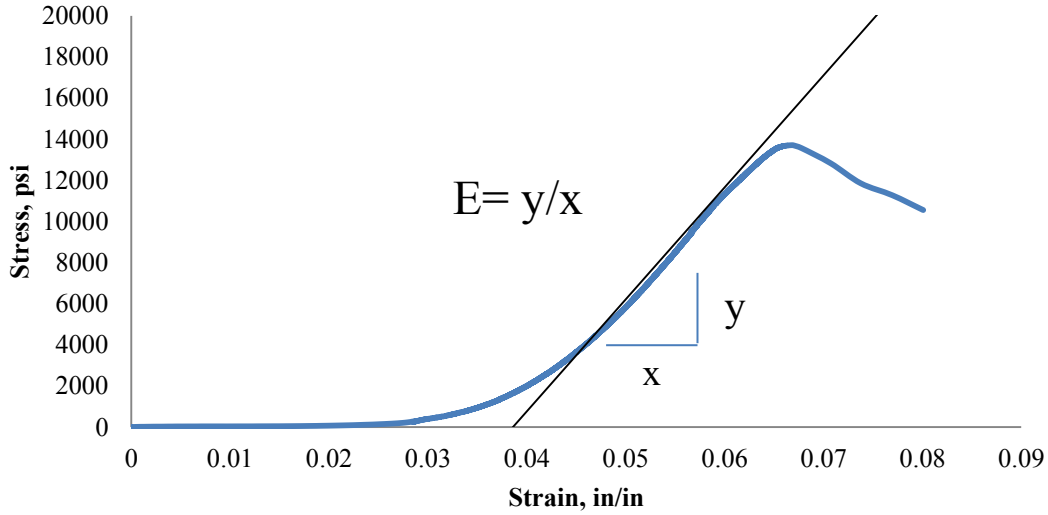

Figure 72: Compression test slope; Modulus of Elasticity (E)

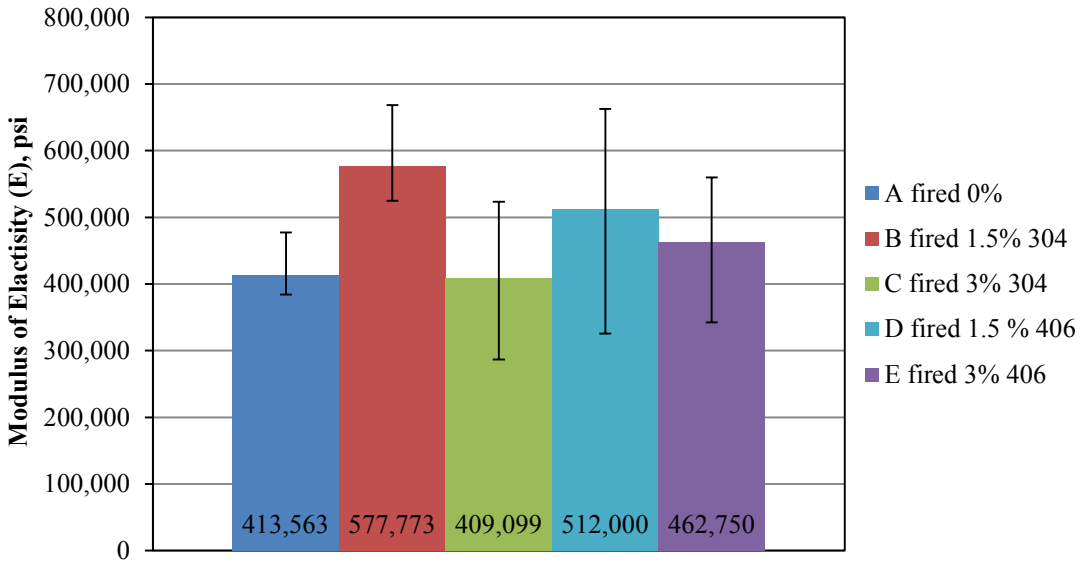

Figure 73 Modulus of Elasticity (E) values from all fired samples.

6.2.4 Pressure Profile

Finally, a pressure profile (Figure 74) could be established by using Hooke's Law while assuming that the ends were restrained (zero movement allowed on each side).

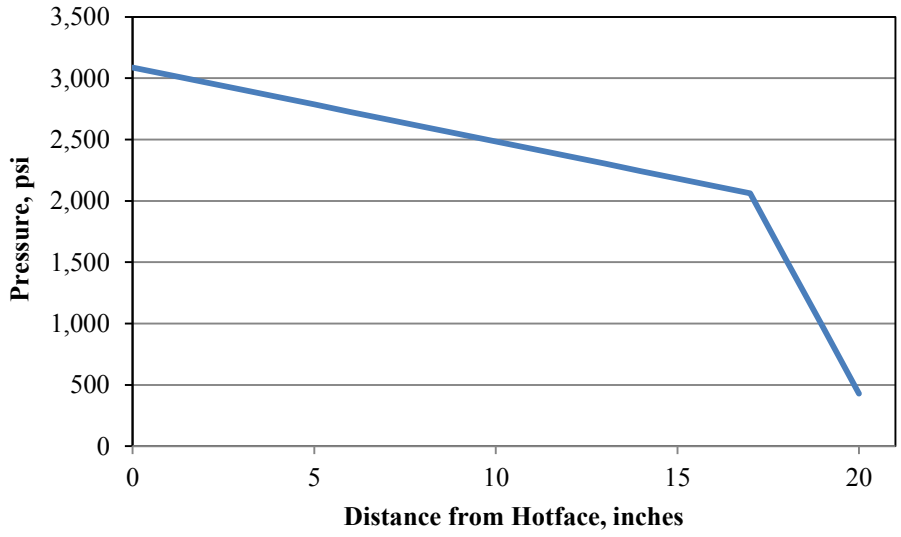

Figure 74: Pressure Profile, assuming a restrained condition

6.3 Finite Element Analysis Model

Ansys computer software was used to generate Finite Element Model of the block. Figures 75 and 76 show the precast block's loading and restraint. For simplification of the modeling process, the curb geometry was represented as a 12 inch x 12 inch x 20 inch rectangular block. Loading from 6.2.4 was fed into the model and results were generated for deformation and strain.

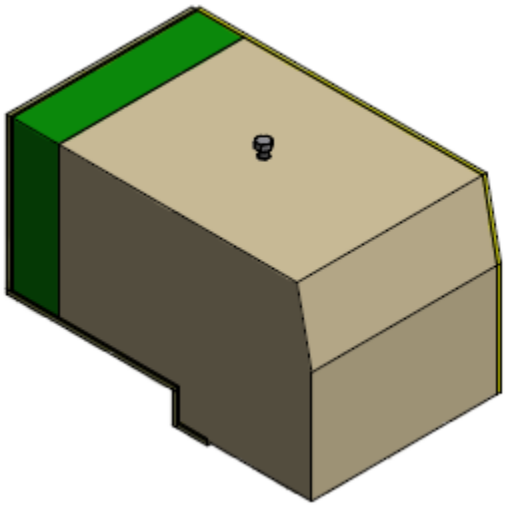

Figure 75: 3D Model of Curb

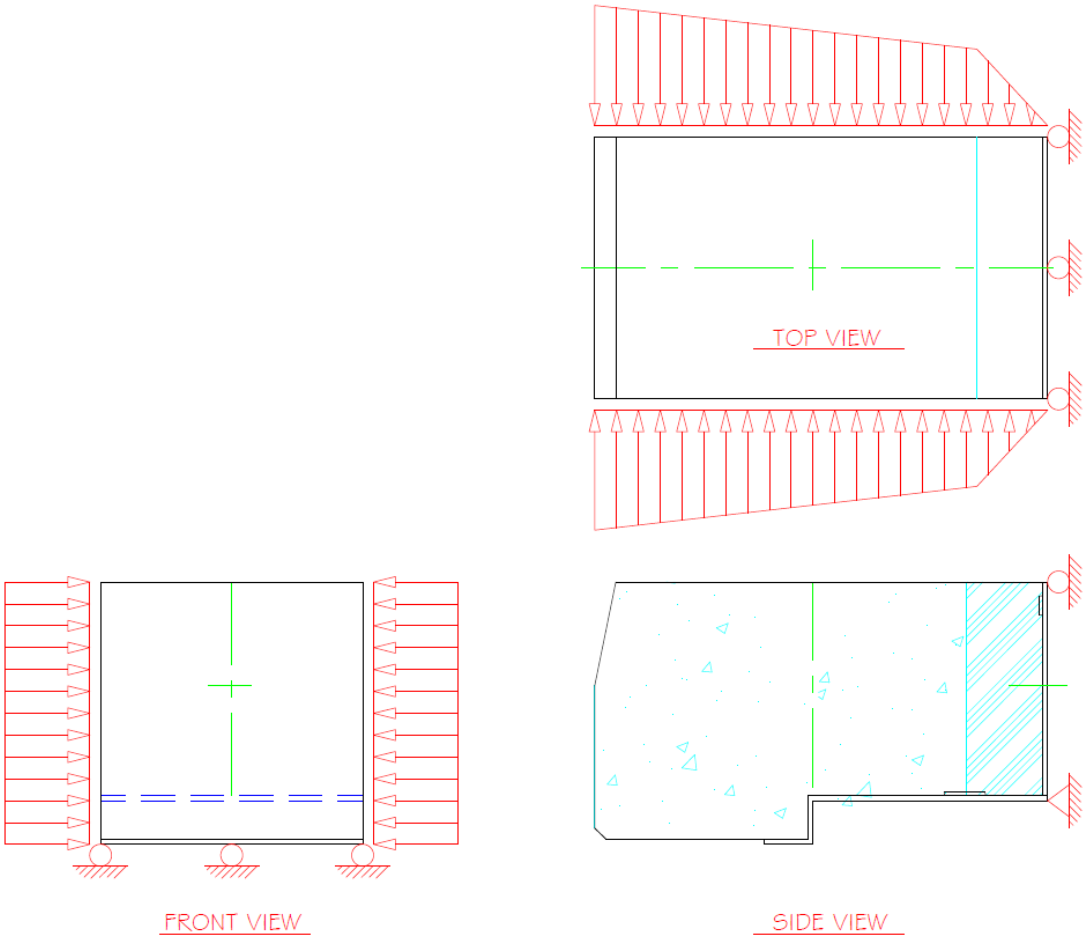

Figure 76: Curb Loading

6.3.1 Deformation

Deformations due to the prescribed pressures show that the block, when confined, will bulge forward towards the unrestrained hot face (Figures 77, 78, 79, and 80). Because of the non-uniform loading, the deformation is not uniform causing differential strains and stresses throughout the block. The surface of the block generates stresses upwards of 2000 psi (2280 psi), which is not over the MOR stress limit of the material, however, the fact that the material is unconfined at the hot face and being forced away, may cause failures over time. This type of failure was seen on Northshore Mining's Furnace 6 where the curb was not allowed to expand and the face had spalled off (Figure 81).

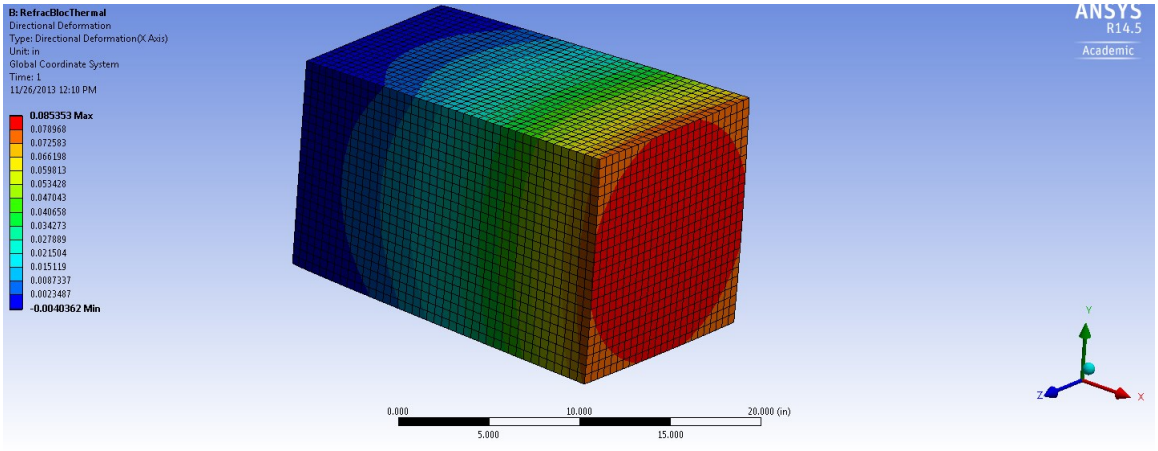

Figure 77: Directional Deformation (x-axis)

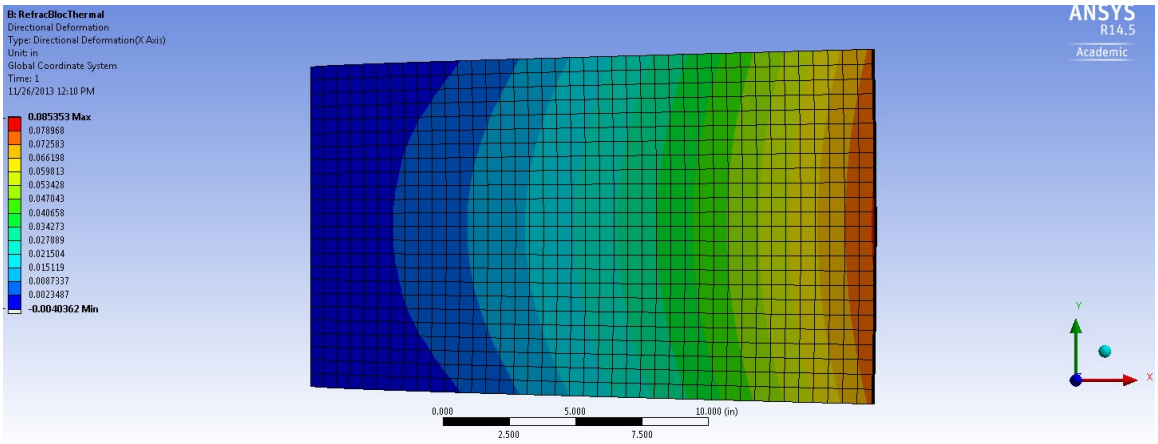

Figure 78: Directional Deformation (x-axis)

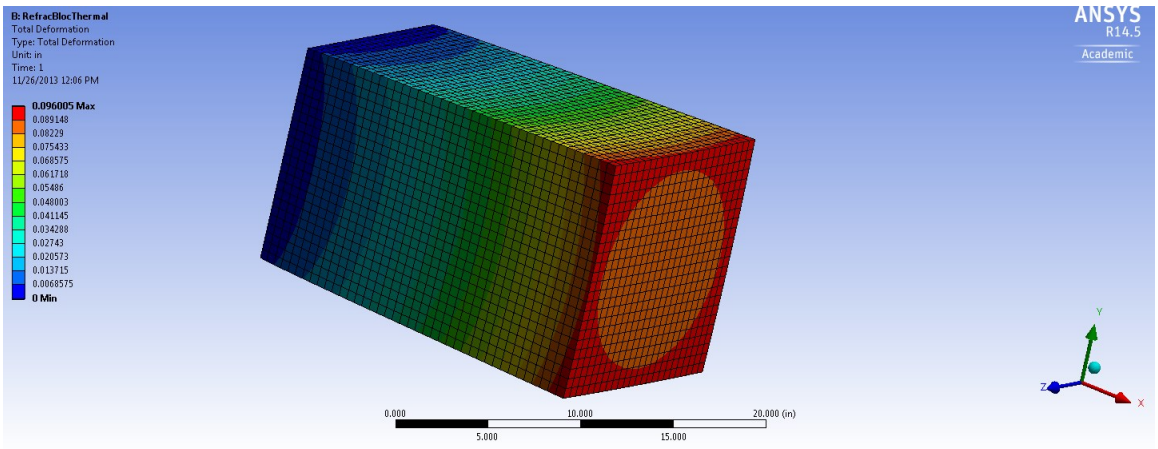

Figure 79: Total Deformation

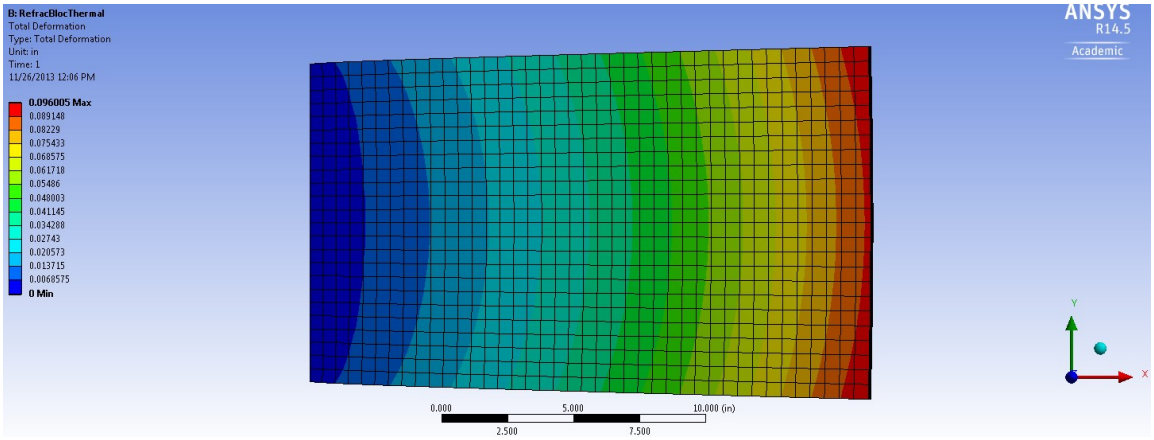

Figure 80: Total Deformation

Figure 81: Curb Failure Furnace 6

6.4 Stress Analysis Summary

The results from this FEA analysis showed that during furnace operating conditions compression forces parallel with the furnace wall would not exceed the compression strength of the material. It also showed that stresses perpendicular to the face would not exceed the tensile material strength of the material, however, adequate expansion joints can eliminate these stresses altogether and thus minimize the risk of failure over time.

CHAPTER 7: SUMMARY, CONCLUSIONS, AND RECOMMENDATIONS

7.1 Summary

This study set out to investigate an optimal reinforcing needle design for a monolithic precast refractory curb shape in a straight-grate taconite iron oxidizing furnace. It explored several different stainless steel alloys at several different weight concentrations in a known high alumina castable refractory. The study executed most standard physical property ASTM tests pertaining refractory with set formulations. This was in an effort to compare the studied material against existing data on materials, specifications, and standards. Cold Compressive Strength, Cold Modulus of Rupture, Hot Modulus of Rupture and Thermal Dilation tests provided much information to support design decisions made, with the most revealing being the Thermal Shock test.

Stainless steel needle material properties were also explored, of those, revelations of the needle alloy corrosion were the most beneficial in supporting the thesis presented.

At the same time, the study also explored and followed a real-world design application of a furnace reline at Cliff's Northshore Mine in Silver Bay, Minnesota. The study used lab data gathered to improve and maximize the engineering design while using in-the-field feedback information to improve lab tests and information generated by a lab and maximize the usefulness of this research.

7.2 Findings

7.2.1 Major Findings

The thesis also concluded the following about reinforcing added to this refractory:

• Under initial conditions of pouring, drying, and curing refractory, stainless steel needle reinforcing reduces Compressive Strength and Modulus of Rupture properties.

• Needles help retain integrity of refractory under thermal shock conditions by holding the refractory together and controlling cracking when cycled to furnace conditions based on tests performed to ASTM specifications.

• Oxidation is a key consideration in reinforcement selection. Corrosion by oxidation degrades the needles creating stresses and strains leading to lack of performance.

• 406 ALFA 1 stainless steel alloy is far superior to 304 stainless steel alloy in this furnace application based on CMOR test performed by this study after a thermal shock situation. This was reaffirmed in the literature review supportive materials and the anecdotal evidence. This is primarily due to the fact that 304 stainless steel operating temperature ranges are exceeded in this design condition.

• A 3% addition (by weight) of 406 ALFA 1 needles added to a TuffCrete 65M vibratory cast refractory performed the best under thermal shock conditions that attempted to mimic a worst case design of furnace conditions.
• Higher needle concentration samples outperformed lower needles concentration samples in a thermal shock loading situation.
• The benefits of refractory reinforced with 3% 406 ALFA 1 stainless steel needles to guard against thermal shock conditions seen in a furnace conditions far outweigh any disadvantages dues to lower physical properties at room temperature when needles are added, while physical strength properties for reinforced refractory still fall well within limits of furnace calculations.

7.2.2 Other Findings

• When ceramic materials experience a phase change from hydraulic to ceramic, non-elastic thermal expansion characteristics become quite complex. This complexity is important to understand in design, installation, or maintenance of this type of furnace lining.
• Geometric needle design was proper for the material and application used in this study based on failure mode.
• Although the study concluded that reinforcing of a 406 stainless steel alloy at 3% concentration is desirable, it failed to find the break point were adding too many needles would not be advantageous. In addition, it did not determine the most economical design.
• Lower sample aspect ratios (length to depth) increase the chances of an unconventional (non-bending) failure mode resulting in data that can skew results.
• The refractory used for a controlled base material in this study was of high quality and consistence with manufacturer's research and data sheets.

7.3 Conclusions

This study concluded that reinforcing refractory with stainless steel needles is beneficial when lining a taconite processing furnace and that needle concentration density along with chemical makeup can be adjusted to optimize the linings mechanical properties performance under thermal loads; however, 304 alloy should no longer be considered at any concentrations as reinforcement in this application since the furnace temperatures are above the service temperatures of 304.

7.4 Future Recommendations

Tests performed in this study were adequate to draw conclusions for a thesis regarding reinforcement, however, further experimentation and study would be valuable in refining details of future furnace relines.

• Install mullite based 65% alumina precast curbs with 3% 406 ALFA 1 stainless steel in future relines of taconite furnaces.
• Complete further studies to establish break point for optimal properties and economical design.
• Because the cost of 406 is approximately double the price of 304 and adds about 20% to the cost of the precast curb. A cost and risk analysis should be reviewed in all decisions.
• Explore other alloys for economic considerations such as higher chrome content (i.e. 310 stainless)
• Educate engineers, operators, and managers at taconite plants on refractory design and maintenance
• Run tests of thermal expansion to as-built and as-installed conditions to understand any unforeseen behaviors that can be engineered out.
• Have manufacturers' data sheets display reversible expansion.
• Use a three point bending model close to ASTM C-78 "Flexural Strength of Concrete" for CMOR testing when true modulus of rupture properties are needed.
• Monitor in-service refractory lining installed as a part of this project.
• Explore more accurate tests of in-service samples at furnace conditions.
• Implement any ideas or changes on upcoming install on Furnace 11
• The information gathered for this study was tested in a cast scenario. The majority of the furnace wall is the same product, only it was shotcreted in. It would be beneficial to test shotcrete material to confirm assumptions and have confidence in the complete liner package.
• Implement destructive testing of precast pieces along with refractory installed in the field. Similar Quality Assurance (QA) tests are done on road and building construction sites with concrete. Shotcrete could be shot onto a board next to material installed in the field, samples could then be tested with same procedures as performed in manufactures Q.C. lab.
• Determine if needle concentration variation is practical in these precast assemblies. Perform FEA analysis to determine optimal needle distribution.
• Research effects of corrosive and more reactive fuels on refractory reinforcement.
• Explore the effects and relationship that the aluminum contained in a 406 needle stainless steel needle has in a high alumina refractory as used in this study.

Engineering is the application of science and is the bridge between data generated from tests done in a lab data and practices executed in the field. How to properly connect the two defines the success of the project. This study was an effort to maintain that spirit by gathering information valuable to engineers working on taconite processing furnace linings.

REFERENCES

[1] E. W. Davis, "Pioneering with Taconite," *Minnesota Historical Society, St. Paul, Minnesota*, 1964

[2] Stephen C. Carniglia and Gordon L. Barna, "Handbook of Industrial Refractories Technology," *Noyes Publications, Park Ridge, New Jersey*, pp 3, 1992

[3] Harbison-Walker, "Modern Refractory Practice, Fifth Edition," *Harbison-Walker, Pittsburgh, PA*, pp PR-19-24, 1992

[4] Charles A. Schacht, "Refractories Linings," *Marcel Dekker, New York, New York*, 1995

[5] Charles A. Schacht, "Refractories Handbook," *CRS Press, Boca Raton, Florida*, 2004

[6] Lloyd E. Hackman, Ribbon Technology Corporation, "Hot Corrosion of Steel Fiber in Refractories,"*American Ceramic Society, Detroit, MI*, 1978

[7] Fibercon International Inc. (n.d.). Table of "Fibercon Standard Alloys". Retrieved October 6, 2013, fromhttp://www.fiberconfiber.com/refractory.html

[8] E.Cailleux, T. Cutard, and G. Bernhart, "Pullout of Steel Fibres from a Refractory Castable: Experiment and Modeling," *Mechanics and Materials*, 2005

[9] R.Nobuhara, Y.Nishimoto, K.Sato, J.Nishiioka, and H.Tetsuyama "Evaluation of Dispersiblity of Stainless Fiber in Reinforced Castable Refractories," *Taikabutsu,* 2000

[10] ASTM International, "C 862-02 Standard Practice for Preparing Refractory Concrete Specimens by Casting," *ASTM International, West Conshohocken, PA*, 2008

[11] L.V.Uzberg, A.A. Malyutin, G.V. Efimova, A.F.Edneral, and N.N. Teplyakov, "A Study of Reinforced Refractory Concrete," *Refractories and Industrial Ceramics*, 1997

[12] G.A. Gogotsi, Ya.L.Grushevskil, A.A. Kurashevskil, and V.A.Artemov, "Strength of Reinforced Refractory Materials," Institute *of Strength of Materials, Ukrainian, SSR*, 1975

[13] I.D. Hashcheev, K.G. Zemlyanoi, S.A.Podkopaev, E.V. Korsukov, L.A.Karpets, and I.V.Kormina, "Use of Carbon Fibers in Refractory Materials, " *Refractories and Industrial Ceramics*, 2009

[14] Cemail Aksel (2003) "The effect of mullite on the mechanical properties and thermal shock behavior of alumina-mullite refractory materials"

[15] Allied Mineral Products, Inc, "TuffCrete 65M Material Data Sheet," *Allied Mineral Products, Inc, Columbus, OH*, 2007

[16] ASTM International, "C 467-97 Standard Classification of Mullite Refractories," *ASTM International, West Conshohocken, PA*, 2008

[17] Mitchell Fibercon,Inc., "Fibercon Facts and Features," *Mitchell Fibercon, Inc., Evan City, PA*, (n.d.)

[18] Fibercon International Inc."Material Data Sheet – 304 Slit-Sheet Fibers," *Fibercon International, Evans City, PA*, 2007

[19] Fibercon International Inc. "Material Data Sheet – 406ALFA-1 Slit-Sheet Fibers",*Fibercon International, Evans City, PA*, 2007

[20] Jim Wunich, "Buying Firebricks," *Ceramic Publication Company, Lithonia, GA*, 2010

[21] ASTM International, "C 862-02 Standard Practice for Preparing Refractory Concrete Specimens by Casting," *ASTM International, West Conshohocken, PA*, 2008

[22] ASTM International, "C 583-10 Standard Test Method of Modulus of Rupture of Refractory Materials at Elevated Temperatures," *ASTM International, West Conshohocken, PA*, 2010

[23] ASTM International, "C 832-00 Standard Test Method of Measuring Thermal Expansion and Creep of Refractories under Load," *ASTM International, West Conshohocken, PA*, 2010

[24] ASTM International, "C 133 Standard Test Method for Cold Crushing Strength and Modulus of Rupture of Refractories," *ASTM International, West Conshohocken, PA*, 2008

[25] ASTM International, "C 1171-05 Standard Test Method for Quantitative Measuring the Effects of Thermal Shock and Thermal Cycling on Refractories," *ASTM International, West Conshohocken, PA*, 2011

[26] ASTM International, "C 1419-99a Standard Test Method for Sonic Velocity in Refractory Materials at Room Temperature and Its Use in Obtaining an Approximate Young's Modulus," *ASTM International, West Conshohocken, PA*, 2009

[27] ASTM International, "C 20-00 Standard Test Method for Apparent Porosity, Water Absorption, Apparent Specific Gravity, and Bulk Density of Burned Refractory Brick and Shapes by Boiling Water,"*ASTM International, West Conshohocken, PA*, 2010

[28] ASTM International, "C 914-09 Standard Test Method for Bulk Density and Volume of Solid Refractories by Wax Immersion,"*ASTM International, West Conshohocken, PA*, 2009

[29] Allegheny Ludlum Steel Division "Technical Data, Blue Sheet, Stainless Steel Allegheny Ludlum ALFA-1 and ALFA II Type 406 Alloys," *Allegheny Ludlum Steel Division, Pittsburgh, PA* ,1990

[30] Gang Engineering (n.d.). "Indurating Machine". Retrieved November 2, 2013, from http://www.gangengineering.com

[31] Shanghai BinQ Mining Equipment Co.,Ltd. (n.d.). "KOBELCO-pelletizing-plant". Retrieved November 2, 2013, from http://www.raymondgrindingmill.com

APPENDIX A: Raw Data

Table 16: Dried Samples, CMOR and Compression Data

PROJECT:	Robb Peterson								Use only if your zero point is 0. If your zero point is the initial bar length, do not use this box.			FILL IN GRAY AREAS			
			Hold Time (hr)	If Firing Temp. Not Listed => Enter Here	Bar Dimensions							TECH:	TRM,SRB,JAK		
Firing Temp.:	1	230° F (110° C)	24		Length	Width	Thick				Spread of Breadth (Bar Span) =	DATE:	3/19/2013		
Furnace Used:		Dryer									7				

		Measurement From Zero Point							Results				Compression			
	Bar #	In. Len.	Fin. Len.	Width	Thick	Mass	Load 1	Load 2	Calc. Den.	PLC	Cold MOR	Bar #	Width	Length	Peak Load (lbs)	Compression Strength (psi)
Material 1:	1	8.996	8.996	2.209	2.503	2074.3	3186		158.9	0.00	2417	1	2.245	2.348	79,670	15,114
As Made	2	8.985	8.985	2.185	2.499	2049.7	3633		159.2	0.00	2796	2	2.228	2.380	72,680	13,706
	3	8.989	8.989	2.178	2.503	2041.7			158.7	0.00		3	2.209	2.373	72,990	13,924
	4	8.985	8.985	2.110	2.500	1974.7	3129		158.7	0.00	2491	4	2.153	2.355	65,370	12,893
	5	8.984	8.984	2.139	2.544	2023.9	3520		157.7	0.00	2670	5	2.186	2.372	82,580	15,926
									158.6	0.00	2593			AVG.=	74,658	14,313
	Bar #	In. Len.	Fin. Len.	Width	Thick	Mass	Load 1	Load 2	Calc. Den.	PLC	Cold MOR	Bar #	Width	Length	Peak Load (lbs)	Compression Strength (psi)
Material 2:	1	8.989	8.989	2.104	2.493	1999.0	3401		161.5	0.00	2731	1	2.049	2.352	64,790	13,444
1.5% 304	2	8.969	8.969	2.250	2.513	2127.3	3707		159.8	0.00	2739	2	2.293	2.389	70,220	12,819
	3	8.980	8.980	2.113	2.509	1993.0	3267		159.5	0.00	2579	3	2.076	2.373	68,490	13,903
	4	8.963	8.963	2.160	2.513	2052.9	3654		160.7	0.00	2813	4	2.232	2.362	73,730	13,985
	5	8.974	8.974	2.140	2.534	2062.8	3581		161.5	0.00	2736	5	2.119	2.383	51,620	10,223
									160.6	0.00	2720			AVG.=	65,770	12,875
	Bar #	In. Len.	Fin. Len.	Width	Thick	Mass	Load 1	Load 2	Calc. Den.	PLC	Cold MOR	Bar #	Width	Length	Peak Load (lbs)	Compression Strength (psi)
Material 3:	1	8.985	8.985	2.139	2.495	2004.1	2489		159.2	0.00	1963	1	2.117	2.370	40,270	8,026
3.0% 304	2	8.985	8.985	2.243	2.499	2120.7	3189		160.4	0.00	2390	2	2.210	2.373	54,190	10,333
	3	9.011	9.011	2.149	2.502	2033.0	3038		159.8	0.00	2371	3	2.129	2.356	47,560	9,482
	4	8.987	8.987	2.156	2.523	2062.5	3398		160.7	0.00	2600	4	2.143	2.340	53,000	10,569
	5	8.987	8.987	2.178	2.505	2048.2	3143		159.1	0.00	2415	5	2.211	2.350	46,260	8,903
									159.9	0.00	2348			AVG.=	48,256	9,463
	Bar #	In. Len.	Fin. Len.	Width	Thick	Mass	Load 1	Load 2	Calc. Den.	PLC	Cold MOR	Bar #	Width	Length	Peak Load (lbs)	Compression Strength (psi)
Material 4:	1	8.972	8.972	2.214	2.552	2131.5	3213		160.2	0.00	2340	1	2.262	2.355	65,060	12,213
1.5% 406	2	8.976	8.976	2.166	2.496	2017.7	2925		158.4	0.00	2276	2	2.187	2.365	43,800	8,468
	3	8.981	8.981	2.210	2.505	2081.7	3351		159.5	0.00	2537	3	2.254	2.385	57,150	10,631
	4	8.982	8.982	2.137	2.498	1996.4	2844		158.6	0.00	2239	4	2.159	2.314	45,050	9,017
	5	8.992	8.992	2.254	2.499	2132.0	3243		160.4	0.00	2419	5	2.292	2.334	38,540	7,204
									159.4	0.00	2362			AVG.=	49,920	9,507
	Bar #	In. Len.	Fin. Len.	Width	Thick	Mass	Load 1	Load 2	Calc. Den.	PLC	Cold MOR	Bar #	Width	Length	Peak Load (lbs)	Compression Strength (psi)
Material 5:	1	8.992	8.992	2.197	2.506	2072.9	3065		159.5	0.00	2333	1	2.176	2.375	66,380	12,844
3.0% 406	2	8.996	8.996	2.189	2.493	2054.6	2993		159.4	0.00	2310	2	2.147	2.350	50,430	9,995
	3	9.001	9.001	2.233	2.497	2120.2	3114		160.9	0.00	2348	3	2.214	2.355	59,140	11,343
	4	8.987	8.987	2.181	2.508	2066.3	3038		160.1	0.00	2325	4	2.167	2.352	51,540	10,112
	5	8.990	8.990	2.138	2.561	2085.5	2978		161.4	0.00	2230	5	2.107	2.347	49,170	9,943
									160.3	0.00	2309			AVG.=	55,332	10,848

Table 17: Fired Data, CMOR and Compression Data

PROJECT:	Robb Peterson			Use only if your zero point is 0. If your zero point is the initial bar length, do not use this box.			FILL IN GRAY AREAS		
		Hold Time (hr)	If Firing Temp. Not Listed => Enter Here	Bar Dimensions			Spread of Breadth (Bar Span) =	TECH:	TRM,SRB,JAK
Firing Temp.:	2	2000° F (1093° C)	5	Length	Width	Thick	7	DATE:	3/19/2013
Furnace Used:		L&L							

		Measurement From Zero Point							Results			Compression				
	Bar #	In. Len.	Fin. Len.	Width	Thick	Mass	Load 1	Load 2	Calc. Den.	PLC	Cold MOR	Bar #	Width	Length	Peak Load (lbs)	Compression Strength (psi)
Material 1:	1	8.989	8.959	2.167	2.489	1983.7	5563		156.4	-0.33	4351	1	2.161	2.341	104,050	20,568
As Made	2	8.989	8.957	2.220	2.495	2044.7	5401		157.0	-0.36	4104	2	2.199	2.386	97,140	18,514
	3	8.990	8.950	2.179	2.487	2017.6	5627		158.5	-0.44	4384	3	2.172	2.364	108,260	21,084
	4	8.974	8.938	2.106	2.488	1952.3	5433		158.8	-0.40	4376	4	2.116	2.362	93,740	18,756
	5	8.980	8.935	2.107	2.559	1959.7	5182		155.0	-0.50	3943	5	2.103	2.374	87,500	17,526
									157.1	-0.41	4232			AVG.=	98,138	19,290

	Bar #	In. Len.	Fin. Len.	Width	Thick	Mass	Load 1	Load 2	Calc. Den.	PLC	Cold MOR	Bar #	Width	Length	Peak Load (lbs)	Compression Strength (psi)
Material 2:	1	8.976	8.957	2.097	2.491	1980.5	4692		161.3	-0.21	3786	1	2.082	2.390	99,910	20,078
1.5% 304	2	8.990	8.967	2.144	2.501	2010.1	4945		159.3	-0.26	3872	2	2.167	2.357	78,680	15,404
	3	9.002	8.979	2.241	2.486	2074.4	5491		158.0	-0.26	4163	3	2.252	2.369	56,200	10,534
	4	9.016	8.966	2.242	2.502	2102.1	5014		159.2	-0.55	3751	4	2.377	2.228	59,280	11,193
	5	8.981	8.934	2.186	2.487	2053.7	5825		161.1	-0.52	4524	5	2.198	2.362	73,650	14,186
									159.8	-0.36	4019			AVG.=	73,544	14,279

	Bar #	In. Len.	Fin. Len.	Width	Thick	Mass	Load 1	Load 2	Calc. Den.	PLC	Cold MOR	Bar #	Width	Length	Peak Load (lbs)	Compression Strength (psi)
Material 3:	1	8.989	8.963	2.174	2.486	2059.4	4466		162.0	-0.29	3490	1	2.162	2.349	75,430	14,853
3.0% 304	2	8.985	8.963	2.200	2.494	2067.9	6081		160.2	-0.24	4666	2	2.156	2.367	65,020	12,741
	3	8.992	8.968	2.206	2.489	2062.0	5455		159.5	-0.27	4191	3	2.192	2.361	65,670	12,689
	4	9.001	8.971	2.166	2.505	2026.3	5301		158.6	-0.33	4095	4	2.178	2.362	70,810	13,764
	5	8.997	8.966	2.215	2.508	2101.8	5095		160.8	-0.34	3840	5	2.212	2.371	63,380	12,085
									160.2	-0.30	4056			AVG.=	68,062	13,226

	Bar #	In. Len.	Fin. Len.	Width	Thick	Mass	Load 1	Load 2	Calc. Den.	PLC	Cold MOR	Bar #	Width	Length	Peak Load (lbs)	Compression Strength (psi)
Material 4:	1	8.977	8.951	2.149	2.527	2012.9	5222		157.8	-0.29	3996	1	2.110	2.370	73,200	14,638
1.5% 406	2	8.968	8.946	2.208	2.492	2052.3	5233		158.8	-0.25	4007	2	2.258	2.358	93,350	17,533
	3	8.981	8.944	2.171	2.492	2027.1	5245		159.6	-0.41	4085	3	2.163	2.331	81,830	16,230
	4	8.978	8.950	2.117	2.491	1951.8	4793		157.5	-0.31	3831	4	2.071	2.344	85,080	17,526
	5	8.980	8.944	2.073	2.492	1916.5	4489		158.0	-0.40	3661	5	2.046	2.343	79,440	16,571
									158.3	-0.33	3916			AVG.=	82,580	16,500

	Bar #	In. Len.	Fin. Len.	Width	Thick	Mass	Load 1	Load 2	Calc. Den.	PLC	Cold MOR	Bar #	Width	Length	Peak Load (lbs)	Compression Strength (psi)
Material 5:	1	8.989	8.958	2.062	2.497	1912.1	4271		157.9	-0.34	3488	1	2.172	2.351	74,520	14,594
3.0% 406	2	8.991	8.954	2.175	2.490	2018.0	4636		158.5	-0.41	3610	2	2.010	2.370	69,430	14,575
	3	8.981	8.954	2.164	2.484	2009.0	4737		159.0	-0.30	3725	3	2.010	2.352	70,330	14,877
	4	8.973	8.943	2.233	2.497	2051.2	4863		156.7	-0.33	3667	4	2.288	2.352	63,800	11,856
	5	8.988	8.965	2.186	2.552	2552.0	5211		194.4	-0.26	3843	5	2.247	2.350	65,560	12,416
									165.3	-0.33	3667			AVG.=	68,728	13,663

Table 18: Work of Fracture Data

	Sample #					
			flexural	flexural	Work of Fracture	WOF Ave
Comp Sample #	Dried to 230F	Peak Load	Strength (psi)	Strength (ave)	lb-in	
34613	A1	3186.0	2416.7	2593	20.908	25
34614	A2	3633.0	2795.6		35.200	
	A3	broke	broke			
34615	A4	3129.0	2491.3		19.982	
34616	A5	3520.0	2669.9		24.303	work to first pt deflection twice
	Fired to 2000F					
34617	A6	5563.0	4351.0	4232	41.645	43
34618	A7	5401.0	4103.6		36.205	
34619	A8	5627.0	4383.9		47.059	
34620	A9	5433.0	4375.9		53.107	
34621	A10	5182.0	3943.5		36.140	
	Dried to 230F					
34622	B1	3401.0	2730.9	2720	19.681	24
34623	B2	3707.0	2739.3		32.984	
34624	B3	3267.0	2578.9		13.317	
34625	B4	3654.0	2812.7		26.185	
34626	B5	3581.0	2736.3		28.178	
	Fired to 2000F					
34627	B6	4692.0	3786.2	4019	35.976	41
34628	B7	4945.0	3871.7		31.251	
34629	B8	5491.0	4162.9		44.443	
34630	B9	5014.0	3751.1		47.191	
34631	B10	5825.0	4523.6		45.639	
	Dried to 230F					
34632	C1	2489.0	1962.7	2348	34.797	26
34633	C2	3189.0	2390.5		31.160	
34634	C3	3038.0	2371.2		19.305	
34635	C4	3398.0	2599.7		23.207	
34636	C5	3143.0	2414.7		22.117	
	Fired to 2000F					
34637	C6	4466.0	3490.2	4056	30.558	46
34638	C7	6081.0	4666.0		53.071	
34639	C8	5455.0	4191.1		51.926	
34640	C9	5301.0	4095.2		44.864	
34641	C10	5095.0	3839.8		50.819	
	Dried to 230F					
34642	D1	3213.0	2339.7	2362	18.084	17
34643	D2	2925.0	2276.0		14.314	
34644	D3	3351.0	2537.2		17.885	
34645	D4	2844.0	2239.4		15.369	
34646	D5	3243.0	2419.1		17.554	
	Fired to 2000F					
34647	D6	5222.0	3995.6	3915	33.367	33
34648	D7	5223.0	3999.6		39.038	
34649	D8	5245.0	4084.9		35.471	
34650	D9	4793.0	3831.1		31.568	
34651	D10	4489.0	3661.4		27.537	
	Dried to 230F					
34652	E1	3065.0	2332.5	2309	19.496	17
34653	E2	2993.0	2310.0		18.445	
34654	E3	3114.0	2348.5		17.345	
34655	E4	3038.0	2325.2		17.401	
34656	E5	2978.0	2229.9		14.717	
	Fired to 2000F					
34657	E6	4271.0	3488.1	3667	28.634	33
34658	E7	4636.0	3609.7		28.327	
34659	E8	4737.0	3725.1		34.991	
34660	E9	4863.0	3667.5		31.042	
34661	E10	5211.0	3843.3		40.728	

Table 19: Hot Modulus of Rupture Data

PROJECT:	Robb Peterson					
TECH:	TRM,SRB,JAK					
DATE:	3/19/2013					
Firing Temp.:	1	2000° F (1093° C)			If Firing Temp. Not Listed => Enter Here	
Furnace Used:		Hot MOR				
Conversion factors=						
Inside pin	2.4821			Pin Used:	Outside pin	
Outside pin	2.8714			Conversion factor:	2.8714	
	Bar Order	Width (Inches)	Thickness (Inches)	Load (In. H2O)	Force (lbs.)	HMOR (PSI)
Material 1: As Made	1	0.999	1.012	40.500	930	5,456
	2	1.021	0.981	34.250	787	4,804
	3	1.004	0.937	28.875	663	4,515
	4	1.024	0.933	28.000	643	4,329
	5	1.011	0.974	33.500	770	4,814
					AVERAGE	4,784
Material 2: 1.5% 304	1	1.017	0.952	33.000	758	4,935
	2	0.995	0.976	29.500	678	4,290
	3	1.015	1.010	30.750	706	4,093
	4	1.010	0.996	28.500	655	3,920
	5	1.115	0.964	35.500	815	4,722
					AVERAGE	4,392
Material 3: 3.0% 304	1	1.028	1.032	31.875	732	4,013
	2	1.007	0.937	25.000	574	3,897
	3	1.007	0.952	26.500	609	4,002
	4	0.991	0.975	32.000	735	4,682
	5	1.013	1.005	33.500	770	4,513
					AVERAGE	4,221
Material 4: 1.5% 406	1	1.001	0.990	36.500	838	5,128
	2	1.037	0.996	34.000	781	4,555
	3	0.986	0.983	28.500	655	4,123
	4	1.038	0.978	28.875	663	4,008
	5	0.972	0.968	27.500	632	4,162
					AVERAGE	4,395
Material 5: 3.0% 406	1	1.007	0.953	17.500	402	2,637
	2	1.008	0.948	29.625	681	4,507
	3	1.016	0.996	26.000	597	3,555
	4	1.000	0.998	28.750	660	3,978
	5	1.003	0.958	26.500	609	3,968
					AVERAGE	3,729

Table 20: Porosity Data

Porosity

Firing Temp.:	1500° F (815.6° C)	TECH:	TRM,SRB,JAK
Furnace Used:	L&L	DATE:	3/19/2013

	Bar #	Dry Wt.	Weight Sat. & Susp.	Sat. Wt.	App. Porosity	Specific Gravity	Bulk Density
Material 1:							
As Made	1	552.3	369.5	585.8	15.5	3.02	159.4
	2	483.8	323.8	513.3	15.6	3.02	159.4
	3	581.0	389.0	616.9	15.8	3.03	159.2
				Avg =	15.6	3.02	159.3

	Bar #	Dry Wt.	Weight Sat. & Susp.	Sat. Wt.	App. Porosity	Specific Gravity	Bulk Density
Material 2:							
1.5% 304	1	471.2	317.0	500.1	15.8	3.06	160.7
	2	536.2	360.6	570.2	16.2	3.05	159.7
	3	545.5	367.0	578.7	15.7	3.06	160.9
				Avg =	15.9	3.06	160.4

	Bar #	Dry Wt.	Weight Sat. & Susp.	Sat. Wt.	App. Porosity	Specific Gravity	Bulk Density
Material 3:							
3.0% 304	1	396.8	268.0	421.0	15.8	3.08	161.9
	2	532.7	360.7	565.5	16.0	3.10	162.4
	3	463.6	313.6	491.8	15.8	3.09	162.4
				Avg =	15.9	3.09	162.3

	Sample	Dry Wt.	Weight Sat. & Susp.	Sat. Wt.	App. Porosity	Specific Gravity	Bulk Density
Material 4:							
1.5% 406	1	555.0	374.0	590.2	16.3	3.07	160.3
	2	473.6	319.0	502.9	15.9	3.06	160.8
	3	583.6	394.5	620.6	16.4	3.09	161.2
				Avg =	16.2	3.07	160.7

	Sample	Dry Wt.	Weight Sat. & Susp.	Sat. Wt.	App. Porosity	Specific Gravity	Bulk Density
Material 5:							
3.0% 406	1	424.2	287.0	452.4	17.0	3.09	160.1
	2	500.1	338.0	534.0	17.3	3.09	159.3
	3	539.8	365.6	575.6	17.0	3.10	160.5
				Avg =	17.1	3.09	160.0

Table 21: Test Data Summary

Technician:	TRM,SRB,JAK	Project Name :	Robb Peterson
Requestor:	DGG	Date :	3/19/2013

		Materials/ Batches					
		TUFFCRETE 65M					
Firing Temp.	Hold Time	As Made	1.5% 304	3.0% 304	1.5% 406	3.0% 406	Kiln Used
Calculated Density (lb/ft^3)							
230° F (110° C)	24	159	161	160	159	160	Dryer
2000° F (1093° C)	5	157	160	160	158	165	L&L
Permanent Linear Expansion (%)							
230° F (110° C)	24	0.00	0.00	0.00	0.00	0.00	Dryer
2000° F (1093° C)	5	-0.41	-0.36	-0.30	-0.33	-0.33	L&L
CMOR - Modulus of Rupture (psi)							
230° F (110° C)	24	2593	2720	2348	2362	2309	Dryer
2000° F (1093° C)	5	4232	4019	4056	3916	3667	L&L
Compression (psi)							
230° F (110° C)	24	14313	12875	9463	9507	10848	Dryer
2000° F (1093° C)	5	19290	14279	13226	16500	13663	L&L
HOT MOR (psi)							
2000° F (1093° C)		4784	4392	4221	4395	3729	Hot MOR
App. Porosity (%)							
2000° F (1093° C)		15.6	15.9	15.9	16.2	17.1	
Apparent Specific Gravity							
2000° F (1093° C)		3.02	3.06	3.09	3.07	3.09	
Bulk Density (lb/ft^3)							
2000° F (1093° C)		159.3	160.4	162.3	160.7	160.0	

FLOW

Product	ASTM Tap or Self Flow	Water Level (mL)	Water Level (%)	Flow (%)	INITIAL SET (hrs:min)	FINAL SET (hrs:min)
As Made	SELF	#REF!	5.9	120	10:00*	14:30*
1.5% 304	SELF	#REF!	6.0	120	8:30*	14:30*
3.0% 304	SELF	#REF!	6.0	119	11:00*	15:00*
1.5% 406	SELF	#REF!	6.0	118	10:00*	14:15*
3.0% 406	SELF	#REF!	6.0	120	10:00*	15:00*

Table 22: Thermal Shock Data

PROJECT:		Robb Peterson							Use only if your zero point is 0. If your zero point is the initial bar length, do not use this box.		
				Hold Time (hr)		If Firing Temp., Not Listed => Enter Here	Bar Dimensions		
Firing Temp.:	1	2000° F (1093° C)					Length	Width	Thick
Furnace Used:		New 20 kVA							

		Measurement From Zero Point							Results		
	Bar #	In. Len.	Fin. Len.	Width	Thick	Mass	Load 1	Load 2	Calc. Den.	PLC	Cold MOR
Material 1:	1			2.147	2.487		9280				4193
A UNSHOCKED	2			2.173	2.425		9255				4346
	3			2.208	2.502		9934				4312
	4			2.195	2.581		11647				4779
	5			2.187	2.501		9059				3973
											4321

		Measurement From Zero Point							Results		
	Bar #	In. Len.	Fin. Len.	Width	Thick	Mass	Load 1	Load 2	Calc. Den.	PLC	Cold MOR
Material 1:	1			2.142	2.502		364				163
A SHOCKED	2			2.181	2.497		875				386
	3			2.236	2.497						
	4			2.185	2.563		1442				603
	5			2.205	2.512		309				133
											321

		Measurement From Zero Point							Results		
	Bar #	In. Len.	Fin. Len.	Width	Thick	Mass	Load 1	Load 2	Calc. Den.	PLC	Cold MOR
Material 1:	1			2.203	2.496		8984				3928
B UNSHOCKED	2			2.183	2.489		11500				5102
	3			2.242	2.499		10816				4635
	4			2.161	2.500		5092				2262
	5			2.237	2.482		8427				3669
											3919

		Measurement From Zero Point							Results		
	Bar #	In. Len.	Fin. Len.	Width	Thick	Mass	Load 1	Load 2	Calc. Den.	PLC	Cold MOR
Material 1:	1			2.205	2.494		1242				543
B SHOCKED	2			2.180	2.497		2506				1106
	3			2.222	2.512		1344				575
	4			2.139	2.503		364				163
	5			2.229	2.505		747				320
											542

		Measurement From Zero Point							Results		
	Bar #	In. Len.	Fin. Len.	Width	Thick	Mass	Load 1	Load 2	Calc. Den.	PLC	Cold MOR
Material 1:	1			2.188	2.492		8142				3595
C UNSHOCKED	2			2.120	2.489		8355				3817
	3			2.211	2.587		8235				3339
	4			2.178	2.515		8900				3876
	5			2.057	2.498		10105				4724
											3870

		Measurement From Zero Point							Results		
	Bar #	In. Len.	Fin. Len.	Width	Thick	Mass	Load 1	Load 2	Calc. Den.	PLC	Cold MOR
Material 1:	1			2.204	2.495		2101				919
C SHOCKED	2			2.140	2.488		8798				3985
	3			2.211	2.516		2813				1206
	4			2.195	2.554		5943				2490
	5			2.163	2.163		7164				4248
											2570

		Measurement From Zero Point							Results		
	Bar #	In. Len.	Fin. Len.	Width	Thick	Mass	Load 1	Load 2	Calc. Den.	PLC	Cold MOR
Material 1:	1			2.169	2.495		8193				3641
D UNSHOCKED	2			2.158	2.505		8823				3909
	3			2.203	2.522		9499				4067
	4			2.184	2.556		9010				3789
	5			2.167	2.489		9214				4118
											3905

		Measurement From Zero Point							Results		
	Bar #	In. Len.	Fin. Len.	Width	Thick	Mass	Load 1	Load 2	Calc. Den.	PLC	Cold MOR
Material 1:	1			2.192	2.498		2802				1229
D SHOCKED	2			2.179	2.491		2243				995
	3			2.211	2.505		2352				1017
	4			2.177	2.544		4917				2094
	5			2.163	2.498		3596				1599
											1387

		Measurement From Zero Point							Results		
	Bar #	In. Len.	Fin. Len.	Width	Thick	Mass	Load 1	Load 2	Calc. Den.	PLC	Cold MOR
Material 1:	1			2.244	2.487		8288				3583
E UNSHOCKED	2			2.149	2.492		7718				3470
	3			2.117	2.557		7680				3329
	4			2.205	2.489		7666				3367
	5			2.215	2.497		7783				3381
											3426

		Measurement From Zero Point							Results		
	Bar #	In. Len.	Fin. Len.	Width	Thick	Mass	Load 1	Load 2	Calc. Den.	PLC	Cold MOR
Material 1:	1			2.226	2.498		2668				1152
E SHOCKED	2			2.225	2.498		4985				2154
	3			2.139	2.500		9799				4398
	4			2.132	2.562		4011				1720
	5			2.267	2.503		2353				994
											2084

Table 23: Thermal Shock, Strength and Work of Fracture Data

	Sample #				
		flexural	flexural	Work of fracture	WOF Ave
Comp San	non-shock	Strength (psi)	Strength (psi) (ave)	lb-in	
34697	A1	4192.9	4,321	92.0	99
34698	A2	4345.5		86.4	
34699	A3	4312.2		114.1	
34700	A4	4779.2		115.1	
34718	A5	3973.3		89.7	
	shock				
34719	A1s	163.3	228	15.0	11
34720	A2s	386.1		11.2	
	A3s				
34721	A4s	0.0		76.2	
34722	A5s	133.2		7.4	
	non-shock				
34738	B1	3927.5	3,920	87.3	95
34739	B2	5102.1		124.5	
34740	B3	4639.3		141.9	
34741	B4	2262.1		40.0	
34742	B5	3669.1		80.8	
	shock				
34723	B1s	543.3	452	16.7	22
34724	B2s	781.9		44.9	
34725	B3s			46.8	
34726	B4s	163.0		14.6	
34727	B5s	320.4		11.2	
	non-shock				
34748	C1	3595.3	3,881	99.3	89
34749	C2	3816.9		75.0	
34750	C3	3391.4		76.5	
34751	C4	3876.2		94.0	
34752	C5	4723.5		101.7	
	shock				
34728	C1s	918.8	1,604	19.4	68
34729	C2s	2581.7		120.7	
34730	C3s	718.1		22.9	
34731	C4s	1718.1		76.0	
34732	C5s	2083.8		103.2	
	non-shock				
34753	D1	3640.8	3,905	72.8	88
34754	D2	3909.3		97.4	
34755	D3	4067.5		88.4	
34756	D4	3788.8		82.2	
34757	D5	4118.0		99.2	
	shock				
34733	D1s	122.9	1,100	29.5	37
34734	D2s	995.4		24.7	29
34735	D3s	821.7		14.6	
34736	D4s	2093.9		72.9	
34737	D5s	1467.0		45.5	
	non-shock				
34758	E1	3582.8	3,426	90.6	78
34759	E2	3470.0		65.3	
34760	E3	3329.1		70.2	
34761	E4	3367.1		83.3	
34762	E5	3381.3		82.7	
	shock				
34743	E1s	1152.5	1,832	31.2	41
34744	E2s	2154.3		45.4	33
34745	E3s	3141.7		70.3	
34746	E4s	1719.7		31.7	
34747	E5s	994.0		25.7	

Table 24: Thermal Shock, Ultrasonic Data

	Sample						
	All samples were originally fired to 2000F						
	Shock	S	Shock was 5 cycles to 2200F then to room temperature inb				4.5
	Non-Shock	NS					0.1143
Sample #	Shock or Non-Shock	Travel Time (us)	time (s)	length (m)	speed (m/s)	density	E (psi)
A5	NS	14.9	0.0000149	0.1143	7671.14094	163	22,284,834
A5	S	43	0.000043	0.1143	2658.13953	163	2,675,747
A2	S	49	0.000049	0.1143	2332.65306	163	2,060,581
A4	S	33	0.000033	0.1143	3463.63636	163	4,543,118
A1	S	37	0.000037	0.1143	3089.18919	163	3,613,920
B1	NS	15.5	0.0000155	0.1143	7374.19355	163	20,592,949
B2	NS	15.4	0.0000154	0.1143	7422.07792	163	20,861,258
B3	NS	15.9	0.0000159	0.1143	7188.67925	163	19,569,859
C1	NS	16.4	0.0000164	0.1143	6969.5122	163	18,394,765
C2	NS	16.4	0.0000164	0.1143	6969.5122	163	18,394,765
C3	NS	16.4	0.0000164	0.1143	6969.5122	163	18,394,765
D1	NS	15.4	0.0000154	0.1143	7422.07792	163	20,861,258
D2	NS	15.4	0.0000154	0.1143	7422.07792	163	20,861,258
E1	NS	15.9	0.0000159	0.1143	7188.67925	163	19,569,859
E2	NS	16.4	0.0000164	0.1143	6969.5122	163	18,394,765
B1	S	44.9	0.0000449	0.1143	2545.65702	163	2,454,083
B2	S	44.4	0.0000444	0.1143	2574.32432	163	2,509,666
B3	S	42.9	0.0000429	0.1143	2664.33566	163	2,688,236
B4	S	34.4	0.0000344	0.1143	3322.67442	163	4,180,854
B5	S	43.4	0.0000434	0.1143	2633.64055	163	2,626,652
C1	S	30.4	0.0000304	0.1143	3759.86842	163	5,353,463
C2	S	31.4	0.0000314	0.1143	3640.12739	163	5,017,907
C3	S	31.4	0.0000314	0.1143	3640.12739	163	5,017,907
C4	S	31.9	0.0000319	0.1143	3583.0721	163	4,861,839
C5	S	31.9	0.0000319	0.1143	3583.0721	163	4,861,839
D1	S	27.9	0.0000279	0.1143	4096.77419	163	6,355,848
D2	S	28.9	0.0000289	0.1143	3955.0173	163	5,923,607
D3	S	28.9	0.0000289	0.1143	3955.0173	163	5,923,607
D4	S	28.4	0.0000284	0.1143	4024.64789	163	6,134,021
D5	S	28.9	0.0000289	0.1143	3955.0173	163	5,923,607
E1	S	28.4	0.0000284	0.1143	4024.64789	163	6,134,021
E2	S	28.9	0.0000289	0.1143	3955.0173	163	5,923,607
E3	S	28.9	0.0000289	0.1143	3955.0173	163	5,923,607
E4	S	28.9	0.0000289	0.1143	3955.0173	163	5,923,607
E5	S	29.9	0.0000299	0.1143	3822.74247	163	5,534,005

Table 25: Thermal Shock Data Summary

Technician:			Project Name :	Robb Peterson	
Requestor:			Date :	3/22/2013	
Specimen	**A**	**B**	**C**	**D**	**E**
% Water Added	5.9	6.0	6.0	6.0	6.0
ASTM Flow (mm)	-	-	-	-	-
Self-Flow (mm)	120	120	119	118	120
Prefire Temp (°F)	2200	2200	2200	2200	2200
Shock Temp (°F)	2200	2200	2200	2200	2200
CMOR - Modulus of Rupture (psi)					
Unshocked Data (psi)	4321	3919	3870	3905	3426
Shocked Data (psi)	321	542	2570	1387	2084
% Loss	**92.6**	**86.2**	**33.6**	**64.5**	**39.2**
Thermal Cycle	0=	1=	2=	3=	4=
Crack Rating Scale	No cracking	Slight Cracking	Cracking	Severe Cracking	Failure
Cycle 1					
Cycle 2					
Cycle 3					
Cycle 4					
Cycle 5					

Table 26: In-service Data Summary

Technician:	TRM		Project Name :	Robb Peterson (In Service Samples)			
Requestor:			Date :	4/3/2013			
		Materials/ Batches					
Firing Temp.	**Hold Time**	**Sample A**	**Sample B**	**Sample C**	**Sample D**	**Kiln Used**	
Calculated Density (lb/ft^3)							
2000° F (1093° C)		**156**	**154**	**-**	**-**		
Permanent Linear Expansion (%)							
2000° F (1093° C)		**-0.24**	**-0.18**	**-**	**-**		
CMOR - Modulus of Rupture (psi)							
2000° F (1093° C)		**1652**	**2033**	**-**	**-**		
Compression (psi)							
2000° F (1093° C)		**12272**	**10833**	**7684**	**9196**		
App. Porosity (%)							
2000° F (1093° C)		**17.4**	**15.5**	**15.7**	**15.9**		
Apparent Specific Gravity							
2000° F (1093° C)		**3.10**	**3.06**	**3.03**	**3.06**		
Bulk Density (lb/ft^3)							
2000° F (1093° C)		**160.2**	**161.3**	**159.5**	**161.0**		

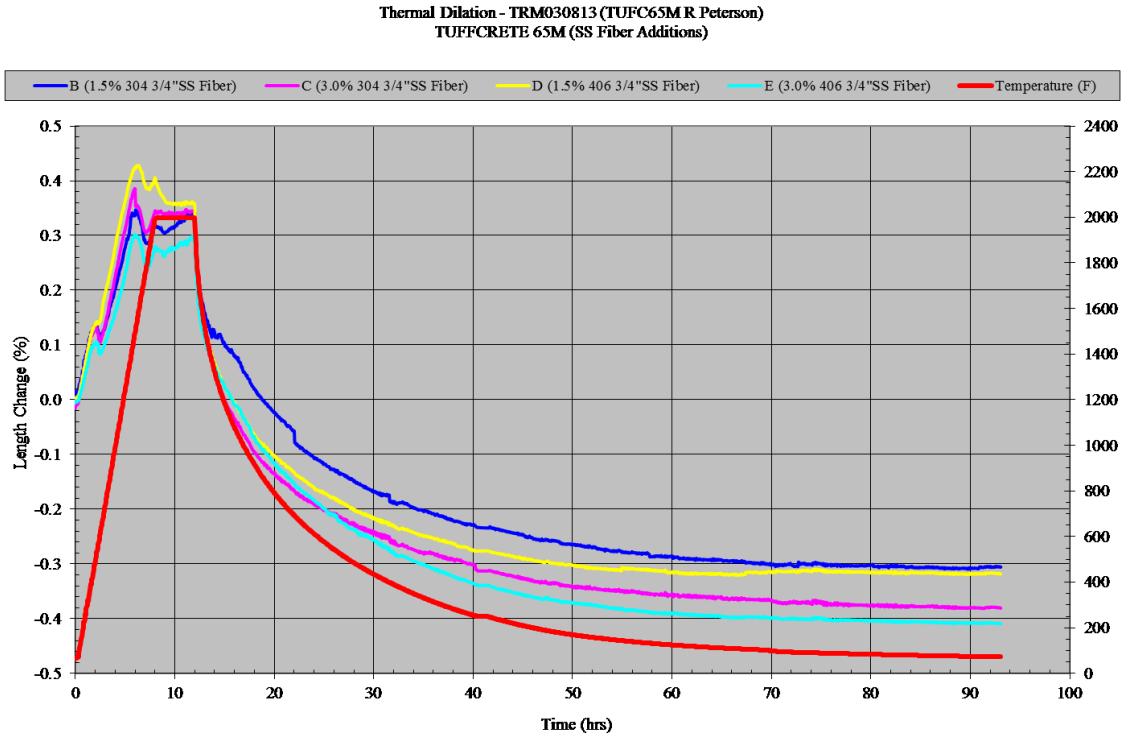

Figure 82: Thermal Dilation Time Graph, First Run

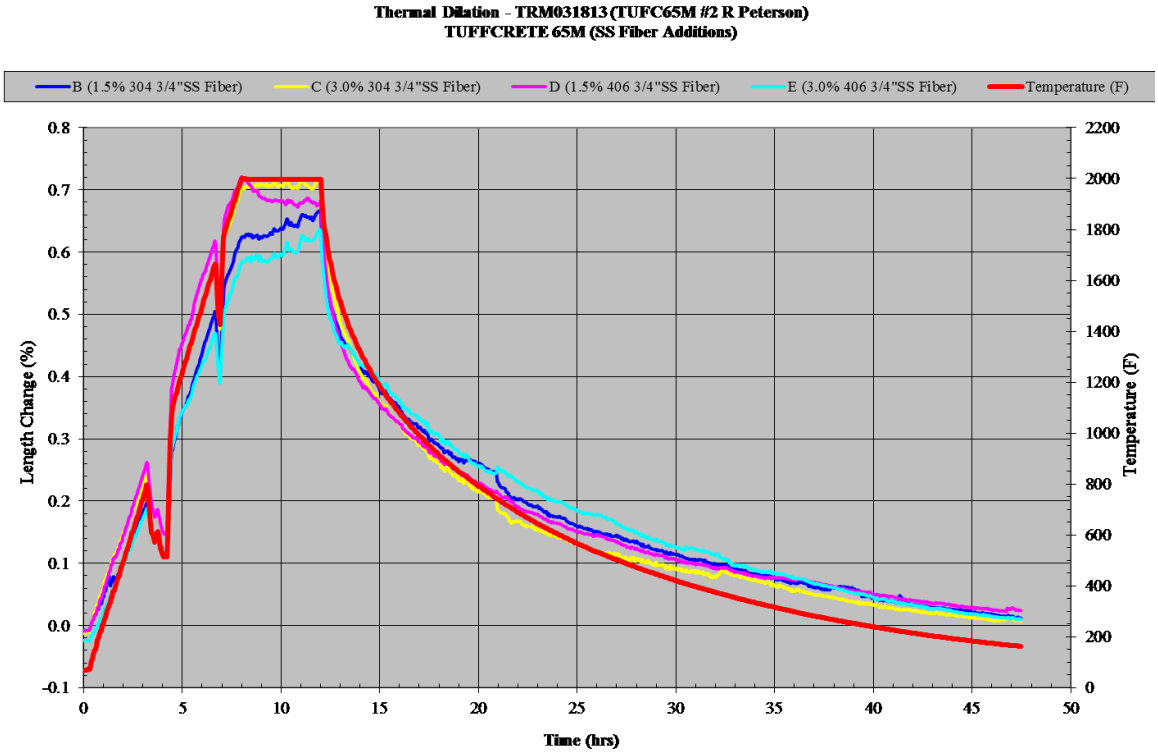

Figure 83: Thermal Dilation Time Graph, Second Run